Manuscript Details

Manuscript number	EARTH_2017_210_R1
Title	Mineralogical and geochemical evidence for polybaric fractional crystallization of continental flood basalts and implications for identification of their source lithologies
Article type	Review Article

Abstract

Continental flood basalts undergo crystallization at a variety of pressures in the crust and sometimes even in the mantle. Polybaric fractionation, when magmas may pause and undergo crystallization at different pressures, results in complex fractionation of major elements. Crystallization at high pressures where clinopyroxene is an early crystallizing phase can result in erupted compositions that have major element characteristics which mimic those expected for melts derived from pyroxenite-rich sources. The trace element compositions of early-crystallizing olivine can add further detail to crystallization histories and potentially allow an examination of the crystallization of basalts from melt segregation to the surface. The North Atlantic Igneous Province (NAIP) comprises sub-regions which had diverse crystallization histories. Plateau basalts of the British Palaeogene Igneous Province (BPIP) were generated by partial melting of mantle peridotite starting at ~3.8 GPa with melting ceasing by ~2.7 GPa. Major elements indicate that some basalts crystallized at <1 GPa with plagioclase joining the liquidus before clinopyroxene. However, the majority of BPIP magmas crystallized clinopyroxene before plagioclase feldspar over the pressure range 1.0-2.0 GPa. Trace elements in olivine indicate crystallization of olivine + clinopyroxene over the pressure interval 1.6-2.0 GPa. However, olivine data also show that some near-primary magmas reached near-surface pressures without substantial modification by fractional crystallization. Olivines formed at ≥1.6 GPa have Ni and Ca contents that are consistent with an origin by partial melting of mantle peridotite with no role for pyroxenite being detected. This contrasts with the low pressure dominated crystallization histories exhibited by lavas from West Greenland and Iceland. Whole-rock data for many BPIP lavas exhibit CaO depletion at a given MgO content compared with those from West Greenland and Iceland, which might be cited as an indicator of pyroxenite in their source, but this is solely a consequence of augite fractionation at depth. An absence of augite phenocrysts in lavas may have resulted either from augite crystallization in the mantle or from a change from augite saturation to under-saturation with decreasing pressure, and consequent augite dissolution. The lack of any significant contribution from recycled oceanic crust to magmatism in the NAIP suggests that the petrological structure of the mantle source from which NAIP lavas were derived does not conform with the generally accepted models for mantle plumes such as those responsible for magmatism in Hawaii and the Siberian Traps.

Keywords	Continental flood basalts; polybaric fractional crystallization; olivine chemistry; pyroxenite; model primary magmas

Corresponding Author	Malcolm Hole
Order of Authors	Malcolm Hole

Suggested reviewers	Jussi Heinonen, Claude Herzberg, Tyrone Rooney, Sally Gibson

Submission Files Included in this PDF

File Name [File Type]

Hole-ESR-Letter-Reply.doc [Cover Letter]

Hole-ESR-Response.doc [Response to Reviewers]

Hole-MJ-ESR-Final-Revisions.doc [Revised Manuscript with Changes Marked]

Hole-Abstract.doc [Abstract]

Hole-MJ-ESR-Final-Revised-MS.doc [Manuscript File]

Hole-Fig-1.jpg [Figure]

Hole-Fig-2.jpg [Figure]

Hole-Fig-3.jpg [Figure]

Hole-Fig-4.jpg [Figure]

Hole-Fig-5.jpg [Figure]

Hole-Fig-6.jpg [Figure]

Hole-Fig-7.jpg [Figure]

Hole-Fig-8.jpg [Figure]

Hole-Fig-9.jpg [Figure]

Hole-Fig-10.jpg [Figure]

Hole-Fig-11.jpg [Figure]

Hole-Fig-12.jpg [Figure]

Hole-Fig-13.jpg [Figure]

To view all the submission files, including those not included in the PDF, click on the manuscript title on your EVISE Homepage, then click 'Download zip file'.

Research Data Related to this Submission

Data set https://data.mendeley.com/datasets/3psjbpjb3r/draft?a=04945c5f-a324-478b-9bb1-061c8c5f0808

Data for: Mineralogical and geochemical evidence for polybaric fractional crystallization of continental flood basalts and implications for identification of their source lithologies

Primary magma models for Skye and Mull picrutes

Department of Geology & Petroleum Geology
Meston Building
King's College
Aberdeen AB24 3UE
Telephone: 01224 273434
e-mail:m.j.hole@abdn.ac.uk
13/09/2017

Mineralogical and geochemical evidence for polybaric fractional crystallization of continental flood basalts and implications for identification of their source lithologies
Malcolm J. Hole.

A revised manuscript has been uploaded. In addition to the reviewer's minor comments (all of which have been addressed in the revised manuscript) the following more substantial revisions have been made;

1) A map of the NAIP and BPIP has been included as Fig. 1.
2) Sub-figures have been re-lettered so that they are referred to in a more logical order
3) Fig. 9 has been modified to show the same samples as Fig. 8. This has been done to improve the discussion on Fe/Mn and clinopyroxene crystallization (reviewer's comment 17).
4) **Pressure of crystallization of clinopyroxene (major comment).** This has been clarified in a number of places in the text, including in the abstract; in lines 238 to 251 and in the conclusions. section in the revised manuscript. In addition, the fact that the Ol+Pl+Cpx barometer used by Herzberg (2004) is only calibrated to 1.0 GPa has been noted, and Fig. 3b has been modified to show data for Skye Cone Sheets which have been demonstrated to have crystallized at low pressure (1atm) by other workers.
5) **Discussion and conclusions**. In the light of the reviewer's comments (19) I have expanded the scope of the discussion and included section 8 entitled "The NAIP – a peridotite-dominated LIP". This section outlines the important differences between the NAIP and continental and oceanic LIPs that are dominated by pyroxenite and addresses the issues relating to the larger geodynamical implications of monolithological peridotite source melting displayed by the NAIP, as suggested by Prof. Herzberg.
6) Lambart (2017; Geochem. Persp. Lett. 4, 7-12.) was published while this paper was in review, and this has added a timely context for the discussion.
7) Fig. 13 has been added and is a summary model showing that the Ni contents of olivine from Iceland does not require, but does not preclude and role for pyroxenite in the petrogenesis of Icelandic lavas. This addresses some issues arising from Lambart (2017)

I hope that this is all satisfactory.

Malcolm

Malcolm J. Hole BSc, MSc, PhD.
Senior Lecturer in Geology
Department of Geology & Petroleum Geology
University of Aberdeen.

UNIVERSITY OF ABERDEEN

Department of Geology & Petroleum Geology
Meston Building
King's College
Aberdeen AB24 3UE
Telephone: 01224 273434
e-mail:m.j.hole@abdn.ac.uk
13/09/2017

Mineralogical and geochemical evidence for polybaric fractional crystallization of continental flood basalts and implications for identification of their source lithologies
Malcolm J. Hole.

A revised manuscript has been uploaded. In addition to the reviewer's minor comments (all of which have been addressed in the revised manuscript) the following more substantial revisions have been made;

1) A map of the NAIP and BPIP has been included as Fig. 1.
2) Sub-figures have been re-lettered so that they are referred to in a more logical order
3) Fig. 9 has been modified to show the same samples as Fig. 8. This has been done to improve the discussion on Fe/Mn and clinopyroxene crystallization (reviewer's comment 17).
4) **Pressure of crystallization of clinopyroxene (major comment).** This has been clarified in a number of places in the text, including in the abstract; in lines 238 to 251 and in the conclusions. section in the revised manuscript. In addition, the fact that the Ol+Pl+Cpx barometer used by Herzberg (2004) is only calibrated to 1.0 GPa has been noted, and Fig. 3b has been modified to show data for Skye Cone Sheets which have been demonstrated to have crystallized at low pressure (1atm) by other workers.
5) **Discussion and conclusions**. In the light of the reviewer's comments (19) I have expanded the scope of the discussion and included section 8 entitled "The NAIP – a peridotite-dominated LIP". This section outlines the important differences between the NAIP and continental and oceanic LIPs that are dominated by pyroxenite and addresses the issues relating to the larger geodynamical implications of monolithological peridotite source melting displayed by the NAIP, as suggested by Prof. Herzberg.
6) Lambart (2017; Geochem. Persp. Lett. 4, 7-12.) was published while this paper was in review, and this has added a timely context for the discussion.
7) Fig. 13 has been added and is a summary model showing that the Ni contents of olivine from Iceland does not require, but does not preclude and role for pyroxenite in the petrogenesis of Icelandic lavas. This addresses some issues arising from Lambart (2017)

I hope that this is all satisfactory.

Malcolm

Malcolm J. Hole BSc, MSc, PhD.
Senior Lecturer in Geology
Department of Geology & Petroleum Geology
University of Aberdeen.

Mineralogical and geochemical evidence for polybaric fractional crystallization of continental flood basalts and implications for identification of peridotite and pyroxenite source lithologies.

M.J. Hole[a]

a. Department of Geology & Petroleum Geology, University of Aberdeen, Aberdeen AB243UE, UK.

Abstract Continental flood basalts undergo crystallization at a variety of pressures in the crust and sometimes even in the mantle. Polybaric fractionation, when magmas may pause and undergo crystallization at different pressures, results in complex fractionation of major elements. Crystallization at high pressures where clinopyroxene is an early crystallizing phase can result in erupted compositions that have major element characteristics which mimic those expected for melts derived from pyroxenite-rich sources. The trace element compositions of early-crystallizing olivine can add further detail to crystallization histories and potentially allow an examination of the crystallization of basalts from melt segregation to the surface. The North Atlantic Igneous Province (NAIP) comprises sub-regions which had diverse crystallization histories. Plateau basalts of the British Palaeogene Igneous Province (BPIP) were generated by partial melting of mantle peridotite starting at ~3.8 GPa with melting ceasing by ~2.7 GPa. Major elements indicate that some basalts crystallized at <1 GPa with plagioclase joining the liquidus before clinopyroxene. However, the majority of BPIP magmas crystallized clinopyroxene before plagioclase feldspar over the pressure range 1.0-2.0 GPa. Trace elements in olivine indicate crystallization of olivine + clinopyroxene over the pressure interval 1.6-2.0 GPa. However, olivine data also show that some near-primary magmas reached near-surface pressures without substantial modification by fractional crystallization. Olivines formed at ≥1.6 GPa have Ni and Ca contents that are consistent with an origin by partial melting of mantle peridotite with no role for pyroxenite being detected. This contrasts with the low pressure dominated crystallization histories

exhibited by lavas from West Greenland and Iceland. Whole-rock data for many BPIP lavas exhibit CaO depletion at a given MgO content compared with those from West Greenland and Iceland, which might be cited as an indicator of pyroxenite in their source, but this is solely a consequence of augite fractionation at depth. An absence of augite phenocrysts in lavas may have resulted either from augite crystallization in the mantle or from a change from augite saturation to under-saturation with decreasing pressure, and consequent augite dissolution. The lack of any significant contribution from recycled oceanic crust to magmatism in the NAIP suggests that the petrological structure of the mantle source from which NAIP lavas were derived does not conform with the generally accepted models for mantle plumes such as those responsible for magmatism in Hawaii and the Siberian Traps.

1. Introduction

Continental flood basalts (CFB) must traverse continental lithosphere before eruption at the surface. For the North Atlantic Igneous Province (NAIP; Fig. 1), where the mantle was anomalously hot (T_P ~1450-1550°C; Herzberg and Gazel, 2009; Hole and Millett, 2016; Matthews et al. 2016) melting of mantle peridotite was initiated at ~3.7-4.5 GPa (Hole and Millett, 2016; Hole, 2015) and melting ceased when magmas rising by adiabatic ascent along the olivine liquidus reached the asthenosphere-lithosphere boundary (LAB), which is also the final pressure of melting (P*f*). The depth to the LAB varies throughout the province from ~100 km beneath Disko Island (west of Greenland) to ~60 km beneath Baffin Island (Hole and Millett, 2016; Matzen et al., 2017). During ascent from the initial melting pressure (P*i*) to the LAB, it is generally accepted that magmas crystallize olivine alone (e.g. Herzberg and Asimow, 2008; 2015; Putirka 2008; 2011). However, Herzberg and Asimow (2008) state that augite fractionation can occur in the mantle, an assertation that is corroborated by the existence of clinopyroxene-bearing xenoliths in Hawaiian lavas that are consistent with crystallization from a tholeiitic liquid at 110-150 km depth (Keshav et al., 2007). Magmas

may pause at the LAB or within the lithosphere prior to eruption, and in the British Palaeogene Igneous Province (BPIP), which is a sub-province of the NAIP, there is a large body of evidence that suggests that magmas paused at the Moho at about 30km depth, or equivalent to ~0.9±0.15 GPa (Thompson, 1974; 1982; Hole et al., 2015a; Millett et al., 2016). Individual batches of magma may have undergone polybaric fractionation. Thompson (1974; 1982) on the basis of melting experiments, as well as major, trace element and isotopic compositions of lavas, proposed that some mafic BPIP lavas underwent fractionation at 1.6-1.7 GPa as well as at ~0.9 GPa. Conversely, at Disko Island, very primitive and near primary magmas were erupted through ~100km of lithosphere and seem not to have paused to fractionate to any great extent in the crust (Larsen and Pedersen, 2000; 2009; Hole and Millett, 2016; Matzen et al., 2017).

O'Hara (1968) showed that with increasing pressure of crystallization, the liquidus fields of olivine and clinopyroxene contracted and that the field for clinopyoxene crystallization expanded at the expense of olivine. Experimental phase equilibria (e.g. Villiger et al., 2004; 2007; Whitaker et al., 2007) show that for fractional crystallization of peridotite-derived magmas at ~1 GPa, clinopyroxene (Cpx) crystallizes in compositions with Mg# (molecular % $MgO/MgO+FeO+Fe_2O_3$) ≤65 whereas the same magma crystallizing at 1 atm would have olivine as the sole liquidus phase at Mg# 65. With increasing pressure of fractionation, Cpx becomes a liquidus phase at progressively higher Mg# (Fig. 2) which results in an expansion of the Cpx stability field at the expense of olivine as noted by O'Hara (1968). For a typical BPIP primary magma generated by volatile-free melting of mantle peridotite (see Hole and Millett, 2016 for a compilation of primary magma compositions) at 1 atm, ~25% olivine crystallization would be expected before plagioclase joins the liquidus, whereas at 1.6 GPa, only about 10% crystallization of olivine alone would occur in the same magma before Cpx joins olivine on the liquidus (Fig. 2). This also means that the minimum

Mg# (or Fo content) of olivine when it is the sole liquidus phase also increases with increasing pressure (Fig. 2). Derivative liquids formed by Ol+Cpx fractionation at ~1 GPa, which may ultimately erupt at the surface as lavas, will also have a lower CaO content for a given MgO content than lavas that crystallize olivine alone because Cpx is a CaO-rich phase and strongly fractionates MgO from CaO (Fig. 3A).

It is generally accepted that the source lithology for CFB and their oceanic equivalents is not exclusively mantle peridotite, and that magmas derived from partial melting of pyroxenite are an important component of CFB magmatism (e.g Herzberg, 2011). The pyroxenite source components in LIPs is generally considered to have been derived from oceanic crust recycled to lower mantle depths as a result of subduction tectonics (Herzberg, 2011; Sobolev et al., 2007). In the broadest terms, two distinct lithologies of pyroxenite can be recognized on the basis of SiO_2 content. Primary or very primitive melts derived from high SiO_2 pyroxenite (silica+pyroxene) are recognized because they plot on the SiO_2-rich side of the orthopyroxene-calcium Tschermaks component (Opx–Cpx–CaTs) join in the molecular projection of the system olivine–Opx–CaTs–silica (Ol–Opx–CaTs–SiO_2; Herzberg, 2011). Conversely, melts derived from low SiO_2 pyroxenite (olivine+pyroxene) plot to the SiO_2-poor side of the same plane. Since the Opx–Cpx–CaTs join is a thermal divide at pressures associated with mantle melting i.e. 3-7 GPa, derivative magmas from the melting of high and low SiO_2 pyroxenite have divergent fractionation histories. At near melting pressures, low SiO_2 pyroxenite may undergo mixing with melts of mantle peridotite to form hybrid magmas, whereas melt derived from high SiO_2 pyroxenite cannot (Herzberg, 2011)

Distinguishing between pyroxenite- and peridotite-derived magmas in the lavas erupted at LIPs using major or trace major element geochemical data is fraught with problems. A commonly used indicator of the involvement of pyroxenite-derived melt in basalt

petrogenesis is that pyroxenite-derived magmas tend to be too deficient in CaO at a given MgO content to be derived from melting of volatile-free mantle peridotite (Herzberg and Asimow, 2008). However, fractionation of CaO relative to MgO is sensitive to the bulk mineral/melt partition coefficient for CaO (*D*CaO) in a magma, and some pyroxenites appear to have *D*CaO > 1 and others < 1 regardless of the initial concentration of CaO in the solid pyroxenite (e.g. Herzberg, 2011; Jennings and Holland 2015; Jennings et al., 2016). Residual clinopyroxene during melting of pyroxenite is likely to result in the generation of CaO deficient derivative lavas and therefore depends on the extent of melting at which clinopyroxene is partially consumed (Lambart et al., 2016). A significant difficulty is using CaO and MgO contents of mafic lavas to identify pyroxenite involvement is that lavas derived from CaO-poor pyroxenite will fall in the same region of an MgO-CaO diagram as peridotite-derived melts that have fractionated Ol+Cpx at crustal pressures (Herzberg and Asimow, 2008; Fig. 3A). Another effect of crystallization of peridotite-derived magmas at the Ol+Cpx+L cotectic is to drive liquids to progressively more SiO_2-undersaturation with decreasing Mg#. Consequently, crystallization of a peridotite-derived melt at ~1.0 GPa can result in a CaO depleted, Si-undersaturated liquid composition that is indistinguishable from a magma derived from the melting of low SiO_2 pyroxenite such as those found at the Canary Islands and Madeira (Herzberg, 2011; Gurenko et al., 2013). Furthermore, recycled pyroxenite is also known to be far more heterogeneous than mantle peridotite, both chemically and mineralogically, and produces a diverse range of derivative magmas that may be very similar to peridotite-derived magmas (Keshav et al., 2004; Herzberg, 2011; Lambart et al., 2012; 2013; 2016;). For most high SiO_2 pyroxenite-derived magmas, covariations between SiO_2 and CaO provide a reasonable discriminant from peridotite-derived magmas, because most high Mg#, high SiO_2 lavas derived from mantle peridotite are silica saturated or silica oversaturated olivine or quartz tholeiites, and they owe their high SiO_2 contents to

olivine fractionation at near-surface pressures; as a consequence, any deficiency in CaO at a given MgO content is most likely attributable to high SiO_2 pyroxenite.

Olivine phenocrysts in mafic lavas provide a mineralogical narrative about magmatic processes in Earth's crust and mantle and olivine records in its chemistry the widespread occurrence of magma chamber fractional crystallization, recharge, and mixing (Herzberg and O'Hara, 2002; Herzberg, 2011; Herzberg et al., 2016; Sobolev et al., 2007). Olivine contains readily measurable concentrations of trace elements Ni, Ca and Mn and the partitioning of these element between olivine and coexisting melt is well-understood (e.g. Beattie et al. 1991; Beattie, 1994; 1995; Herzberg and O'Hara, 2002; Matzen et al., 2013; 2017). Fractional crystallization can never be perfect in natural systems and so olivine in mafic lavas may be able to record episodes of fractionation that are not evident from whole-rock data, particularly in magmatic provinces such as the BPIP where polybaric fractionation is most likely to have occurred. Olivine also records the melting of recycled crust as a distinct pyroxenite lithology. In the case of Hawaii, many of the shield-forming lavas (e.g. Mauna Kea) have Ni contents that are too high, and Ca contents that are too low, to have been derived by partial melting of mantle peridotite and they are more likely to be derived from a pyroxenite-rich source (Sobolev et al., 2005; Herzberg, 2006; 2011).

Before an understanding of the possible source lithology for MPLF lavas can be made, it is clearly necessary to firstly constrain the fractionation histories of the magmas to enable an assessment of the role of Cpx fractionation in causing CaO depletion in basic. Only if this is understood can the contribution of low CaO pyroxenite to the source of the basalts be assessed. To this end, a combination of whole-rock and component olivine chemistry has been utilized to examine the fractionation history of some continental flood basalts from the British Palaeogene Igneous Province (BPIP) which is part of the wider North Atlantic Igneous Province (NAIP).

2. Magmatism in the BPIP

The BPIP is a sub-province of the large NAIP. Magmatism in the BPIP began at ~60 Ma and continued until ~58 Ma. The majority of the lavas of the BPIP are mildly alkaline slightly *Ne*-normative alkali olivine basalts and *Hy*-normative olivine tholeiites. The Mull Plateau Lava Formation (MPLF; Williamson and Bell, 2012) is made of a sequence of ~1 km thickness of plateau-forming lavas dominated by picrites and basalts with local occurrences of hawaiite, mugearite and trachyte (Kerr 1998; Kerr et al. 1995; 1999). The MPLF is overlain locally by the Central Mull Formation (CMF; Williamson and Bell, 2012) which comprises olivine tholeiite lavas and associated hypabyssal intrusions. The Skye Main Lava Series (SMLS; Thompson, 1982) is petrologically very similar to the MPLF although it is probably slightly older.

A number of the mafic (>8 wt% MgO) CMF tholeiites which equilibrated at ~1 atm, reached their erupted compositions by crystallization of olivine alone. For 49 of these lavas and intrusions Hole & Millett (2016) generated model primary magma compositions using PRIMELT3 (Herzberg and Asimow, 2008; 2015). Primitive parental melts to CMT erupted compositions required a mantle potential temperature (T_P) ~1500°C and MgO ~17.5 wt%. The initial pressure of melting (P*i*) was ~3.6 GPa with melting stopping by ~2.7 GPa giving a melt fraction for accumulated fractional melting (F-AFM) of ~0.16. Spice et al. (2016) applied the aluminium-spinel-olivine thermometer of Coogan et al. (2014) to Skye and Mull picrites (Mg# 78-85) which yielded crystallization temperatures of 1410°C and 1380°C relative to MORB primitive magmas, which are in excellent agreement with olivine-liquid crystallization temperatures for MPLF lavas given by Hole et al. (2015a). Four of the whole-rock samples of Spice et al. (2016) also provide PRIMELT3 solutions (Appendix 1) indicating T_P in the range 1524-1568°C and with P*f* of 3.4-3.6 GPa. However, MPLF lavas do not yield PRIMELT3 solutions, although olivine-hosted melt inclusions do provide model

primary magmas which indicate T_P~1480°C (Hole and Millett, 2016). The reason why MPLF lavas do not allow the generation of model primary magmas is because they are too deficient in CaO at a given MgO content to have been derived by olivine fractionation alone from mantle peridotite (Fig. 2). As has already been noted, such CaO deficiency can be caused augite fractionation or can be a characteristic of the source region for pyroxenite-derived magmas.

2.1 Estimates of equilibration pressure of BPIP plateau lavas from major element chemistry.

Based on experimentally determined phase relationships for SMLS lavas containing 11.1 wt% MgO, Thompson (1974; 1982) proposed that most Mg-rich picrites of the SMLS and MPLF reached their erupted compositions at pressures up to about 1.7 GPa, and that the remaining basic magmas of the BPIP have compositions related to cotectic equilibria at approximately 0.9±0.15 GPa, which is near the base of the crust beneath the Province (Thompson 1982). The melting experiments of Thompson (1974) showed that the general sequence of phase relationships with decreasing T and MgO at ~1.0 GPa is Ol+liquid (L); Ol+Cpx+L; Ol+Cpx+Pl+L; whereas at 1 atm, plagioclase is a liquidus phase before clinopyroxene. With increasing pressure, the stability field for clinopyroxene expands at the expense of olivine, and at ~1.7 GPa olivine is replaced by clinopyroxene as first crystallizing phase in the system for compositions with >11 wt% MgO. However, augite in typical Plateau-type basalts occurs as groundmass poikilitic anhedra and never forms phenocrysts (Thompson, 1982) and the dominant phenocryst phase in mafic plateau lavas is olivine.

Fig. 3 illustrates the relationships between CaO, MgO and Mg# for MPLF lavas with ≥8 wt% MgO. The liquid lines of descent (LLD) for a model primary magma at varying pressures from 1 atm to 2.0 GPa is also shown. The primary magma composition chosen for the forward model was the PRIMELT3 solution to Skye lava SK982, which is representative of a typical peridotite-derived magma in this region (Hole and Millett, 2016). Additionally,

SK982 has εNd_{58} = +8.9 and $^{206}Pb/^{204}Pb$=17.5 which means that it is largely unmodified by interaction with the continental crust (Thompson et al., 1986; Hole et al., 2015a). Forward models of fractional crystallization have been generated using Petrolg3 (Danyushevsky and Plechov 2011) using the parameters given in the caption to Fig 2. Forward modelling of all 49 BPIP model primary magmas shows that the relationship between T, MgO, Mg# and the pressure at which clinopyoxene appears on the liquidus is given by the approximations;

$$Mg\# = -0.554P^2 + 9.81P + 55.9 \quad (1)$$

$$T = 6.277P^2 + 141.9P + 1154.4 \quad (2)$$

For MgO the uncertainty is ±0.6% and for Mg# ±2.0. Thus, for a BPIP magma crystallizing at 1.0 GPa, clinopyroxene would join olivine on the liquidus at MgO = 10.6±0.6 wt% or Mg# = 65.2±2.0.

Inspection of Fig. 3B reveals the situation where CaO decreases with decreasing Mg# for the assemblage Ol+Cpx+L and thereafter, CaO may increase or decrease with Mg#, depending on pressure, for the assemblage Ol+Cpx+Pl+L. However, the overall variation in CaO once clinopyroxene joins the crystallizing assemblage is not great. Thus, for the SK982 primary magma crystallizing at 1.0 GPa, CaO decreases from ~12.6 to 12.1 wt% for a change in Mg# of 61-65 and then remains nearly constant (CaO=11.7-12.0 wt%) along the Ol+Cpx+Pl+L cotectic. This feature of Mg#-CaO covariations will be returned to later in the discussion regarding olivine chemistry. It is also noticeable from Fig. 3 that data for the majority of MPLF plateau lavas plots to the left and below the 1 atm Ol+L LLD and close to the Ol+Cpx cotectics for various pressures. Data for CMF and Baffin Island lavas, all of which yield PRIMELT3 solutions, plot close to the predicted olivine liquidus. Since PRIMELT3 only provides solutions for the melting of mantle peridotite for erupted compositions that have crystallized only olivine, then data for such lavas must plot on or above the Ol+L LLD, as they do in Fig. 3. It is logical to assume, therefore, that the reason

for the MPLF lavas yielding few PRIMELT3 solutions is that they underwent augite fractionation at ≥1.0 GPa, as proposed by Thompson (1974; 1982).

Herzberg (2004) provided a method of estimating pressure of equilibration of MORB tholeiitic basalts using a molecular projection in the system Anorthite-Diopside-Enstatite. However, this method has an inherent uncertainty of ±0.28 GPa for olivine tholeiites, can only be applied to liquids that fall along the Ol+Pl+Cpx+L cotectic, and is calibrated only up to ~1.0 GPa. It has already been shown that for BPIP lavas, the initiation of clinopyroxene crystallization is pressure and composition dependent. Consideration of Fig. 3B shows that the predicted plagioclase-in position has a curvilinear relationship with Mg#. The equation for this curve for the forward models of SK982 is;

$$CaO = 0.0658[Mg\#]^2 - 6.99[Mg\#] + 194.8 \quad (3)$$

Data for most Central Mull Formation lavas which are predicted to have been simultaneously saturated in olivine + plagioclase + augite fall above the 0.8 GPa crystallization trajectory in Fig. 3A. Application of the Herzberg (2004) method for estimating P_{eq} gives values in the range 0.0-1.0 GPa which are in good agreement with the estimates from Fig. 3B. Most CMF lavas also yield PRIMELT3 solutions for melting of dry peridotite (Hole and Millet, 2016) and therefore have CaO contents at a given MgO content that are consistent with their derivation from mantle peridotite. Bell et al. (1994) presented extensive mineral chemical and geochemical evidence for near 1 atm fractionation of the Skye cone sheets and data for these intrusions and these plot close to the 1 atm Ol+Pl+Cpx+L cotectic in Fig. 3B. There is, therefore, ample evidence of fractionation of MPLF and SMLS lavas in the range 1atm to >1 GPa, which is consistent with the results from the melting experiments of Thompson (1974) and other published estimates (e.g. Scarrow and Cox, 1995; Kerr et al., 1999; Hole et al., 2015a). However, many MPLF lavas plot in positions in Fig. 3 that suggest they underwent crystallization of Ol+Cpx at pressures up to 2.0 GPa.

Interaction between mafic lavas and sialic crust is an integral part of the fractionation history of BPIP magmas. Kerr et al. (1995) provided isotopic evidence for crustal assimilation during turbulent magma ascent for MPLF lavas and there is strong evidence to support the interaction between at least two discrete compositions of sialic crust and mantle derived magma in the BPIP (Thompson et al., 1982; 1986; Hole et al., 2015a). The isotopic compositions of BPIP lavas exhibit extreme variability, with εNd_{60} varying from −30 to +10 and $^{206}Pb/^{204}Pb$ 14.3-18.5 which reflects the antiquity of the contaminants involved in petrogenesis. For MPLF lavas, variations in εNd_{60} are a more modest −8 to +8. Because the Archean sialic component had εNd_{60} ~−50, and was light rare earth element (LREE) enriched, whereas many BPIP magmas are LREE depleted, the total amount of crustal contamination required to reach εNd_{60} −8 was small and possibly only a few % (Hole et al., 2015a). However, Thompson et al. (1986) noted that interaction with Archean granulite facies crust was a feature of plateau lavas that fractionated at ~1.0 GPa, whereas upper-crustal contamination occurred during crystallization along the 1 atm Ol+Pl+Cpx cotectic. Peate et al. (2012), using data from olivine-hosted melt inclusions, showed that the crustal assimilation in some magmas must have taken place prior to growth of the olivines, but in others the inclusions have less contaminated compositions than the whole-rocks and crustal assimilation must have taken place both during and after growth of the olivines. Necessarily, the evidence of crustal interaction is entirely from trace element and isotopic compositions. During this study, no relationship was found between isotopic compositions and major element chemistry of lavas, except for concentrations of K_2O and TiO_2 which tend to be elevated and reduced respectively in lavas that suffered crustal contamination relative to uncontaminated lavas.

Major element data therefore suggest that the majority MPLF lavas crystallized Ol+Cpx at ≥1 GPa. Consequently, the position occupied by these lavas in Fig. 3B, which is

below the peridotite-pyroxenite divide of Herzberg and Asimow (2008) could either be because of their fractionation history or because they were derived from a CaO depleted pyroxenite source. Consequently, major elements alone are not sufficient to identify the course lithology of many MPLF lavas.

3. Models for trace element behaviour during olivine crystallization

3.1 Calculation methods – Ni in olivine

The methods for calculating model olivine Ni and Ca compositions of primary magmas used here follow those of Beattie et al. (1991), Beattie (1994; 1995), Herzberg and O'Hara (2002), Toplis (2005), Herzberg (2011) and Matzen et al. (2013; 2017) and Gavrilenko et al. (2016). Equations and assumptions pertinent to the current study are given below.

Fractional crystallization of primary magmas produces olivines that are expected to crystallize along a liquid line of descent (LLD); such olivine compositions have been appropriately termed "crystal line of descent," or CLD (Putirka et al. 2011). Forward models to define a CLD for olivine have been generated using Petrolog3 (Danyuchesvky and Plechov, 2011) for model BPIP primary magmas (Hole and Millett, 2016) to give an LLD. The predicted CaO, NiO and MnO concentrations in olivines formed in equilibrium with liquids along the LLD have then been calculated using the parameters embedded in PRIMELT3, or modifications of these, which are detailed below.

The forsterite (Fo) content of olivine in equilibrium with a melt is calculated using the partitioning of Fe and Mg between olivine and melt;

$$K_D^{Ol/L}{}_{(FeO/MgO)} = D^{OL/L}{}_{FeO}/D^{Ol/L}{}_{MgO} \qquad (4)$$

$K_D^{Ol/L}{}_{(FeO/MgO)}$ varies of a function of pressure, temperature and composition (*P, T, X;* e.g. Toplis 2005). Herzberg and O'Hara (2002) provide a method for calculating $K_D^{Ol/L}{}_{(FeO/MgO)}$ for the crystallization of a primary magma along the olivine liquidus from the pressure of

melting to the surface, and this calculation method is available to the user in Petrolog3. However, for magmas that pause in the crust, then it is $K_D^{Ol/L}{}_{(FeO/MgO)}$ at the depth at which olivine crystallization occurs that is relevant and not necessarily the ascent path to the surface along the olivine liquidus. The thermodynamical parameterization of Toplis (2005) allows for the calculation of $K_D^{Ol/L}{}_{(FeO/MgO)}$ at a given pressure for a known magma composition. The Toplis (2005) model has been investigated using Petrolog3 for BPIP primary magma compositions and the results are illustrated in Fig. 4 for three BPIP magmas with different MgO contents which cover the range of T_P estimates for the region (Hole and Millet, 2016). The final pressure of melting (P*f*) was used as a proxy for pressure of melt segregation which for BPIP primary magmas is typically ~2.7 GPa (Hole and Millett, 2016). This gives values of $K_D^{Ol/L}{}_{(FeO/MgO)}$ ~0.338 for derivative magmas at 2.7 GPa formed from primary magmas containing 17.5 wt% MgO or equivalent to T_P=1500°C (Fig. 4A). For near-surface crystallization, $K_D^{Ol/L}{}_{(FeO/MgO)}$ for the same magma would be 0.30-0.31. At a fixed pressure $K_D^{Ol/L}{}_{(FeO/MgO)}$ exhibits a negative covariation with Mg/Fe_{Liq} (cationic Mg/Fe of the liquid) for liquids with Mg/Fe in the range 1.5-3.3 (Fig. 4B), which is equivalent to the composition of near-primary magmas to moderately evolved basalts with ~8.0 wt% MgO. Conversely, the Herzberg and O'Hara (2002) calculation method defines a relationship between Mg/Fe_{liq} and $k_D^{Ol/L}{}_{(FeO/MgO)}$ that is necessarily positive and curvilinear to account for *P, T, X* variability during ascent along the olivine liquidus, but without magma pausing in the crust. The practical use of this is that the point of intersection between the Herzberg and O'Hara (2002) crystallization trajectory and a Toplis (2005) crystallization contour allows both $K_D^{Ol/L}{}_{(FeO/MgO)}$ and Mg/Fe_{liq} at the contoured pressure to be estimated, which are unique to a given primary magma. For example, considering a magma that segregated at 2.7 GPa and then paused in the crust and crystallized olivine at 1.0 GPa, it can be assumed that the magma follows the Herzberg and O'Hara (2002) curve in Fig. 4B from the point of magma

segregation to 1.0 GPa, crystallizing olivine along the CLD. The melt then pauses at 1.0 GPa and crystallizes more olivine. The point at which the Herzberg and O'Hara (2002) LLD intersects the 0.5 GPa Toplis (2005) contour, which in this example is at Mg/Fe_{liq}=1.7 and $K_D^{Ol/L}{}_{(FeO/MgO)}$=0.317 (Fig. 4B), is the taken as the compositional starting point for 1 GPa olivine crystallization. From that point onwards, $K_D^{Ol/L}{}_{(FeO/MgO)}$ is estimated from Mg/Fe_{Liq} using the Toplis (2005) parameterization at a fixed pressure of 1.0 GPa. Whereas the intersection point in Fig. 4b is unique to a specific primary magma, it is mainly influenced by Mg/Fe (and therefore also T_P and P*i*) of the primary magma and P*f*. Consequently, for a magmatic province with relatively consistent values T_P and P*f* such as the BPIP (Hole and Millett 2016) a single crystallization model is probably sufficient to describe the LLD of most basalts and the CLD of their component olivines, and that is the approach which has been taken here.

An additional complication comes from the expansion of the clinopyroxene stability field at the expense of olivine with increasing pressure (Fig. 2; Whitaker et al., 2007; Villger et al., 2007). Magmas that pause in the crust are likely to crystallize on the Ol+Cpx+Liq cotectic rather than along the olivine liquidus. Investigations using Petrolog3 show that $K_D^{Ol/L}{}_{(FeO/MgO)}$ remains nearly constant for the Ol+Cpx+L crystallization interval, but the role of olivine in the crystallizing assemblage diminishes substantially with continuing crystallization (Fig. 2). Consequently, for crystallization at elevated crustal pressures, olivine should be less abundant than for crystallization of the same magma near the surface. This probably naturally limits the number of olivine analyses that can be generated for olivines that crystallized on the Ol+Cpx+L cotectic. For the purposes of this study it has been assumed that for crystallization of Ol+Cpx+L, $K_D^{Ol/L}{}_{(FeO/MgO)}$ is constant at the pressure of interest.

The method used for estimating the Ni content of a primary magma was that of Herzberg (2011);

$$\text{Ni ppm} = 21.6\text{MgO} - 0.32\text{MgO}^2 + 0.051\text{MgO}^3 \quad (5)$$

$D^{Ol/L}_{NiO}$ was determined using the method of Beattie et al. (1991) which was re-examined by Herzberg et al. (2016) and found to remain applicable in the light of new experimental results;

$$D^{Ol/L}_{NiO} = 3.346\, D^{Ol/L}_{MgO} - 3.665 \quad (6)$$

Because $D^{Ol/L}_{MgO}$ is determined from $K_D{}^{Ol/L}_{(FeO/MgO)}$ then magmas which pause at depth in the crust are pressure-compensated for $D^{OL/L}_{NiO}$ by the $K_D{}^{Ol/L}_{(FeO/MgO)}$ calculation method outlined above and in Fig. 4.

Matzen et al. (2013; 2017) showed that the temperature dependence of $D^{Ol/L}_{NiO}$ can ultimately result in olivine crystallizing from near-primary magmas at near-surface pressures, having higher Ni contents than olivine crystallizing from the same magma at the pressure of melt segregation. The relationship between the NiO content of an olivine crystallizing from the same magma at 1 bar and at the pressure of melt segregation is given by;

$$NiO^{Ol}T_{P0}/NiO^{Ol}T_{Pf} = \exp\,(4505 - (1/T_{P0} - 1/T_{Pf})) \quad (7)$$

Where $Ni^{Ol/L}T_{P0}$ and $NiO^{OL/L}T_{Pf}$ are the NiO contents, in weight units, of olivine crystallizing from magma at the surface and close to the pressure of melt segregation respectively, and T_{P0} and T_{Pf} are the temperatures of the olivine saturated magma at 0 GPa and at the pressure of melt segregation respectively. Olivine-saturated T_{Pf} was taken from T_{Ol} of the PRIMELT3 solution for the magma of interest (Herzberg and Asimow, 2015; Hole and Millett, 2016). Since subsequent crystallization was assumed to take place near to the surface $K_D{}^{Ol/L}_{(FeO/MgO)}$=0.30 was used in all calculations. Application of equation (7) to primary magma compositions therefore yields the maximum possible Ni content of an olivine

crystallizing from a primary magma at near-surface pressure. Such olivines are referred to hereafter as 'Matzen olivines'.

3.2 Calculation methods – Ca in olivine

Three different methods are available for calculating the model olivine Ca compositions of primitive magmas. Two of these (Beattie et al., 1991; Herzberg and O'Hara, 2002) are based on variation in $D^{Ol/L}_{CaO}$ as a function of $D^{Ol/L}_{MgO}$. The Beattie et al. (1991) method, which is appropriate to near-surface pressures, and is given by;

$$D^{Ol/L}_{CaO} = 0.0056\, D^{Ol/L}_{MgO} + 0.0135 \quad (8)$$

And for pressures close to those of melt segregation in the range 3-7 GPa, the equation of Herzberg and O'Hara (2002) can been applied;

$$D^{Ol/L}_{CaO} = -0.019\, D^{Ol/L}_{MgO} + 0.007\, D^{Ol/L}_{MgO} + 0.0063/\, D^{Ol/L}_{MgO} \quad (9)$$

Gavrilenko et al. (2016) provided a further method of calculating $D^{Ol/L}_{CaO}$ using only the MgO content of an anhydrous magma based on new melting experiments. This method is applicable over a wide range of pressures (1atm to 14 GPa) and temperatures (1150-2050°C). For magmas containing <11.1 wt% MgO;

$$D^{Ol/L}_{CaO} = -0.0043\ \mathrm{MgO} + 0.072 \quad (10)$$

And for magmas containing >11.1 wt% MgO;

$$D^{Ol/L}_{CaO} = 0.00042\ \mathrm{MgO} + 0.0196 \quad (11)$$

Fig. 5A shows Petrolog3 forward crystallization models of two BPIP model primary magmas (SK982 and MU1.1) at a nominal pressure of 1 atm for the three olivine-liquid CaO partitioning models given in equations (8)-(11). In addition, the CaO contents of olivine in equilibrium with 49 model primary BPIP magmas calculated for equations (8)-(11) are also shown in Fig. 5A. The uncertainty in $D^{Ol/L}_{CaO}$ (±0.004) for the Gavrilenko et al. (2016) model for compositions with >11.0 wt% MgO propagates to ±300 ppm Ca in Fig. 5. The Beattie et

al. (1991) and Gavrilenko et al. (2016) models predict very similar primary equilibrium olivine compositions for BPIP magmas, but exhibit significant differences in slope of the CLD, with the Gavrilenko et al. (2016) model initially predicting lower $D^{Ol/L}_{CaO}$ than the Beattie et al. (1991) model for the same range of Fo contents. However, at around 85-87% Fo, equivalent to a whole rock MgO content of 11 wt% (see equations (10) and (11) above) the Gavrilenko et al. (2016) model exhibits a sharp increase in olivine Ca content with decreasing Fo compared to the Beattie et al. (1991) model. The Herzberg and O'Hara (2002) model predicts lower Ca contents of primary olivine than either of the other two models.

Fig 4b illustrates the effects of crystallization of magmas at varying pressures on Ca and Fo contents of olivine. A single model primary BPIP magma (SK982) has been selected and Petrolog3 forward models at pressures in the range 1atm to 2.2 GPa generated. CLDs for olivine have then been calculated from equations (9)-(11). The Beattie et al. (1991) model has not been investigated because it is applicable only to crystallization at 1 atm. The key features of Fig. 5 are that both the Herzberg and O'Hara (2002) and Gavrilenko et al. (2016) models develop an inflection on the CLD at the point at which clinopyroxene joins the crystallizing assemblage, which is also reflected in the major element data for BPIP lavas (Fig. 3). According to the Gavrilenko et al. (2016) model, crystallization of the assemblage Ol+Cpx+L causes the Ca contents of equilibrium olivine to decrease relative to the primary olivine compositions, whereas the Herzberg and O'Hara (2002) model suggests a buffering of Ca content of equilibrium olivine for the same aasemblage. Additionally, for the Gavrilenko et al. (2016) model, the CLD for Fo and Ca for the assemblage Ol+L has a relatively shallow slope for Fo contents in the range 85.5-91.5, which is equivalent to about 11 wt% MgO in the whole rock (see equation (11)). For the purposes of consistency, the most recent parameterizations for $D^{Ol/L}_{CaO}$ of Gavrilenko et al. (2016) are primarily used below, but the Herzberg and O'Hara model (2002) is also considered if necessary.

Also shown in Fig. 5B are data for natural olivines in near-primary Siqueiros Fracture Zone MORB. These have Ca=2060±63 ppm at Fo=89.9±0.5 (64 samples from Gavrilenko et al., 2016). Olivine in equilibrium with PRIMELT3 model primary magma compositions (Herzberg and Asimow 2015) have predicted Ca=2204±58 ppm and Fo= 89.9±0.3 using the method of Gavrilenko et al. (2016), which is lower than the observed abundances. However, for MORB, predicted and observed data fall within the limits of the regressions used in the Gavrilenko et al. (2016) model.

4. Olivine in MPLF lavas

Data for olivine in MPLF lavas are taken from Sobolev et al. (2007) who analyzed olivine grains from 14 different samples giving a total data set of 842 individual determinations. Spice et al. (2016) provide a further 64 analyses from Skye, Mull and Rum picrites all of which have whole-rock MgO contents in the range 24.8-31.9 wt% MgO. These picrites will be treated as a separate group of rocks from the MPLF because their stratigraphical affinity is unclear they are unlike any samples found within the main MPLF lava pile.

Covariations between Fo content and Ni content for selected analyses are shown in Fig. 6. The data have been selected to be representative of all MPLF olivine, and particularly the range of Fo contents which is from ~75-90, although the bulk of the data have Fo >80. Olivine with compositions in the range Fo 80-90 would be in equilibrium with whole-rock compositions with Mg# 54-73 and MgO 7.7-15.8 wt% at 1 atm based on forward models of the primary magma to SK982. This range in whole-rock compositions encompasses the majority of that for MPLF lavas (Fig. 3). The CLDs in Fig. 6 were calculated both for the Beattie et al. (1991) and the Herzberg and O'Hara (2002) models. For olivine in MPLF lavas, Ni correlatives positively with Fo and the data falls into two distinct groups which relate to the position of data relative to the 1 atm Beattie CLD; data for samples BR2, BR6 and BHL15 (Fig. 6A) plots closer to the 1 atm CLD than the remaining samples, the latter all

having a higher Ni for a given Fo content than, for example, sample BR2. Olivine from picrites from Mull, Skye and Rum (Spice et al. 2016) plot close to the position expected of olivine in equilibrium with primary magmas. Using these data and equation (7) above, gives Matzen olivines with Fo 91.2–91.8 and Ni = 3560-3570 ppm which are within the range of the analyzed values for olivine in the Skye and Mull picrites. Indeed, Matzen olivines calculated to be in equilibrium with all 49 BPIP PRIMELT3 primary magmas (Fig. 6B) show considerable overlap with the olivine data from Spice et al. (2016). The picrites of Spice et al. (2016) which contain high Fo and high Ni olivines must therefore have been formed by rapid emplacement of a near-primary magma at the surface followed by olivine crystallization at close to 1 atm. This allows the maximum Ni content of BPIP olivines to be constrained to ~3600 ppm at Fo ~91.5, values which are within the normal range expected for dry melting of mantle peridotite at T_P ~1500°C (Matzen et al., 2017) and within the range of those calculated for lavas from west Greenland (Herzberg et al., 2016; Matzen et al., 2017).

Since it is likely that MPLF lavas equilibrated at pressures ≥1.6 GPa, the CLD for SK982 at 1.6 GPa has been calculated and is shown in in Fig. 6. It shows a remarkable correspondence with the data from MPLF samples BR2, BR6 and BHL15, including an apparent inflection in the data trend which corresponds to clinopyroxene joining the liquidus. The inflection occurs because $D^{Cpx/L}_{NiO}$ ~0.25 × $D^{OL/L}_{NiO}$, (Herzberg et al., 2016) and therefore crystallization along the Ol+Cpx+L cotectic results in a smaller bulk mineral-melt distribution coefficient for Ni than for olivine crystallization alone. This, in turn, results in liquid compositions that have fractionated Ol+Cpx having higher Ni contents than for the same liquid fractionating only olivine, at the same Mg#. It is also noticeable that the data for near CLD MPLF lavas terminates at the Ol+Cpx+Pl+L cotectic. Mixing between primary and derivative magmas along the LLD and their subsequent crystallization of olivine would produce olivine compositions that fall on the mixing lines shown in Fig. 6. The remaining

data for MPLF olivines fall along these mixing lines. This is a similar situation to that described by Herzberg et al. (2016) for mixing relationships in olivines and primary and derivative magmas from Theistareykir, Iceland. The mixing lines shown in Fig. 5 relate to specific MgO contents of the derivative magma along the LLD. So, for sample BR5, mixing between a primary magma and a derivative magma with ~6 wt% MgO could produce the observed array of olivine compositions, whereas sample BHL34 would require a derivative magma with higher MgO content to produce its component olivine compositions.

Fig. 7 shows covariations between Fo and Ca content of the same olivines as shown in Fig. 6. Because Ca is incompatible with respect to olivine ($D^{Ol/L}_{CaO}$ typically 0.025-0.031) then a negative covariation between Fo and Ca content might be expected, but this is not observed. A feature of Fo-Ca covariations in MPLF olivines is the relatively consistent Ca content of 1800-2400 ppm over a range of Fo = 80-89. The predicted range of olivine compositions calculated for the fractional crystallization of 49 BPIP PRIMELT3 solutions from primary MgO contents to 8 wt% MgO, using the Beattie et al. (1991) 1atm crystallization and Gavrilenko et al. (2016) olivine liquidus models are also shown in Fig. 7. The field for olivine calculated using the Beattie *et al.* (1991) model has a considerably steeper slope than that for the Gavrilenko et al. (2016) model. It is noticeable that olivine in the Skye picrites mostly fall within the range of the Beattie et al. (1991) model and close to primary olivine compositions predicted by the Gavrilenko et al. (2016) model, which is also consistent with their position in Ni–Fo space (Fig. 6). Olivine in Mull picrites appear to have consistently lower Ca for a given Fo content than the Skye olivines.

Very few of the data for olivine grains from MPLF lavas fall within the region reserved for 1 atm olivine crystallization from primary and derivative magmas using the Gavrilenko et al. (2016) model. CLDs at varying pressures, calculated as described earlier, are also shown in Fig. 7, and mirror the data trends shown in Fig. 3 such that once Cpx joins olivine on the

liquidus, the CaO content of olivine decreases slightly at a given pressure. Therefore, as in Fig. 4 for whole-rock data, some of the MPLF olivines exhibit patterns of distribution of Fo and CaO that are consistent with crystallization along the Ol+Cpx+L cotectic. However, the position of isobars in Fig. 7 cannot be predicted with certainty because the CaO abundances of BPIP primary magmas vary considerably, such that at ~1.6 GPa the variation within primary magmas is equivalent to a variation of ~500 ppm Ca in the olivine data set. In addition, slow diffusion of Ca in olivine can result in consistent Ca but variable Fo contents in individual grains, which is not evident for faster-diffusing Ni data (Coogan et al., 2005; Chakraborty, 2010). Consequently, the apparent sub-horizontal arrays delineated by olivines from individual MPLF samples could in part be a result of slow Ca diffusion, and it is the Ca content of the most Fo-rich samples that best reflects crystallization conditions. However, the Ca and Fo content of the MPLF lavas shown in Fig. 7 seems to require crystallization at ≥1.4 GPa

Covariations between NiO and CaO are shown in Fig. 8 for all the Ca partitioning models in equations (8)-(11) based on the primary magma to Skye lava SK982, and for the Herzberg and O'Hara (2002) and Gavrilenko et al. (2016) methods, at varying pressures. Ca-Ni covariations for the Gavrilenko et al. (2016) model exhibit a series of negative 'spikes' which relate to the composition at which clinopyroxene joins olivine in the crystallizing assemblage, which is a predictable consequence of augite fractionation. Because clinopyroxene joins the crystallizing assemblage at progressively higher MgO contents with increasing pressure (Fig. 3), the negative 'spikes' occur at higher Ni contents with increasing pressure. However, an added complication is that for pressures >1.2 GPa, clinopyroxene joins the crystallizing assemblage at >11.1wt% MgO so equation (11) applies to the assemblages Ol+L and Ol+Cpx+L, whereas for pressures <1.2 GPa clinopyroxene joins the crystallizing assemblage at <11.1wt% MgO and so equation (11) only applies to the olivine liquidus.

Once crystallization takes place along the Ol+Cpx+Pl+L cotectic Ni-Ca variations define shallow concave upwards trends, Ca contents decreasing with increasing pressure of fractionation. The Herzberg and O'Hara (2002) model is less complex and predicts lower Ca for a given Ni content than the Gavrilenko et al. (2016) model.

Data for olivine in Skye picrites falls close to the extension of the trajectory for low pressure (~1 atm) crystallization of Ol+L and close to the position of Matzen olivines calculated to be in equilibrium with BPIP primary magmas at 1 atm. Data for olivine in Mull picrites generally hove lower Ca for a given Fo than those from Skye picrites, and lower than the model Matzen olivines. This may suggest that the Mull picrites may have experienced clinopyroxene fractionation in the mantle (Herzberg and Asimow, 2008). The data for MPLF olivines shown in Fig 7c plots significantly below the olivine liquidus of Gavrilenko et al. (2016) and close to, or below, the olivine liquidus for the Herzberg and O'Hara (2002) model. Consequently, data for the samples shown in Figs 6 and 7 are consistent with crystallization of Ol+Cpx+L at elevated pressures up to ~2.2 GPa. Given that the final pressure of melting for many BPIP lavas is ~2.7 GPa (Hole and Millett, 2016) then in some cases, crystallization of olivine must have commenced at or close to the lithosphere-asthenosphere boundary, as suggested by Matzen et al. (2017). In Fig. 8A data are shown for MPLF olivines that falls between the Gavrilenko et al. (2016) and Herzberg and O'Hara (2002) olivine liquidii, and therefore close to the expected range of Ca and Ni content for crystallization of the assemblage Ol+L. BPIP Matzen olivines fall on the extension of the Ol+L trajectory and have higher Fo contents ~92 (Fig. 7) than the observed values for MPLF lavas (maximum ~Fo88). Crystallization of ~15-20% olivine from a Skye picrite composition could produce the observed Ni, Ca and Fo contents of the MPLF olvines shown in Figs 7A and 8A. On the basis of Ni and Ca distributions in olivines discussed above all MPLF lavas could have been generated by crystallization from a peridotite-derived magma at

variable, but elevated pressures of up to ~2.2 GPa. Consequently, there is no evidence to suggest the involvement of pyroxenite in the source of the MPLF lavas.

Herzberg (2011) showed that Fe/Mn>70 at any Fo content is characteristic of olivine that crystallizes from pyroxenite compared to Fe/Mn 60-70 for olivine in peridotite-derived magmas. The mean Fe/Mn for MPLF lavas is 69.2±2.6 (Fig. 9) but two samples (BCH14 and AM7a) fall exclusively above 70 with a maximum Fe/Mn of 75 (Fig. 9A). However, Herzberg et al. (2013) demonstrated that clinopyroxene fractionates Fe from Mn causing elevated Fe/Mn in lavas that undergo clinopyroxene fractionation. Consequently, the elevated Fe/Mn in the MPLF lavas that crystallized at the highest pressures (Fig. 9B) may solely be due to clinopyroxene fractionation and not because they were derived from pyroxenite. Furthermore, the lavas shown in Fig. 9B contain olivine which carry a lower pressure crystallization signature than those in Fig. 9A, and also have Fe/Mn<70. Low and high SiO_2 pyroxenite-derived lavas from Hawaii (HSDP-2) contain olivines with Fe/Mn = 73.8±1.7 and up to a maximum of 81 all of which are higher than the MPLF samples again suggesting that pyroxenite was not an important component of the course of MPLF lavas.

5. Olivine in magmas from Iceland, Baffin Island and west Greenland

The distribution of Ni in olivines in lavas from Thesitareykir (Iceland), Baffin Island and Disko Island (west of Greenland) were discussed in detail by Herzberg et al. (2016). A feature of olivines within lavas from Theistareykir are the existence of two populations, one primitive population crystallizing close to the 1 atm CLD and the other falling on mixing lines with derivative magmas along the CLD (Herzberg et al., 2016). However, the two populations of olivines are mutually exclusive with respect to their host lavas. When the same data are considered in terms of Ni-Ca covariations (Fig. 10A), olivines that exhibit evidence of an origin by magma mixing in terms of Fo-Ni correlations, have lower CaO contents over the same range of Ni contents than the more primitive olivines that fall close to the 1 atm

CLD. Simple magma mixing cannot account for these variations because mixing lines for reasonable MgO contents of derivative magmas (≥7 wt% MgO) do not intersect both groups of olivines. Indeed, mixing between a primary magma formed at depth with magmas formed at progressively shallower levels would necessarily fall along the predicted pathway for the Herzberg and O'Hara (2002) Ni-Ca partitioning model (Fig, 9). Similarly, mixing between primitive or near primary magmas (those which would crystallize Matzen olivines) and derivative magmas close to the surface would follow the predicted pathway for the Beattie et al. (1991) Ni-Ca partitioning model.

Inspection of Fig. 7 shows that for BPIP lavas crystallizing only olivine, Ca contents of olivines should be lower for crystallization occurring at higher pressures compared to those at lower pressures. Maclennan et al. (2003) showed that some lavas at Theistareykir crystallized at >0.8 GPa and showed evidence of crystallization along the Ol+Cpx+L cotectic. So, rather than being a result of mixing it is more likely the low CaO olivines found in some Theistareykir lavas are those which crystallized at ~1.0 GPa. The variation in $D^{Ol/L}{}_{NiO}$ because of fractionation at higher T (Matzen et al. 2017) would not be great enough to cause any discernible variation in Ni content between high and lower pressure olivines. Nevertheless, $K_D{}^{Ol/L}{}_{(FeO/MgO)}$ would be higher (~0.310) for the higher pressure olivines than those which crystallized at 1 atm (~0.298) thus resulting in differences in distribution of the data in terms of Ni-Fo covariations. Also, because crystallization along the Ol+Cpx+L cotectic results in a smaller bulk mineral-melt distribution coefficient for Ni than for olivine crystallization alone, liquid compositions that have fractionated Ol and Cpx have higher Ni contents than for the same liquid fractionating only olivine, resulting in higher Ni contents in olivine for a given Fo content, as is observed at Theistareykir.

Covariations between Ca and Ni in data for olivines from Baffin Island (Fig. 10B) follow the predicted CLDs defined by the Beattie et al. (1991) and Gavrilenko et al. (2016)

models and the data therefore follow trends that are consistent with crystallization at or near the surface. The most Ni-rich and Ca-poor olivines overlap with the composition of Matzen olivines calculated to be in equilibrium with PRIMELT3 primary magmas Consequently, some of the olivines in Baffin Island lavas can be considered to be truly primary and crystallized after rapid emplacement of magma close to the surface. Importantly, there is no evidence for crystallization along the Ol+Cpx+L cotectic, the projection of which falls well below the observed data in Fig. 10B. Olivines in lavas from Disko Island (Fig. 10C) have systematically lower Ca contents at a given Fo content compared to the values predicted by the Gavrilenko et al. (2016) model for crystallization at 1 atm, and lower Ca contents than olivines from Baffin Island with similar Fo contents. Hole and Millett (2016) showed that at Baffin Island P*f*~2.1 GPa whereas at Disko island P*f* ~2.8 GPa which most likely reflects a deeper asthenosphere-lithosphere boundary at Disko Island Baffin Island (Matzen et al., 2017). One possibility is that Disko Island magmas underwent minor clinopyroxene fractionation in the mantle before being emplaced, whereas the Baffin Island magmas only crystallized olivine and underwent rapid emplacement to shallow levels. Alternatively, the low Ca and high Ni contents of some Disko Island olivines could be interpreted as a result of their derivation from a low CaO pyroxenite source. However, the involvement of pyroxenite cannot be substantiated by the Fe/Mn for Disko Island olivines (Fig. 9). Consequently, the observed differences between Baffin and Disko island olivines might relate to the differences in magmatic plumbing at the two locations rather than to source heterogeneities.

6. Clinopyroxene stability during polybaric fractionation

MPLF and SMLS lavas do not contain augite phenocrysts, only olivine. Augite tends to form as groundmass poikilitic anhedra in sparsely olivine-phyric lavas regardless of Mg# (Thompson, 1982; Bailey et al., 1923). Nevertheless, there appears to be ample evidence to

suggest that augite was an important crystallizing phase during the evolution of the BPIP plateau lavas, which sets them apart from other NAIP lavas. On a regional scale, there were large volumes of pyroxene gabbro intruded throughout the lifetime of the BPIP. The Ben Buie gabbro complex on Mull forms part of the intrusive complex beneath the Mull volcano and is considered to be a product of the crystallization of a tholeiitic magma (Thompson 1982).

The estimates of ~1.0 GPa crystallization pressure of some of the more evolved lavas along the Ol+Cpx+Pl+L cotectic, coupled with the high pressure Ol+L or Ol+Cpx+L crystallization trends evident in the olivine data, strongly suggests that polybaric fractional crystallization was important in the BPIP, as was originally postulated by Thompson *et al.* (1980) and developed further by other workers (e.g. Kerr et al., 1999; Fowler et al., 2003; Font et al., 2008; Hole et al., 2015a). Herzberg and Asimow (2008) noted that deep crystallization of high CaO augite can have the same effect as shallow augite fractionation on the CaO contents of high MgO primary magmas, and Keshav et al. (2007) argued that clinopyroxene can accumulate in the mantle and evidence of its existence is found in mantle xenoliths. Consequently, the Ni-Ca relationships shown in Fig. 8 for MPLF lavas could result from initial crystallization of augite at mantle depths, close to the top of the melting column (~2.7 GPa) in the region. The distribution of the most Fo-rich olivines (Fo~92) from Mull in Fig. 8B, and the fact that they have lower Ca content but the same Ni contents as Matzen olivine compositions suggests that mantle augite accumulation is a possibility. Furthermore, olivines in Skye picrites exhibit Ni-Ca covariations that are suggestive of limited or no mantle augite accumulation (Fig. 8B). As discussed above, the sub-horizontal arrays delineated by the MPLF lavas in Fig. 8B might be a result of slower diffusion of Ca relative to Ni in olivine (Coggan et al., 2005; Chakraborty, 2010) and the Ca contents of these olivines reflect the accumulation of augite in the mantle.

An alternative explanation for the lack of early-formed augite phenocrysts in MPLF lavas relates to differences in clinopyroxene and olivine stability in primitive melts. Sugawara (2000) and Chen and Zhang (2008; 2009) provide empirical relationships between pressure, temperature and the MgO and CaO content of olivine and pyroxene saturated liquids. The Sugarawa (2000) parameterizations show that for a given melt MgO content and pressure, augite saturation occurs at ~50°C lower temperature than olivine saturation. The Chen and Zhang (2008; 2009) studies relate to the dissolution of mantle clinopyroxene (diopside $Wo_{49.5}En4_{8.5}Fs_{2.0}$) in basaltic melt. It is appreciated that extrapolating such a study to pyroxenes with compositions of around $Wo_{45}En_{41}Fs_{14}$ such as those found in mafic BPIP magmas (Hole et al. 2015a) may not be strictly valid, but these are the most applicable parameterizations in the literature. Chen and Zhang (2009) showed that saturation of Mg- and Ca-rich clinopyroxene may be determined by the three major components MgO, CaO and SiO_2. Chen and Zhang (2009) developed a relationship between $C_0^{MgO} \times C_0^{CaO}$, pressure and temperature to define clinopyroxene stability in a basaltic melt, where C_0^{MgO} C_0^{CaO} are the concentrations of MgO and CaO in a liquid at the point of saturation. Fig. 11 is a plot of CaO *versus* MgO for the MPLF whole-rock samples from which olivine data were derived plotted alongside clinopyroxene and olivine saturation curves calculated from Chen and Zhang (2008; 2009). Here it is assumed that polybaric fractional crystallization took place in two distinct phases; firstly at 1.5 GPa with Cpx joining the liquidus at ~1390°C (the Cpx-in temperature for SK982 at 1.5 GPa) and secondly at 1.0 GPa with an accompanying fall in temperature to 1365°C (~55°CGPa^{-1}; Sugawara, 2000; Matzen et al., 2017). Olivine saturation is independent of CaO content of the liquid, and over the temperature interval in question, olivine saturation is little effected. However, augite saturation occurs at considerably higher CaO content for a given MgO at 1.0 GPa compared to its saturation at 1.5 GPa. The whole-rock analyses of MPLF lavas fall close to the join the between olivine

and clinopyroxene saturation curves at 1.5 GPa. However, at 1.0 GPa the same liquid composition is saturated with respect to olivine, but not with respect to clinopyroxene. Consequently, is it possible during polybaric fractional crystallization under the range of pressure conditions applicable to the MPLF, to render clinopyroxene unstable. Consequently, the lack of observed phenocrysts of augite in MPLF lavas might result from their dissolution during magma storage and fractionation at ≤1.0 GPa.

7. Predicting pyroxenite in the source of continental flood basalts

Olivines from low SiO_2-pyroxenite-derived magmas from Mauna Loa (HSDP-2) have Ni contents of ~4000 ppm at Fo ~90 whereas high SiO_2 pyroxenite derived magmas from Koolau (Makapuu stage) have even more extreme Ni contents of up to 4660 ppm at Fo ~89 (Herzberg, 2006; 2011; Sobolev et al., 2005). Both of these Ni contents are in excess of the highest Ni Matzen olivines from Disko Island which have ~3600 ppm Ni at Fo ~91.5. Since the Matzen olivines from West Greenland represent the highest possible Ni contents attainable for olivines in the NAIP, the values of up to 3000 ppm Ni at Fo ~90 for MPLF lavas does not require a high Ni pyroxenite source. Additionally, CaO contents of low and high SiO_2 pyroxenite-dervied magmas are <2000 and <1700 ppm respectively which are lower than the most CaO-poor MPLF lavas (Figs 5 & 6).

Olivines from mafic magmas in some Karoo LIP lavas (e.g. N356 of Sobolev et al., 2007) which have whole-rock with ~6wt% CaO at ~15wt% MgO (Ellam and Cox 1989) exhibit extreme depletions in Ca (100-1400 ppm), enrichment in Ni (up to 4500 ppm at Fo 88) and have Fe/Mn 75-82. However, sample N356 comes from the Lebombo monocline and is one of a suite of high TiO_2 lavas with εNd_{190}= −4 to −10 and εHf_{190}=−3 to −11 and is likely to be a sample of Proterozoic lithosphere (Ellam and Cox, 1989; 1992; Ellam et al., 1992; Ellam, 2006) and not necessarily recycled oceanic crust in the sense of Sobolev (2005) and Herzberg (2006). Extreme depletions in CaO (~8 wt% at MgO ~9.5 wt%) in Si-oversaturated

(SiO_2 ~54 wt%) whole rock samples from part of the Karoo LIP in the Falkland Islands were also reported by Hole et al. (2015b) and these too have εNd_{190} as low as −11, although they are olivine-free. It is beyond the scope of the current study to discuss the role of pyroxenite in continental LIPs, but a picture is emerging that the continental lithosphere might also be a source of pyroxenite which contributes to CFB magmatism. Data for olivines in lavas from the Siberian Traps (Sobolev et al. 2007; 2009) have Ni contents of ~3200ppm at $Fo_{83.0}$ which would project to higher Ni contents than those of Matzen olivines (~3200ppm at $Fo_{91.8}$) calculated from PRIMELT3 solutions at the same Fo content, regardless of pressure of crystallization. These same olivine phenocrysts contain <2000 ppm Ca. Consequently, the olivines must have crystallized from partial melt of pyroxenite, and not from mantle peridotite (Sobolev et al. 2009).

Given the intricacies of interpreting the whole-rock and olivine record of fractionation of magmas in the crust, it is not surprising that the positive identification of pyroxenite involvement in magmagenesis at LIPs using major elements is highly problematical. It is quite clear that any attempts to utilize CaO content of lavas to identify pyroxenite sources will be ambiguous in their outcomes. Perhaps a step closer can be made by considering the fractionation of basaltic magmas at varying pressures without utilizing CaO abundances. Fig. 12 shows SiO_2/MgO versus Mg# for basalts from Hawaii (HSDP-2), the MPLF and Theistareykir. LLDs at 1 atm have been calculated from PRIMELT3 primary magmas using Petrolog3, including for HSDP samples, a few of which are derived from mantle peridotite (Herzberg and Gazel 2009). Because Cpx is saturated with respect to silica, when it joins the liquidus it fractionates SiO_2 and MgO relative to one another at a different rate from olivine crystallization resulting in infections on the LLD as seen in Fig. 12. Data for HSDP lavas mostly fall on the 1 atm LLD implying olivine crystallization alone is responsible for their evolution. The majority of HSDP samples have lower CaO for a given MgO than would be

expected for olivine crystallization alone and consequently the source from which they were derived must be similarly CaO deficient indicating a role for pyroxenite which is also consistent with olivine trace element data (e.g. Sobolev et al., 2005; Herzberg, 2006). By contrast, MPLF lavas show significant deviations from the 1 atm LLD as a result of crystallization of Ol+Cpx. Consequently, the CaO deficiency of these lavas need not be attributed to the involvement of pyroxenite, which the olivine trace element data also indicates. For Theistareykir, the majority of lavas follow the 1 atm LLD with some deviation at Mg# <65 towards lower SiO_2/MgO than the 1 atm LLD, which is most likely a consequence of the crystallization of Ol+Cpx. Crystallization of Ol+Cpx at ~0.8 GPa is consistent with the melt inclusion studies of Maclennan et al., (2003) as well as the olivine trace element data discussed above. So, whereas the representation of data in Fig. 12 cannot be used to identify pyroxenite in the source of LIPs, it can be used to identify lavas that have crystallized Cpx+Ol at depth, without the use of CaO data, which therefore removes some ambiguity from the interpretation of MgO and CaO data for continental flood basalts.

8. The NAIP – a peridotite-dominated LIP

It is generally accepted that many of the shield-building lavas of Hawaii are likely to have been derived from melting of a pyroxenite-rich source lithology (e.g. Herzberg 2006; 2011; Sobolev et al., 2005; 2007). This pyroxenite is thought to be derived from the recycling of oceanic crust at depth and was subsequently entrained in a mantle plume. The transformations that oceanic crust may undergo during recycling are complex and involve rock-melt, melt-melt and rock-rock interactions (e.g. Herzberg, 2011; Lambart et al., 2016; Lambart, 2017). Sobolev et al. (2005; 2007) argued that the rising mantle plume beneath Hawaii contains eclogite bodies that start melting at about 190–180km depth. Melting of eclogite produces high SiO_2 initial melts which infiltrate into, and react with, the adjacent peridotite eliminating olivine and producing a solid pyroxenite. Both the reaction pyroxenite

and unreacted peridotite melt at depths between 140 and 100 km, producing hybrid magmas by mixing in conduits and crustal magma chambers. Nevertheless, data from Mauna Kea reveal that low- and high-SiO_2 pyroxenite-sourced magmas coexist as discrete batches along with peridotite-derived magmas (Rhodes et al., 2012; Sobolev et al., 2005; 2007) leading Herzberg (2011) to promote the hypothesis that melts of pure pyroxenite may segregate from their source without mixing and be erupted at the surface as lavas.

In the case of LIPs formed above thick continental lithosphere (e.g. Siberian Traps and parts of the NAIP) the composition of magmas should be almost exclusively controlled by the melting of reaction pyroxenite because thick lithosphere restricts the amount of melt that can be derived from mantle peridotite (Sobolev et al., 2005; 2007; 2009; Hole and Millett, 2016). The model proposed by Sobolev et al. (2005; 2009) for the petrogenesis of lavas of the Siberian Traps relies on the fact that SiO_2 rich olivine-free pyroxenite (that which plots to the right of the Cpx-CaTs-Opx plane) has a lower solidus temperature at a given pressure than peridotite (Sobolev et al., 2005; Lambart et al., 2012; 2016; Lambart 2017) and consequently for a given T_P, pyroxenite will melt at a higher pressure than peridotite. On this basis, Sobolev et al. (2009) concluded that early tholeiites from the Gudchikhinsky Formation of the Siberian Traps were 100% pyroxenite melts with the contribution from pyroxenite decreasing to 40-50% (Tuklonsky and Nadezhdinsky formations) as peridotite was entrained in the melting zone. Sobolev et al. (2009) further argued that differences in the compositions of lavas from the Hawaii and Siberian LIPs was simply a function of lithospheric thickness and not the amount of recycled material present in the mantle, implying that all mantle plumes could have, and should have, a similar petrological structure.

Matzen et al. (2017) provided estimates of 100 and 32 km for the depths to the LAB beneath Disko Island and Iceland rift zones respectively. Hole and Millett (2016) showed that P_f was ~2.7 GPa for BPIP magmas and was not significantly different from that for

Disko Island, West Greenland (P*f*~2.8 GPa) suggesting a similar depth to the LAB in both areas. A pyroxenite melting signature would therefore be expected to be most evident in lavas of the MPLF and Disko Island (Fig. 13). However, it is apparent that none of the NAIP lavas under consideration here provide any evidence of melting of 100% pyroxenite, or indeed any significant proportion of pyroxenite, once the effect of high pressure fractionation on major element compositions is accounted for. In the case of Iceland, existing studies provide estimates for the overall contribution from pyroxenite which vary from <5% (Brown and Lesher, 2014) through 10% (Sobolev et al., 2007; Lambart, 2017) to 30% (Matthews et al., 2016). Lambart (2017) showed that the observed crust thickness of the Icelandic rift zones is consistent with about 10% of recycled crust in the form of a *low* SiO_2 pyroxenite lithology and that diversity of trace element and isotopic compositions observed in Icelandic rift zone basalts does not require a contribution from melts derived directly from a recycled basalt component, but results from the melting of hybrid olivine-bearing lithologies formed by solid state reactions between recycled crust and peridotite (Lambart, 2017).

Low SiO_2 olivine pyroxenites (those which plot to the left of the Cpx-CaTs-Opx plane) melt under P-T conditions that are not much different from that of peridotite but are characterized by higher melt productivity than peridotite at the same temperature and pressure (e.g. Lambart et al., 2016; Lambart, 2017). A contribution from low SiO_2 pyroxenite is therefore most likely to take the form of a hybrid lithology formed by solid state reactions (Lambart, 2017) and the resultant melt may not have an identifiable 'pyroxenite signature'. Melting experiments at 2.0 and 2.5 GPa on low SiO_2 pyroxenite SL77-582 (Keshav et al., 2004) show that large extents of melting (>70%) of pyroxenite can produce magmas with whole-rock compositions that are similar to peridotite-derived magmas, and in particular, such melts occupy the same position as some peridotite-derived melts in terms of CaO and MgO contents (Fig. 2). Lambart (2017) further showed that most of the variations in Ni

content of olivine in Icelandic lavas reported by Sobolev et al. (2007) and Shorttle and Maclennan (2011) can be explained by varying the sampling pressure of the aggregated melts in the melting column, with the compositions richest in Ni sampled at the highest pressure where the contribution of pyroxenite is the largest. However, modelling carried out during the current study does not require a pyroxenite source to explain the Ni-Ca-Fo relationships of Icelandic basalts, but merely requires fractionation of olivines at varying pressures. Nevertheless, a contribution from a pyroxenite lithology is not necessarily precluded on the basis of Ni contents of olivines in Icelandic basalts.

Fig. 13 shows the predicted CLDs for Matzen olivines with 0.365 and 0.600 wt% NiO which are in equilibrium with experimental melt #370 (Keshav et al., 2004) which itself represents 70% melt of low SiO_2 pyroxenite SL77-582 at 2.0 GPa and 1385°C. Herzberg et al. (2016) showed that olivine with 0.365 wt% NiO was characteristic of high-precision analysis of olivines having an Mg number of 89.5 that represent near solidus melts of mantle peridotite. Pyroxenite melts, and their near solidus olivines, have considerably higher NiO than melts from peridotite (e.g. Sobolev et al., 2007) and a value of 0.600 wt% NiO in near solidus pyroxenite olivine has been chosen here for illustrative purposes. The CLD for 0.365 wt% NiO intersects the data for olivine from Theistareykir which crystallized at low pressures (~0 GPa) whereas the CLD for 0.600 wt% NiO intersects the data field for pyroxenite-derived magmas from Mauna Kea recovered during the Hawaiian Scientific Drilling Programme (HSDP-2; Sobolev et al., 2007; Herzberg, 2006). In addition, the 0.600 wt% NiO CLD falls immediately below the field for olivines in lavas from Koolau (Hawaii) which were derived by melting of a high SiO_2 pyroxenite. Reverse modelling from the Matzen olivines shown in Fig. 13 to whole-rock Ni contents gives primary magma compositions which contain 463ppm and 792ppm Ni for 0.365 and 0.600 wt% NiO in olivine respectively; the former is within the estimates for near-primary high SiO_2 pyroxenite-

derived magmas given in Sobolev et al. (2005) and the latter is within the estimates for primary peridotite-derived magmas. Hybridization of melts derived from peridotite and pyroxenite must therefore fall between the 0.600 and 0.365 wt% NiO CLDs and this is indeed the region where data for all olivines from the NAIP are found. However, the Theistareykir olivines with the higher Ni for a given Fo content are also those which fractionated at ~1.0 GPa (Fig. 10) and while their relatively elevated Ni content does not *require* an input from a pyroxenite-derived melt it does not preclude it. Consequently, there is no necessity to involve a significant proportion of pyroxenite in the petrogenesis of any NAIP lavas on the basis of the trace element content of olivine.

It is interesting to speculate on the fact that more than 320 lavas from the NAIP yield PRIMELT3 solutions for melting of dry peridotite (Hole and Millett 2016), which does not include peridotite-derived magmas that crystallized at elevated pressures, compared to ~18 lavas from the Siberian Traps and ~14 lavas from Maua Loa and Mauna Kea, even though the data bases for each area are of a similar magnitude. This is probably also an indication of the dominance of peridotite-derived melt in the NAIP. Why then, if the NAIP was the site of a mantle plume that has been active from ~61 Ma until the present, do lavas show an overwhelming signature of peridotite melting? Variations in the depth to the LAB cannot provide a viable explanation which leads to the conclusion that pyroxenite was never a significant component in the source of the NAIP magmas, and where present, it had thoroughly hybridized with peridotite. If pyroxenite was not present in any significant volume, then this suggests that the NAIP did not have the same petrological structure as that envisaged for the commonly accepted mantle plume models such as those for Hawaii or the Siberian Traps. In this connection, it may be beneficial to consider alternative models for magmatism at LIPs which do not require large scale recycling of oceanic lithosphere (e.g. Foulger 2012; Anderson and Natland 2014).

9. Conclusions

Some plateau forming lavas of the BPIP have major element compositions that indicate they crystallized at <1 GPa with plagioclase joining the liquidus before clinopyroxene, the majority crystallized clinopyroxene before plagioclase feldspar over the pressure range 1.0-2.0 GPa. However, the majority crystallized olivine and clinopyroxene before plagioclase feldspar and therefore must have crystallized at >~1 GPa. Olivine within the plateau lavas have Ni and Ca contents that suggests that magmas paused at >1.6 GPa and crystallized Ol±Cpx at that depth. A few examples of near-primary magmas that underwent crystallization of olivine near the surface are found on Skye and their component olivines can be successfully modelled using the method of Matzen et al. (2017) giving a maximum Ni content for BPIP olivine as 3600 ppm. MPLF lavas which fractionated Ol+Cpx in the crust exhibit a CaO deficieny for a given MgO compared to lavas from west of Greenland and Iceland which crystallized olivine alone near the surface. Low CaO high MgO in lavas is often considered to be a characteristic sign of the involvement of pyroxenite in the source of basalts. However, olivines within MPLF lavas have Fe/Mn <70 and Ni and Ca contents that are entirely consistent with and origin solely from mantle peridotite. Therefore, apparent CaO deficiency in these lavas results from augite crystallization within the crust. The absence of augite phenocrysts in lavas may be a consequence of change from augite saturation to under-saturation with decreasing pressure, and consequent augite dissolution. The commonly accepted petrological structure of mantle plumes involving entrainment of recycled oceanic crust and significant contributions to magmatism from pyroxenite-rich sources cannot be applied to the flood basalts of the NAIP which is dominated by peridotite-derived melts.

Acknowledgements.

Prof. Claude Herzberg is thanked for a thoughtful, critical and technical review of this manuscript. John Millett is thanked for his comments on earlier drafts of the paper. Members of the NAIP workshops at Durham University provided significant background information and a context for this study.

References cited

Anderson, D.L., Natland, J.H., 2014. Mantle updrafts and mechanisms of oceanic volcanism. Proc. Nat. Acad. Sci. Am. 111, E4298-E4304.

Bailey, E.B., Clough, T.C., Wright, W.B., Richey, J.E., Wilson, G.V., 1924. The Tertiary and post-Tertiary geology of Mull, Lochaline and Oban. Mem Geol Surv UK. His Majesty's Stationery Office, Glasgow. 422pp.

Beattie, P.D., Ford, C.E., Russell, D.G., 1991. Partition coefficients for olivine-melt and orthopyroxene-melt systems. Contrib. Mineral. Petrol. 109, 212-224.

Beattie, P.D., 1994. Systematics and energetics of trace-element partitioning between olivine and silicate melts: Implications for the nature of mineral/melt partitioning. Chem. Geol. 117, 57-71.

Beattie, P.D. 1995. Olivine-melt and orthopyroxene-melt equilibria. Contrib. Mineral. Petrol. 115, 103-111.

Bell, B.R., Claydon, R.V., Rogers, G., 1994. The petrology and geochemistry of cone-sheets from the Cuillin igneous complex, Isle of Skye: Evidence for combined assimilation and fractional crystallization during lithospheric extension. J. Petrol. 35, 1055–1094.

Brown, E.L., Lesher, C.E., 2014. North Atlantic magmatism controlled by temperature, mantle composition and buoyancy. Nature Geosci. 7, 820-824.

Chakraborty, S., 2010. Diffusion coefficients in olivine, wadsleyiteand ringwoodite. In: Zhang, Y. & Cherniak, D. J. (eds) Diffusion in Minerals and Melts. Mineralogical Society of America and Geochemical Society, Reviews in Mineralogy and Geochemistry 72, 603–639.

Chen, Y., Zhang, Y., 2008. Olivine dissolution in basaltic melt. Geochim. Cosmochim. Acta 72, 4756-4777.

Chen, Y., Zhang, Y., 2009 Clinopyroxene dissolution in basaltic melt. Geochim. Cosmochim. Acta. 73, 5720-5747.

Coogan, L.A., Hain, A., Stahl, S., Chakraborty, S. 2005. Experimental determination of the diffusion coefficient for calcium in olivine between 900°C and 1500°C. Geochim. Cosmochim. Acta, 14, 3683-3694.

Coogan, L.A., Saunders, A.D., Wilson, R.N., 2014. Aluminium-in-olivine thermometry of primitive basalts: Evidence of an anomalously hot mantle source for large igneous provinces. Chem. Geol. 368, 1-10.

Danyushevsky, L.V., Plechov, P., 2011. Petrolog3: Integrated software for modeling crystallization processes. Geochem. Geophys. Geosys. 12. doi:10.1029/2011GC003516.

Danyushevsky, L.V., 2001. The effect of small amounts of H_2O on crystallization of mid-ocean ridge and back-arc basin magmas. J. Volcanol. Geotherm. Res. 110, 265-280.

Ellam, R.M., 2006. New constraints on the petrogenesis of the Nuanetsi picrite basalts from Pb and Hf isotope data. Earth. Planet. Sci Lett. 245,153-161.

Ellam, R.M., Cox, K.G., 1989. A Proterozoic lithospheric source for Karoo magmatism: evidence from the Nuanetsi picrites. Earth. Planet. Sci. Lett. 92, 207–218.

Ellam, R.M., Cox, K.G., 1991. An interpretation of Karoo picrite basalts in terms of interaction between asthenospheric magmas and the mantle lithosphere. Earth. Planet. Sci. Lett. 105, 330–342.

Ellam, R.M., Carlson, R.W., Shirey, S.B. 1992. Evidence from Re–Os isotopes for plume-lithosphere mixing in Karoo flood basalt magmatism. Nature 359, 718–721.

Font, L., Davidson, J.P., Pearson, D.G., Nowell, G.M., Jerram, D.A. Ottley, C.J. 2008. Sr and Pb Isotope Micro-analysis of Plagioclase Crystals from Skye Lavas: an Insight into Open-system Processes in a Flood Basalt Province. J. Petrol. 49, 1449-1471.

Foulger, G., 2012. Are 'hot spots' hot? J. Geodynamics 58, 1-28.

Fowler, S.J., Bohrson, W.A., Spera, F.J., 2003. Magmatic Evolution of the Skye Igneous Centre, Western Scotland: Modelling of Assimilation, Recharge and Fractional Crystallization. J. Petrol. 45, 2481-2505.

Gavrilenko, M., Herzberg, C., Vidito, C., Carr, M.J., Tenner, T., Ozerov, A., 2016. A calcium-olivine hygrometer and its aoolication to subduction zone magmatism. J. Petrol. 57, 1811-1832.

Gurenko, A.A., Geldmacher, J., Hoernle, K.S., Sobolev, A.V., 2013. A composite, isotopically-depleted peridotite and enriched pyroxenite source for Madeira magmas: Insights from olivine. Lithos 170, 224-238.

Herzberg, C., Asimow, P.D., 2008. Petrology of some oceanic island basalts: PRIMELT2.XLS software for primary magma calculation. Geochem. Geophys. Geosys. 9. Doi: 10.1029/2008GC002057 .

Herzberg, C., Asimow, P.D., 2015. PRIMELT3 MEGA.XLSM software for primary magma calculation: Peridotite primary magma MgO contents from the liquidus to the solidus. Geochem. Geophys. Geosys. 16, 563-578.

Herzberg, C., Gazel, E. 2009. Petrological evidence for secular cooling in mantle plumes. Nature 458, 619-623.

Herzberg, C., O'Hara, M.J. 2002. Plume-associated ultramafic magmas of Phanerozoic age. J. Petrol. 43, 1857-1883.

Herzberg, C. 2004. Partial Crystallization of Mid-Ocean Ridge Basalts in the Crust and Mantle. J Petrol. 45, 2389-2405 .

Herzberg, C. 2006. Petrology and thermal structure of the Hawaiian plume from Mauna Kea volcano. Nature, 444, 605-609.

Herzberg, C., 2011. Identification of source lithology in the Hawaiian and Canary Islands: implications for origins. J Petrol. 52, 113-146.

Herzberg, C., Asimow, P.D., Ionov, D.S., Vidito, C., Jackson, G., Geist, D. 2013. Nickel and helium evidence for melt above the core–mantle boundary. Nature 493, 393-398.

Herzberg, C., Vidito, C., Salter, N. 2016. Nickel–cobalt contents of olivine record origins of mantle peridotite and related rocks. Am. Min. 101, 1952-1966.

Hole, M.J., Millett, J.M. 2016. Controls of mantle potential temperature and lithospheric thickness on magmatism in the North Atlantic Igneous Province. J. Petrol. 57, 417-436.

Hole, M.J., 2015. The generation of continental flood basalts by decompression melting of internally heated mantle. Geology 43, 311-314.

Hole, M.J., Millett, J.M., Rogers, N.W., Jolley, D.W. 2015a. Rifting and mafic magmatism in the Hebridean basins. J. Geol. Soc. Lond. 172, 218-236

Hole, M.J., Ellam, R.M., Macdonald, D.I.M., Kelley, S.P. 2015b. Gondwana break-up related magmatism in the Falkland Islands. J. Geol. Soc. Lond. 173, 108-126.

Jennings, E.S., Holland, T.B.J. 2015. A simple thermodynamic model for melting of mantle peridotite in the system NCFMASOCr. J. Petrol. 56, 869-892.

Jennings, E.S., Holland, T.J.B., Shorttle, O., Mclennan, J., Gibson, S.A. 2016. The composition of melts from a heterogeneous mantle and the origin of ferropicrite: Application of a thermodynamic model. J. Petrol. 57, 2289-2310.

Kashev, S., Gautam, S., Presnall, D.C. 2007. Garnet-bearing Xenoliths from Salt Lake Crater, Oahu, Hawaii: High-Pressure Fractional Crystallization in the Oceanic Mantle. J. Petrol. 48, 1681-1724.

Kerr, A.C., 1998. Mineral chemistry of the Mull-Morvern Tertiary lava succession, western Scotland. Mineral. Mag. 6, 295-312.

Kerr, A.C., Kempton, P.D., Thompson, R.N. 1995. Crustal assimilation during turbulent magma ascent (ATA); new isotopic evidence from the Mull Tertiary lava succession, N. W. Scotland. Contrib. Mineral. Petrol. 119, 142-154.

Kerr, A.C., Kent, R.W., Thomson, B.A., Seedhouse, J.K., Donaldson, C.H. 1999. Geochemical Evolution of the Tertiary Mull Volcano, Western Scotland. J. Petrol. 40, 873-908.

Keshav, S., Gudfinnsson, G., Sen, G., Fei, S., 2004. High-pressure melting experiments on garnet clinopyroxenite and the alkalic to tholeiitic transition in ocean-island basalts. Earth. Planet. Sci. Lett. 223, 365-379.

Kress, V.C., Carmichael, I.S.E., 1988. Stoichiometry of the iron oxidation reaction in silicate melt. Am. Mineral. 73, 1267-1274.

Lambart, S. 2017. No direct contribution of recycled crust in Icelandic basalts. Geochem. Persp. Let. 4, 7-12.

Lambart, S., Laporte, D., Provost, A., Schiano, P., 2012. Fate of pyroxenite-derived melts in the peridotitic mantle: thermodynamic and experimental constraints. J. Petrol. 53,451-476.

Lambart, S., Laporte, D., Provos, A., Schiano, P. 2013. Markers of the pyroxenite contribution in the major-element compositions of oceanic basalts: Review of the experimental constraints. Lithos 160-161, 14-36.

Lambart. S., Baker, M.B., Stopler, E.M., 2016. The role of pyroxenite in basalt genesis: Melt-PX, a melting parameterization for mantle pyroxenites between 0.9 and 5GPa. J. Geophys. Res. doi: 10.1002/2015JB012762.

Larsen, L.M., Pedersen, A.K., 2000. Processes in high-Mg, high-T magmas: evidence from olivine, chromite and glass in Paleogene picrites from West Greenland. J. Petrol. 41,1071–1098.

Larsen, L.M., Pedersen, A.K., 2009. Petrology of the Paleocene picrites and flood basalts on Disko and Nuussuaq, West Greenland. J. Petrol. 50, 1667-1711.

Lawver, L.A., Muller, R.D., 1994. The Iceland hotspot track. Geology 22, 211-214.

Maclennan, J., McKenzie, D.P., Gronvold, K., Shimuzu, N., Eiler, J.M., Kitchen, N. 2003. Melt mixing and crystallization under Theistareykir, northeast Iceland. Geochem. Geophys. Geosys. 4,8624-8664 doi:10.1029/2003GC000558.

Matthews, S., Shorttle, O., Maclennan, J., 2016. The temperature of the Icelandic mantle from olivine-spinel aluminum exchange thermometry. Geochem. Geophys. Geosys. 17, 4725-4752. doi:10.1002/2016GC006497.

Matzen, A.K., Baker, M.B., Beckett, .J.R., Stolper, E.M., 2013. The temperature and pressure dependence of nickel partitioning between olivine and silicate melt. J. Petrol. 54, 2521–2545.

Matzen, A.K., Baker, M.B., Beckett, J.R., Wood, B.J., 2017. The effect of liquid composition on the partitioning of Ni between olivine and silicate melt. Contrib. Mineral. Petrol. 172. DOI 10.1007/s00410-016-1319-8.

Millett, J.M., Hole, M.J., Jolley, D.W., Schofield, N, Campbell, E., 2016. Frontier exploration and the North Atlantic Igneous Province: New insights from a 2.6 km offshore volcanic sequence in the NE Faroe–Shetland Basin. J. Geol. Soc. Lond. 173, 320-336.

O'Hara, M.J. 1968. The bearing of phase equilibria studies in synthetic and natural systems on the origin and evolution of basic and ultrabasic rocks. Earth. Sci. Rev. 4, 69-133.

Peate, D.W., Peat, I.U., Rowe, M.C., Thompson, J.M., Kerr, A.C., 2012. Petrogenesis of High-MgO lavas of the Lower Mull Plateau Lava Formation, Scotland: insights from melt inclusions. J. Petrol. 53, 1867-1886.

Putirka, K.D., 2008. Thermometers and barometers for volcanicsystems. In: Putirka, K. D. & Tepley, F. J., III (eds) Minerals, Inclusions and Volcanic Processes. Mineralogical Society of America and Geochemical Society, Reviews in Mineralogy and Petrology 69, 61–120.

Putirka, K.D., Ryerson, F.J., Perfit, M., Ridley, W.I., 2011. Mineralogy and Composition of the Oceanic Mantle. J. Petrol. 52, 279-313.

Rhodes, J.M., Huang, S., Frey, F.A., Pringle, M., Xu, G., 2012. Compositional diversity of Mauna Kea shield lavas recoveredby the Hawaii Scientific Drilling Project: Inferences on source lithology, magma supply, and the role of multiple volcanoes. Geochem. Geophys. Geosys. 13. Doi: 10.1029/2011GC003812

Scarrow, J.H., Cox, K.G., 1995. Basalts generated by decompressive adiabatic melting of a mantle plume: a case study from the Isle of Skye, NW Scotland. J. Petrol. 36, 3-22.

Sobolev, A.V., Hofmann, A.W., Kuzmin, D.V., Yaxley, G.M., Arndt, N.T., Chun,g S-L,, Danyushevsky, L.V., Elliott, T., Frey, F.A., Garcia, M.O., Gurenko, A.A., Kamenetsky, V.S., Kerr, A.C., Krivolutskaya, N.A., Matvienkov, V.V., Nikogosian, I.K., Rocholl, A., Sigurdsson, I.A., Sushchevskaya, N.M., Teklay, M., 2007. The amount of recycled crust in sources of mantle-derived melts. Science 316, 412-417.

Sobolev, A.V., Krivolutskaya, N.A., Kuzmin, D., 2009. Petrology of the parental melts and mantle sources of Siberian Trap magmatism. Petrology, 17, 253-286.

Sobolev, A.V., Hofmann, A.W., Sobolev, S.V., Nikogosian, I.K., 2005. An olivine-free mantle source of Hawaiian shield basalts. Nature 434, 590-597.

Spice, H.E., Fitton, J.G., Kirstein, L.A., 2016. Temperature fluctuation of the Iceland mantle plume through time. Geochem. Geophys. Geosys. 17, 234-254.

Starkey, A.A., Stuart, F.M., Ellam, R.M., Fitton J.G., S, Basu & Larsen L. M. 2009. Helium isotopes in early Iceland plume picrites: constraints on the composition of high $^{3}He/^{4}He$ mantle. Earth Planet. Sci. Lett. 277, 91-100.

Sugarawa, T., 2000. Empirical relationships between temperature, pressure, and MgO content in olivine and pyroxene saturated liquid. J. Geophys. Res. B4, 8457-8472.

Thompson, R.N., 1974. Primary basalts and magma genesis I: Skye, North-West Scotland. Contrib. Mineral. Petrol. 45, 317-341.

Thompson, R.N., 1982. Magmatism in the British Tertiary Volcanic Province. Scott. J. Geol. 18, 49-107.

Thompson, R.N., Morrison, M.A., Dickin, A.P., Gibson, I.L., Harmon, R.S., 1986. Two contrasting styles of interaction between basic magmas and continental crust in the British Tertiary Volcanic Province. J. Geophys. Res. 91, 5985–5997.

Thompson, R.N., Gibson, I.L., Marriner, G.F., Mattey, D.P., Morrison, M.A., 1980. Trace element evidence of multistage mantle fusion and polybaric fractional crystallisation in the Palaeocene lavas of Skye, NW Scotland. J. Petrol. 21, 265-293

Toplis, M.J., 2005. The thermodynamics of iron and magnesium partitioning between olivine and liquid: criteria for assessing and predicting equilibrium in natural and experimental systems. Contrib. Mineral. Petrol. 149, 22-39.

Villiger, S., Ulmer, P., Muntener, O., 2007. Equilibrium and fractional crystallization experiments at 0.7 Gpa; the effect of pressure on phase relations and liquid compositions of tholeiitic magmas. J. Petrol. 48, 159-184.

Villiger, S., Ulmer, P., Muntener, O., Thompson, B., 2004. The liquid line of descent of anhydrous, mantle-derived, tholeiitic liquids by fractional and equilibrium crystallization—an experimental study at 1.0 GPa. J. Petrol. 45, 2369-2388

Whitaker, M.L., Nekvasil, H., Lindsley, D.H., Difrancesco. N.J., 2007. The role of pressure in producing compositional diversity in intraplate basaltic magmas. J. Petrol. 48, 365-393.

Williamson, I.T., Bell, B.R., 2012. The Staffa Lava Formation: Graben related volcanism, associated sedimentation and landscape character during the early development of the Palaeogene Mull Lava Field, NW Scotland. Scott. J. Geol, 48, 1–46.

Figure Captions.

Fig. 1. (A) Reconstruction of the North Atlantic region at about 65Ma showing the locations referred to in the text. Pecked lines labelled A6 etc., are seafloor magnetic anomalies. Black dots numbered 55-70 are plume-head positions at the time indicated and are taken from Lawver and Müller (1994). JMFZ, Jan Mayen Fracture Zone. After Hole and Millett (2016). (B) detail of the British Pelaeocene Igneous Province showing the position of the main magmatic centres mentioned in the text and the main structural features of the region. After Hole et al. (2015a).

Fig. 2. Schematic representation of the pressure, temperature and composition (*P, T, X*) relationships for the crystallization of a typical BPIP primary magma. (a) Phase relationships calculated using Petrolog3 for the primary magma to Skye lava SK982 (Thompson, 1982; Hole & Millett, 2016). The white dots are the approximate Fo content (Mg#) of olivine that crystallizes at the Ol+Cpx+L cotectic, and the grey dots the same for the Ol+Cpx+Pl+L cotectic. % figures on the arrows are the approximate % of olivine that can crystallize on the Ol+L liquidus at a given pressure before reaching the Ol+Cpx+L cotectic. The olivine saturation curve was calculated using the method of Sugarawa (2000) with the final pressure of melting (P*f*) from PRIMELT3 solutions (Hole & Millett, 2016) acting as a proxy for the pressure of melt segregation.

Fig. 3 (A) CaO (wt%) *versus* Mg# and b) CaO (wt%) *versus* MgO (wt%) for and Mull Plateau Lava Formation (MPLF) lavas (grey dots), Central Mull Formation (CMF; triangles) and Baffin Island lavas (white dots). The Baffin Island and CMF data shown yield PRIMELT3 solutions for melting of dry peridotite. Liquid lines of descent (LLD) were generated using Petrolog3 (Danyushevsky & Plechov, 2011) using the QFM buffer of Kress & Carmichael (1988) and the plagioclase and clinopyroxene melt liquidus associations of Danyuchevsky (2001). Black diamonds; Cpx-in at the pressure indicated; grey diamonds, Plag-in. The LLD shown is for the PRIMELT3 solution for Syke lava SK982 (Thompson, 1982) which has the following characteristics; Fe^{2+}/Fe_T=0.905 (Fe_2O_3/TiO_2=1.0); T_P=1500°C; MgO=17.4 wt%; P*i*=3.5 GPa; P*f*=2.9 GPa; F-AFM=0.17 (Hole & Millett, 2016). In a) note that for pressures <0.6 GPa the crystallization order is Ol+L → Ol+Pl+L → Ol+Pl+Cpx+L whereas for pressures >0.6 GPa the order is Ol+L → Ol+Cpx+L → Ol+Cpx+Pl+L. In (B) the dividing lines between pyroxenite- and peridotite-derived magmas and the range of possible peridotite-derived primary magmas (fine pecked lines) are taken from Herzberg & Asimow (2008). The black dots in each diagram are the samples for which high-precision olivine trace element data is available (Sobolev *et al.* 2007).

Fig. 4. (A) $K_D^{Ol/L}{}_{(FeO/MgO)}$ *versus* pressure for three BPIP model primary magmas calculated using Petrolog3 for the thermodynamical model of Toplis (2005). MgO contents of the model primary magmas were derived from PRIMELT3 the final pressure of melting (P*f*) being used as a proxy for the pressure of melt segregation PRIMELT3 solutions for S006 (16.0 wt% MgO) and SK982 (17.5 wt% MgO) are given in Hole & Millett (2016) and for MU1.1 (20.0 wt% MgO) in the electronic appendix. (B) variation in $K_D^{Ol/L}{}_{(FeO/MgO)}$ and Mg/Fe_{Liq} (cationic Mg/Fe of the liquid) during crystallization of the model primary magma to SK982 for the Toplis (2005) model at fixed pressures from 0.0 to 2.0 GPa (solid lines). Also shown is the parameterization of Herzberg & O'Hara (2002) SK982 which assumes magma ascent and crystallization along the olivine liquidus from the pressure of melt segregation to the surface. The grey diamonds represent the intersections of the Toplis (2005) contours for a fixed pressure with the Herzberg & O'Hara (2002) ascent path – see text for details. The pecked line is the approximate position of Cpx-in, with the vertical shading on the Ol+Cpx+L side of the cotectic.

Fig. 5 (A) Calculated Fo and Ca content for crystal lines of descent (CLD) for equilibrium olivines crystallizing from two BPIP model primary magmas (SK982 and MU1.1) at 1atm pressure for the models given in equations (8)-(11) in the text. Crystallization models were calculated using Petrolog3 with the following parameters; QFM Buffer of Kress and Carmichael (1988); plagioclase and clinopyroxene equilibria of Danyushevsky (2001). Crosses are at 1% crystallization intervals. The composition of 49 olivines in equilibrium with model BPIP primary magmas (Hole and Millett 2016) are also shown for each calculation method. (B) CLDs for the model primary magma to SK982 at variable pressures for; grey lines, Herzberg and O'Hara (2002); black lines, Gevrilenko et al. (2016) calculation methods (equations (9)-(11) in the text). Pressure in GPa is indicated for each CLD. Grey squares, points at which clinopyroxene joins the crystallizing assemblage for each pressure. SQFZ, Siqueiros Fracture Zone MORB measured olivine compositions (filled triangles) from Gavrilenko et al. (2016) and compositions calculated (open triangles) using the Gavrilenko et al. (2016) model. Vectors relating to various petrological parameters are from Gavrilenko et al. (2016). The line with dot terminations is the approximate uncertainty in Ca content propagated from equation (10) in the text.

Fig. 6. (A) & (B) Ni content (ppm) *versus* Fo content for olivines in MPLF lavas. The CLDs shown were calculated for the primary magma to SK982 and are for; (i) the Beattie *et al.* (1991) model at 1 atm (short dashes line); (ii) the Herzberg & O'Hara (2002) model for crystallization and ascent along the olivine liquidus (long dashes) and (iii) the Herzberg & O'Hara (2002) model until 1.6 GPa and then at a fixed pressure of 1.6 GPa (solid back line). For model (iii) $K_D^{Ol/L}{}_{(FeO/MgO)}$ values were calculated from Mg/Fe_{Liq} as shown in Fig. 2(A), propagating to give $D^{Ol/L}{}_{NiO}$ from equation (3) in the text. The large white diamond represents the Fo content for

Cpx-in, and at this pojnt $D^{Cpx/L}_{NiO}$ was assumed to be 0.25 $D^{Ol/L}_{NiO}$. Grey curves are mixing lines between the primary magma composition and derivative magmas along the CLD (see also Herzberg *et al.,* 2016) with the approximate MgO content of the derivative magma indicated. It was assumed that mixing was complete and that neither liquid contained phenocrysts at the time of mixing. 'Matzen olivines' are model olivine compositions for BPIP primary magmas segregating at P*f*, undergoing rapid emplacement at the surface without crystallizing any olivine, and then crystallizing olivine at 1 atm (equation (7) in the text. The cross-hatched field in (a) is for olivines from Siqueiros Fracture Zone MORB (Sobolev et al. 2007; Gavrilenko et al. 2016) and is shown for comparison. In (b) Skye and Mull olivines are near-primary olivines in picrites (Spice *et al.*, 2016). These include sample MU1.1 for which a Toplis model is shown in Fig. 2.

Fig. 7. (A) and (B) Ca content (ppm) *versus* Fo content for olivines for the same MPLF lavas as in Fig. 6. The cross-hatched area delimits the range of Ca and Fo contents of olivines for 49 forward crystallization models of BPIP primary magmas at 1 atm using the Beattie *et al.* (1991) parameterization for $D^{Ol/L}_{CaO}$ given in equation (4) in the text. The stippled field uses the same primary magma data but for the Gavrilenko et al. (2016) method of calculating $D^{Ol/L}_{CaO}$ given in equations (10) and (11) in the text. Grey squares are the composition at which clinopyroxene joins the crystallizing assemblage. The field labelled SQFZ encompasses measured olivine compositions for Siqueiros Fracture Zone MORB from Gavrilenko et al. (2016)

Fig. 8. (A) calculated CLDs for Ca and Ni content of olivines at variable pressures using the Ni and Ca model of Herzberg and O'Hara (2002) and the Ca model of Gavrilenko et al. (2016). The Ni model has been modified for appropriate final pressure of equilibration as discussed in the text and shown in Fig. 3. The black lines with arrows are for the Herzberg and O'Hara (2002) Ca model at the pressures in indicted in GPa. Fine lines with various ornaments are for the Ni model of Herzberg and O'Hara (2002) with Ca calculated according to the Gavrilenko et al. (2016) model, and the thick grey line if for 1 atm pressure, which is the same as the olivine. Grey squares are the compositions at which clinopyroxene joins the crystallizing assemblage for a given pressure and the white squares the same for plagioclase feldspar. The curved inflections giving negative 'spikes' for pressures >1.2 GPa result from clinopyroxene joining the liquidus before 11 wt% MgO, the MgO content at which the calculation $D^{CaO}_{OL/L}$ changes from equations (10) to (11) in the text. Matzen olivines are for olivine in equilibrium with 49 BPIP model primary magmas. The double-headed arrow illustrates the effect of crystallization of ~15% olivine at 1 atm. (B) and (C) Ni and Ca contents of MPLF olivines. The cross hatched area represents the range of compositions for forward crystallization of BPIP model primary magmas at 1 atm and therefore represents the olivine liquidus. The thick grey line is the CLD for

sample SK982 at 1 atm, and the lines labelled 'Beattie' and 'H&O' are 1atm CLDs for the Beattie et al. (1991) and Herzberg and O'Hara (2002) calculation methods.

Fig. 9. Fe/Mn (ppm) *versus* Fo content for olivine in BPIP, Baffin Island and West Greenland (Disko Island) lavas. The fields for primary olivines derived from melts of mantle peridotite are labelled with their source mineralogy i.e. harzburgite or lherzolite. The two pecked horizontal lines (Fe/Mn 60 and 70) are the upper and lower boundaries respectively for olivines that crystallize from peridotite-derived magmas. After Herzberg (2011).

Fig. 10. covariations between Ni and Ca content of lavas from (A) Theistareykir, Iceland, (B) Baffin Island and (C) Disko Island, west Greenland. Stippled areas are the range of predicted Ni and Ca contents for the crystallization of model primary magmas (Hole and Millett 2016) at 1 atm from each location. The grey line on each diagram is the calculated Ol+L CLD at 1 atm for a model primary magma from each location. Model primary magmas are as follows; Disko Island, #410188 (Larsen and Pedersen 2000); Baffin Is, BI/CS/14 (Starkey et al. 2009); Theistareykir, #9302 (Maclennan et al. 2003). In (c) grey symbols are olivines considered by Herzberg et al. (2016) to be near primary, and open circles are olivines considered by Herzberg et al. (2016) to be the result of crystallization from mixed magmas. The Ni content of Matzen olivines were calculated from PRIMELT3 solutions using equation (7) and the Ca content using equation (10). The cross-hatched area is the field for olivine data from MPLF sample BHL15 for comparison with Fig. 7. Data are from Sobolev *et al.* (2007) and Herzberg *et al.* (2016).

Fig. 11 Olivine (vertical lines) and clinopyroxene (curves) saturation calculated using the method of Chen & Zhang (2008; 2009). To the left of the curves, liquids are undersaturated with rescpect to olivine or clinopyroxene. At 1.5 GPa, the temperature estimate of 1390°C is the temperature estimate immediately prior to the Cpx-in temperature from a Petrolog3 forward crystallization model for the primary magma to lava SK982. The temperature at 1.0 GPa assumes a 55°CGPa^{-1} gradient on the olivine liquidus (Sugawara 2000; Matzen et al. 2017). Black dots are the whole-rock compositions of the MPLF lavas for which olivine data are available. The shaded area is the region of instability of Cpx in the melt caused by decompression.

Fig. 12. SiO_2/MgO versus Mg# for (A) Hawaii Scientific Drilling Project lavas, (B) MPLF lavas and (C) lavas from Theistareykir. For each sample set forward crystallization models have been generated at varying pressures from 0.0 to 1.8 GPa using Petrolog3, and starting with PRIMELT3 primary magma compositions. The shaded area on each diagram is the field for

Ol+Cpx+L. The insets are CaO *versus* MgO for the same lavas, the black line indicating the dividing line between peridotite- (above the line) and pyroxenite-derived magmas taken from Herzberg & Asimow (2008). The CaO-MgO relationships for MPLF lavas are shown in Fig. 2. Note the extended scale in (C).

Fig. 13. Ni (ppm) *versus* %Fo in olivine for basalts from Theistareykir, and pyroxenite-derived lavas recovered during the Hawaii Scientific Drilling Project (HSDP-2) and from Koolau (shield stage). Only olivine with Fo>86 are given in Sobolev et al. (2007) for HSDP-2. The open diamond is the composition of Matzen olivine, assuming an NiO content 0.365 wt%, in equilibrium with experimentally generated melt #370 of Keshav et al. (2004) which represents 70% melt of pyroxenite SL77-582. The whole-rock content of this magma would be ~460 ppm Ni which is within the range for natural olivine in peridotite-derived magmas. Black diamond is the composition of Matzen olivine, assuming and NiO content of 0.600 wt%, in equilibrium with melt #370. In this case the whole-rock composition would be 792 ppm Ni which is within the range of parental melts to Hawaiian pyroxenite-derived magmas (Sobolev et al., 2005). The pecked lines represent the CLD at 1 atm from the Matzen olivine indicated.

Abstract Continental flood basalts undergo crystallization at a variety of pressures in the crust and sometimes even in the mantle. Polybaric fractionation, when magmas may pause and undergo crystallization at different pressures, results in complex fractionation of major elements. Crystallization at high pressures where clinopyroxene is an early crystallizing phase can result in erupted compositions that have major element characteristics which mimic those expected for melts derived from pyroxenite-rich sources. The trace element compositions of early-crystallizing olivine can add further detail to crystallization histories and potentially allow an examination of the crystallization of basalts from melt segregation to the surface. The North Atlantic Igneous Province (NAIP) comprises sub-regions which had diverse crystallization histories. Plateau basalts of the British Palaeogene Igneous Province (BPIP) were generated by partial melting of mantle peridotite starting at ~3.8 GPa with melting ceasing by ~2.7 GPa. Major elements indicate that some basalts crystallized at <1 GPa with plagioclase joining the liquidus before clinopyroxene. However, the majority of BPIP magmas crystallized clinopyroxene before plagioclase feldspar over the pressure range 1.0-2.0 GPa. Trace elements in olivine indicate crystallization of olivine + clinopyroxene over the pressure interval 1.6-2.0 GPa. However, olivine data also show that some near-primary magmas reached near-surface pressures without substantial modification by fractional crystallization. Olivines formed at ≥1.6 GPa have Ni and Ca contents that are consistent with an origin by partial melting of mantle peridotite with no role for pyroxenite being detected. This contrasts with the low pressure dominated crystallization histories exhibited by lavas from West Greenland and Iceland. Whole-rock data for many BPIP lavas exhibit CaO depletion at a given MgO content compared with those from West Greenland and Iceland, which might be cited as an indicator of pyroxenite in their source, but this is solely a consequence of augite fractionation at depth. An absence of augite phenocrysts in lavas may have resulted either from augite crystallization in the mantle or from a change

from augite saturation to under-saturation with decreasing pressure, and consequent augite dissolution. The lack of any significant contribution from recycled oceanic crust to magmatism in the NAIP suggests that the petrological structure of the mantle source from which NAIP lavas were derived does not conform with the generally accepted models for mantle plumes such as those responsible for magmatism in Hawaii and the Siberian Traps.

Mineralogical and geochemical evidence for polybaric fractional crystallization of continental flood basalts and implications for identification of peridotite and pyroxenite source lithologies.

M.J. Hole[a]

a. Department of Geology & Petroleum Geology, University of Aberdeen, Aberdeen AB243UE, UK.

Abstract Continental flood basalts undergo crystallization at a variety of pressures in the crust and sometimes even in the mantle. Polybaric fractionation, when magmas may pause and undergo crystallization at different pressures, results in complex fractionation of major elements. Crystallization at high pressures where clinopyroxene is an early crystallizing phase can result in erupted compositions that have major element characteristics which mimic those expected for melts derived from pyroxenite-rich sources. The trace element compositions of early-crystallizing olivine can add further detail to crystallization histories and potentially allow an examination of the crystallization of basalts from melt segregation to the surface. The North Atlantic Igneous Province (NAIP) comprises sub-regions which had diverse crystallization histories. Plateau basalts of the British Palaeogene Igneous Province (BPIP) were generated by partial melting of mantle peridotite starting at ~3.8 GPa with melting ceasing by ~2.7 GPa. Major elements indicate that some basalts crystallized at <1 GPa with plagioclase joining the liquidus before clinopyroxene. However, the majority of BPIP magmas crystallized clinopyroxene before plagioclase feldspar over the pressure range 1.0-2.0 GPa. Trace elements in olivine indicate crystallization of olivine + clinopyroxene over the pressure interval 1.6-2.0 GPa. However, olivine data also show that some near-primary magmas reached near-surface pressures without substantial modification by fractional crystallization. Olivines formed at ≥1.6 GPa have Ni and Ca contents that are consistent with an origin by partial melting of mantle peridotite with no role for pyroxenite being detected. This contrasts with the low pressure dominated crystallization histories

exhibited by lavas from West Greenland and Iceland. Whole-rock data for many BPIP lavas exhibit CaO depletion at a given MgO content compared with those from West Greenland and Iceland, which might be cited as an indicator of pyroxenite in their source, but this is solely a consequence of augite fractionation at depth. An absence of augite phenocrysts in lavas may have resulted either from augite crystallization in the mantle or from a change from augite saturation to under-saturation with decreasing pressure, and consequent augite dissolution. The lack of any significant contribution from recycled oceanic crust to magmatism in the NAIP suggests that the petrological structure of the mantle source from which NAIP lavas were derived does not conform with the generally accepted models for mantle plumes such as those responsible for magmatism in Hawaii and the Siberian Traps.

1. Introduction

Continental flood basalts (CFB) must traverse continental lithosphere before eruption at the surface. For the North Atlantic Igneous Province (NAIP; Fig. 1), where the mantle was anomalously hot (T_P ~1450-1550°C; Herzberg and Gazel, 2009; Hole and Millett, 2016; Matthews et al. 2016) melting of mantle peridotite was initiated at ~3.7-4.5 GPa (Hole and Millett, 2016; Hole, 2015) and melting ceased when magmas rising by adiabatic ascent along the olivine liquidus reached the asthenosphere-lithosphere boundary (LAB), which is also the final pressure of melting (P*f*). The depth to the LAB varies throughout the province from ~100 km beneath Disko Island (west of Greenland) to ~60 km beneath Baffin Island (Hole and Millett, 2016; Matzen et al., 2017). During ascent from the initial melting pressure (P*i*) to the LAB, it is generally accepted that magmas crystallize olivine alone (e.g. Herzberg and Asimow, 2008; 2015; Putirka 2008; 2011). However, Herzberg and Asimow (2008) state that augite fractionation can occur in the mantle, an assertation that is corroborated by the existence of clinopyroxene-bearing xenoliths in Hawaiian lavas that are consistent with crystallization from a tholeiitic liquid at 110-150 km depth (Keshav et al., 2007). Magmas

may pause at the LAB or within the lithosphere prior to eruption, and in the British Palaeogene Igneous Province (BPIP), which is a sub-province of the NAIP, there is a large body of evidence that suggests that magmas paused at the Moho at about 30km depth, or equivalent to ~0.9±0.15 GPa (Thompson, 1974; 1982; Hole et al., 2015a; Millett et al., 2016). Individual batches of magma may have undergone polybaric fractionation. Thompson (1974; 1982) on the basis of melting experiments, as well as major, trace element and isotopic compositions of lavas, proposed that some mafic BPIP lavas underwent fractionation at 1.6-1.7 GPa as well as at ~0.9 GPa. Conversely, at Disko Island, very primitive and near primary magmas were erupted through ~100km of lithosphere and seem not to have paused to fractionate to any great extent in the crust (Larsen and Pedersen, 2000; 2009; Hole and Millett, 2016; Matzen et al., 2017).

O'Hara (1968) showed that with increasing pressure of crystallization, the liquidus fields of olivine and clinopyroxene contracted and that the field for clinopyoxene crystallization expanded at the expense of olivine. Experimental phase equilibria (e.g. Villiger et al., 2004; 2007; Whitaker et al., 2007) show that for fractional crystallization of peridotite-derived magmas at ~1 GPa, clinopyroxene (Cpx) crystallizes in compositions with Mg# (molecular % $MgO/MgO+FeO+Fe_2O_3$) ≤65 whereas the same magma crystallizing at 1 atm would have olivine as the sole liquidus phase at Mg# 65. With increasing pressure of fractionation, Cpx becomes a liquidus phase at progressively higher Mg# (Fig. 2) which results in an expansion of the Cpx stability field at the expense of olivine as noted by O'Hara (1968). For a typical BPIP primary magma generated by volatile-free melting of mantle peridotite (see Hole and Millett, 2016 for a compilation of primary magma compositions) at 1 atm, ~25% olivine crystallization would be expected before plagioclase joins the liquidus, whereas at 1.6 GPa, only about 10% crystallization of olivine alone would occur in the same magma before Cpx joins olivine on the liquidus (Fig. 2). This also means that the minimum

Mg# (or Fo content) of olivine when it is the sole liquidus phase also increases with increasing pressure (Fig. 2). Derivative liquids formed by Ol+Cpx fractionation at ~1 GPa, which may ultimately erupt at the surface as lavas, will also have a lower CaO content for a given MgO content than lavas that crystallize olivine alone because Cpx is a CaO-rich phase and strongly fractionates MgO from CaO (Fig. 3A).

It is generally accepted that the source lithology for CFB and their oceanic equivalents is not exclusively mantle peridotite, and that magmas derived from partial melting of pyroxenite are an important component of CFB magmatism (e.g Herzberg, 2011). The pyroxenite source components in LIPs is generally considered to have been derived from oceanic crust recycled to lower mantle depths as a result of subduction tectonics (Herzberg, 2011; Sobolev et al., 2007). In the broadest terms, two distinct lithologies of pyroxenite can be recognized on the basis of SiO_2 content. Primary or very primitive melts derived from high SiO_2 pyroxenite (silica+pyroxene) are recognized because they plot on the SiO_2-rich side of the orthopyroxene-calcium Tschermaks component (Opx−Cpx−CaTs) join in the molecular projection of the system olivine−Opx−CaTs−silica (Ol−Opx−CaTs−SiO_2; Herzberg, 2011). Conversely, melts derived from low SiO_2 pyroxenite (olivine+pyroxene) plot to the SiO_2-poor side of the same plane. Since the Opx−Cpx−CaTs join is a thermal divide at pressures associated with mantle melting i.e. 3-7 GPa, derivative magmas from the melting of high and low SiO_2 pyroxenite have divergent fractionation histories. At near melting pressures, low SiO_2 pyroxenite may undergo mixing with melts of mantle peridotite to form hybrid magmas, whereas melt derived from high SiO_2 pyroxenite cannot (Herzberg, 2011)

Distinguishing between pyroxenite- and peridotite-derived magmas in the lavas erupted at LIPs using major or trace major element geochemical data is fraught with problems. A commonly used indicator of the involvement of pyroxenite-derived melt in basalt

petrogenesis is that pyroxenite-derived magmas tend to be too deficient in CaO at a given MgO content to be derived from melting of volatile-free mantle peridotite (Herzberg and Asimow, 2008). However, fractionation of CaO relative to MgO is sensitive to the bulk mineral/melt partition coefficient for CaO (*D*CaO) in a magma, and some pyroxenites appear to have *D*CaO > 1 and others < 1 regardless of the initial concentration of CaO in the solid pyroxenite (e.g. Herzberg, 2011; Jennings and Holland 2015; Jennings et al., 2016). Residual clinopyroxene during melting of pyroxenite is likely to result in the generation of CaO deficient derivative lavas and therefore depends on the extent of melting at which clinopyroxene is partially consumed (Lambart et al., 2016). A significant difficulty is using CaO and MgO contents of mafic lavas to identify pyroxenite involvement is that lavas derived from CaO-poor pyroxenite will fall in the same region of an MgO-CaO diagram as peridotite-derived melts that have fractionated Ol+Cpx at crustal pressures (Herzberg and Asimow, 2008; Fig. 3A). Another effect of crystallization of peridotite-derived magmas at the Ol+Cpx+L cotectic is to drive liquids to progressively more SiO_2-undersaturation with decreasing Mg#. Consequently, crystallization of a peridotite-derived melt at ~1.0 GPa can result in a CaO depleted, Si-undersaturated liquid composition that is indistinguishable from a magma derived from the melting of low SiO_2 pyroxenite such as those found at the Canary Islands and Madeira (Herzberg, 2011; Gurenko et al., 2013). Furthermore, recycled pyroxenite is also known to be far more heterogeneous than mantle peridotite, both chemically and mineralogically, and produces a diverse range of derivative magmas that may be very similar to peridotite-derived magmas (Keshav et al., 2004; Herzberg, 2011; Lambart et al., 2012; 2013; 2016;). For most high SiO_2 pyroxenite-derived magmas, covariations between SiO_2 and CaO provide a reasonable discriminant from peridotite-derived magmas, because most high Mg#, high SiO_2 lavas derived from mantle peridotite are silica saturated or silica oversaturated olivine or quartz tholeiites, and they owe their high SiO_2 contents to

olivine fractionation at near-surface pressures; as a consequence, any deficiency in CaO at a given MgO content is most likely attributable to high SiO_2 pyroxenite.

Olivine phenocrysts in mafic lavas provide a mineralogical narrative about magmatic processes in Earth's crust and mantle and olivine records in its chemistry the widespread occurrence of magma chamber fractional crystallization, recharge, and mixing (Herzberg and O'Hara, 2002; Herzberg, 2011; Herzberg et al., 2016; Sobolev et al., 2007). Olivine contains readily measurable concentrations of trace elements Ni, Ca and Mn and the partitioning of these element between olivine and coexisting melt is well-understood (e.g. Beattie et al. 1991; Beattie, 1994; 1995; Herzberg and O'Hara, 2002; Matzen et al., 2013; 2017). Fractional crystallization can never be perfect in natural systems and so olivine in mafic lavas may be able to record episodes of fractionation that are not evident from whole-rock data, particularly in magmatic provinces such as the BPIP where polybaric fractionation is most likely to have occurred. Olivine also records the melting of recycled crust as a distinct pyroxenite lithology. In the case of Hawaii, many of the shield-forming lavas (e.g. Mauna Kea) have Ni contents that are too high, and Ca contents that are too low, to have been derived by partial melting of mantle peridotite and they are more likely to be derived from a pyroxenite-rich source (Sobolev et al., 2005; Herzberg, 2006; 2011).

Before an understanding of the possible source lithology for MPLF lavas can be made, it is clearly necessary to firstly constrain the fractionation histories of the magmas to enable an assessment of the role of Cpx fractionation in causing CaO depletion in basic. Only if this is understood can the contribution of low CaO pyroxenite to the source of the basalts be assessed. To this end, a combination of whole-rock and component olivine chemistry has been utilized to examine the fractionation history of some continental flood basalts from the British Palaeogene Igneous Province (BPIP) which is part of the wider North Atlantic Igneous Province (NAIP).

2. Magmatism in the BPIP

The BPIP is a sub-province of the large NAIP. Magmatism in the BPIP began at ~60 Ma and continued until ~58 Ma. The majority of the lavas of the BPIP are mildly alkaline slightly *Ne*-normative alkali olivine basalts and *Hy*-normative olivine tholeiites. The Mull Plateau Lava Formation (MPLF; Williamson and Bell, 2012) is made of a sequence of ~1 km thickness of plateau-forming lavas dominated by picrites and basalts with local occurrences of hawaiite, mugearite and trachyte (Kerr 1998; Kerr et al. 1995; 1999). The MPLF is overlain locally by the Central Mull Formation (CMF; Williamson and Bell, 2012) which comprises olivine tholeiite lavas and associated hypabyssal intrusions. The Skye Main Lava Series (SMLS; Thompson, 1982) is petrologically very similar to the MPLF although it is probably slightly older.

A number of the mafic (>8 wt% MgO) CMF tholeiites which equilibrated at ~1 atm, reached their erupted compositions by crystallization of olivine alone. For 49 of these lavas and intrusions Hole & Millett (2016) generated model primary magma compositions using PRIMELT3 (Herzberg and Asimow, 2008; 2015). Primitive parental melts to CMT erupted compositions required a mantle potential temperature (T_P) ~1500°C and MgO ~17.5 wt%. The initial pressure of melting (P*i*) was ~3.6 GPa with melting stopping by ~2.7 GPa giving a melt fraction for accumulated fractional melting (F-AFM) of ~0.16. Spice et al. (2016) applied the aluminium-spinel-olivine thermometer of Coogan et al. (2014) to Skye and Mull picrites (Mg# 78-85) which yielded crystallization temperatures of 1410°C and 1380°C relative to MORB primitive magmas, which are in excellent agreement with olivine-liquid crystallization temperatures for MPLF lavas given by Hole et al. (2015a). Four of the whole-rock samples of Spice et al. (2016) also provide PRIMELT3 solutions (Appendix 1) indicating T_P in the range 1524-1568°C and with P*f* of 3.4-3.6 GPa. However, MPLF lavas do not yield PRIMELT3 solutions, although olivine-hosted melt inclusions do provide model

primary magmas which indicate T_P~1480°C (Hole and Millett, 2016). The reason why MPLF lavas do not allow the generation of model primary magmas is because they are too deficient in CaO at a given MgO content to have been derived by olivine fractionation alone from mantle peridotite (Fig. 2). As has already been noted, such CaO deficiency can be caused augite fractionation or can be a characteristic of the source region for pyroxenite-derived magmas.

2.1 Estimates of equilibration pressure of BPIP plateau lavas from major element chemistry.

Based on experimentally determined phase relationships for SMLS lavas containing 11.1 wt% MgO, Thompson (1974; 1982) proposed that most Mg-rich picrites of the SMLS and MPLF reached their erupted compositions at pressures up to about 1.7 GPa, and that the remaining basic magmas of the BPIP have compositions related to cotectic equilibria at approximately 0.9±0.15 GPa, which is near the base of the crust beneath the Province (Thompson 1982). The melting experiments of Thompson (1974) showed that the general sequence of phase relationships with decreasing T and MgO at ~1.0 GPa is Ol+liquid (L); Ol+Cpx+L; Ol+Cpx+Pl+L; whereas at 1 atm, plagioclase is a liquidus phase before clinopyroxene. With increasing pressure, the stability field for clinopyroxene expands at the expense of olivine, and at ~1.7 GPa olivine is replaced by clinopyroxene as first crystallizing phase in the system for compositions with >11 wt% MgO. However, augite in typical Plateau-type basalts occurs as groundmass poikilitic anhedra and never forms phenocrysts (Thompson, 1982) and the dominant phenocryst phase in mafic plateau lavas is olivine.

Fig. 3 illustrates the relationships between CaO, MgO and Mg# for MPLF lavas with ≥8 wt% MgO. The liquid lines of descent (LLD) for a model primary magma at varying pressures from 1 atm to 2.0 GPa is also shown. The primary magma composition chosen for the forward model was the PRIMELT3 solution to Skye lava SK982, which is representative of a typical peridotite-derived magma in this region (Hole and Millett, 2016). Additionally,

SK982 has εNd_{58} = +8.9 and $^{206}Pb/^{204}Pb$=17.5 which means that it is largely unmodified by interaction with the continental crust (Thompson et al., 1986; Hole et al., 2015a). Forward models of fractional crystallization have been generated using Petrolg3 (Danyushevsky and Plechov 2011) using the parameters given in the caption to Fig 2. Forward modelling of all 49 BPIP model primary magmas shows that the relationship between T, MgO, Mg# and the pressure at which clinopyoxene appears on the liquidus is given by the approximations;

$$Mg\# = -0.554P^2 + 9.81P + 55.9 \quad (1)$$

$$T = 6.277P^2 + 141.9P + 1154.4 \quad (2)$$

For MgO the uncertainty is ±0.6% and for Mg# ±2.0. Thus, for a BPIP magma crystallizing at 1.0 GPa, clinopyroxene would join olivine on the liquidus at MgO = 10.6±0.6 wt% or Mg# = 65.2±2.0.

Inspection of Fig. 3B reveals the situation where CaO decreases with decreasing Mg# for the assemblage Ol+Cpx+L and thereafter, CaO may increase or decrease with Mg#, depending on pressure, for the assemblage Ol+Cpx+Pl+L. However, the overall variation in CaO once clinopyroxene joins the crystallizing assemblage is not great. Thus, for the SK982 primary magma crystallizing at 1.0 GPa, CaO decreases from ~12.6 to 12.1 wt% for a change in Mg# of 61-65 and then remains nearly constant (CaO=11.7-12.0 wt%) along the Ol+Cpx+Pl+L cotectic. This feature of Mg#-CaO covariations will be returned to later in the discussion regarding olivine chemistry. It is also noticeable from Fig. 3 that data for the majority of MPLF plateau lavas plots to the left and below the 1 atm Ol+L LLD and close to the Ol+Cpx cotectics for various pressures. Data for CMF and Baffin Island lavas, all of which yield PRIMELT3 solutions, plot close to the predicted olivine liquidus. Since PRIMELT3 only provides solutions for the melting of mantle peridotite for erupted compositions that have crystallized only olivine, then data for such lavas must plot on or above the Ol+L LLD, as they do in Fig. 3. It is logical to assume, therefore, that the reason

for the MPLF lavas yielding few PRIMELT3 solutions is that they underwent augite fractionation at ≥1.0 GPa, as proposed by Thompson (1974; 1982).

Herzberg (2004) provided a method of estimating pressure of equilibration of MORB tholeiitic basalts using a molecular projection in the system Anorthite-Diopside-Enstatite. However, this method has an inherent uncertainty of ±0.28 GPa for olivine tholeiites, can only be applied to liquids that fall along the Ol+Pl+Cpx+L cotectic, and is calibrated only up to ~1.0 GPa. It has already been shown that for BPIP lavas, the initiation of clinopyroxene crystallization is pressure and composition dependent. Consideration of Fig. 3B shows that the predicted plagioclase-in position has a curvilinear relationship with Mg#. The equation for this curve for the forward models of SK982 is;

$$CaO = 0.0658[Mg\#]^2 - 6.99[Mg\#] + 194.8 \quad (3)$$

Data for most Central Mull Formation lavas which are predicted to have been simultaneously saturated in olivine + plagioclase + augite fall above the 0.8 GPa crystallization trajectory in Fig. 3A. Application of the Herzberg (2004) method for estimating P_{eq} gives values in the range 0.0-1.0 GPa which are in good agreement with the estimates from Fig. 3B. Most CMF lavas also yield PRIMELT3 solutions for melting of dry peridotite (Hole and Millet, 2016) and therefore have CaO contents at a given MgO content that are consistent with their derivation from mantle peridotite. Bell et al. (1994) presented extensive mineral chemical and geochemical evidence for near 1 atm fractionation of the Skye cone sheets and data for these intrusions and these plot close to the 1 atm Ol+Pl+Cpx+L cotectic in Fig. 3B. There is, therefore, ample evidence of fractionation of MPLF and SMLS lavas in the range 1atm to >1 GPa, which is consistent with the results from the melting experiments of Thompson (1974) and other published estimates (e.g. Scarrow and Cox, 1995; Kerr et al., 1999; Hole et al., 2015a). However, many MPLF lavas plot in positions in Fig. 3 that suggest they underwent crystallization of Ol+Cpx at pressures up to 2.0 GPa.

Interaction between mafic lavas and sialic crust is an integral part of the fractionation history of BPIP magmas. Kerr et al. (1995) provided isotopic evidence for crustal assimilation during turbulent magma ascent for MPLF lavas and there is strong evidence to support the interaction between at least two discrete compositions of sialic crust and mantle derived magma in the BPIP (Thompson et al., 1982; 1986; Hole et al., 2015a). The isotopic compositions of BPIP lavas exhibit extreme variability, with εNd_{60} varying from −30 to +10 and $^{206}Pb/^{204}Pb$ 14.3-18.5 which reflects the antiquity of the contaminants involved in petrogenesis. For MPLF lavas, variations in εNd_{60} are a more modest −8 to +8. Because the Archean sialic component had εNd_{60} ~−50, and was light rare earth element (LREE) enriched, whereas many BPIP magmas are LREE depleted, the total amount of crustal contamination required to reach εNd_{60} −8 was small and possibly only a few % (Hole et al., 2015a). However, Thompson et al. (1986) noted that interaction with Archean granulite facies crust was a feature of plateau lavas that fractionated at ~1.0 GPa, whereas upper-crustal contamination occurred during crystallization along the 1 atm Ol+Pl+Cpx cotectic. Peate et al. (2012), using data from olivine-hosted melt inclusions, showed that the crustal assimilation in some magmas must have taken place prior to growth of the olivines, but in others the inclusions have less contaminated compositions than the whole-rocks and crustal assimilation must have taken place both during and after growth of the olivines. Necessarily, the evidence of crustal interaction is entirely from trace element and isotopic compositions. During this study, no relationship was found between isotopic compositions and major element chemistry of lavas, except for concentrations of K_2O and TiO_2 which tend to be elevated and reduced respectively in lavas that suffered crustal contamination relative to uncontaminated lavas.

Major element data therefore suggest that the majority MPLF lavas crystallized Ol+Cpx at ≥1 GPa. Consequently, the position occupied by these lavas in Fig. 3B, which is

below the peridotite-pyroxenite divide of Herzberg and Asimow (2008) could either be because of their fractionation history or because they were derived from a CaO depleted pyroxenite source. Consequently, major elements alone are not sufficient to identify the course lithology of many MPLF lavas.

3. Models for trace element behaviour during olivine crystallization

3.1 Calculation methods – Ni in olivine

The methods for calculating model olivine Ni and Ca compositions of primary magmas used here follow those of Beattie et al. (1991), Beattie (1994; 1995), Herzberg and O'Hara (2002), Toplis (2005), Herzberg (2011) and Matzen et al. (2013; 2017) and Gavrilenko et al. (2016). Equations and assumptions pertinent to the current study are given below.

Fractional crystallization of primary magmas produces olivines that are expected to crystallize along a liquid line of descent (LLD); such olivine compositions have been appropriately termed "crystal line of descent," or CLD (Putirka et al. 2011). Forward models to define a CLD for olivine have been generated using Petrolog3 (Danyuchesvky and Plechov, 2011) for model BPIP primary magmas (Hole and Millett, 2016) to give an LLD. The predicted CaO, NiO and MnO concentrations in olivines formed in equilibrium with liquids along the LLD have then been calculated using the parameters embedded in PRIMELT3, or modifications of these, which are detailed below.

The forsterite (Fo) content of olivine in equilibrium with a melt is calculated using the partitioning of Fe and Mg between olivine and melt;

$$K_D^{Ol/L}{}_{(FeO/MgO)} = D^{OL/L}{}_{FeO}/D^{Ol/L}{}_{MgO} \qquad (4)$$

$K_D^{Ol/L}{}_{(FeO/MgO)}$ varies of a function of pressure, temperature and composition (*P, T, X;* e.g. Toplis 2005). Herzberg and O'Hara (2002) provide a method for calculating $K_D^{Ol/L}{}_{(FeO/MgO)}$ for the crystallization of a primary magma along the olivine liquidus from the pressure of

melting to the surface, and this calculation method is available to the user in Petrolog3. However, for magmas that pause in the crust, then it is $K_D^{Ol/L}{}_{(FeO/MgO)}$ at the depth at which olivine crystallization occurs that is relevant and not necessarily the ascent path to the surface along the olivine liquidus. The thermodynamical parameterization of Toplis (2005) allows for the calculation of $K_D^{Ol/L}{}_{(FeO/MgO)}$ at a given pressure for a known magma composition. The Toplis (2005) model has been investigated using Petrolog3 for BPIP primary magma compositions and the results are illustrated in Fig. 4 for three BPIP magmas with different MgO contents which cover the range of T_P estimates for the region (Hole and Millet, 2016). The final pressure of melting (P*f*) was used as a proxy for pressure of melt segregation which for BPIP primary magmas is typically ~2.7 GPa (Hole and Millett, 2016). This gives values of $K_D^{Ol/L}{}_{(FeO/MgO)}$ ~0.338 for derivative magmas at 2.7 GPa formed from primary magmas containing 17.5 wt% MgO or equivalent to T_P=1500°C (Fig. 4A). For near-surface crystallization, $K_D^{Ol/L}{}_{(FeO/MgO)}$ for the same magma would be 0.30-0.31. At a fixed pressure $K_D^{Ol/L}{}_{(FeO/MgO)}$ exhibits a negative covariation with Mg/Fe_{Liq} (cationic Mg/Fe of the liquid) for liquids with Mg/Fe in the range 1.5-3.3 (Fig. 4B), which is equivalent to the composition of near-primary magmas to moderately evolved basalts with ~8.0 wt% MgO. Conversely, the Herzberg and O'Hara (2002) calculation method defines a relationship between Mg/Fe_{liq} and $k_D^{Ol/L}{}_{(FeO/MgO)}$ that is necessarily positive and curvilinear to account for *P, T, X* variability during ascent along the olivine liquidus, but without magma pausing in the crust. The practical use of this is that the point of intersection between the Herzberg and O'Hara (2002) crystallization trajectory and a Toplis (2005) crystallization contour allows both $K_D^{Ol/L}{}_{(FeO/MgO)}$ and Mg/Fe_{liq} at the contoured pressure to be estimated, which are unique to a given primary magma. For example, considering a magma that segregated at 2.7 GPa and then paused in the crust and crystallized olivine at 1.0 GPa, it can be assumed that the magma follows the Herzberg and O'Hara (2002) curve in Fig. 4B from the point of magma

segregation to 1.0 GPa, crystallizing olivine along the CLD. The melt then pauses at 1.0 GPa and crystallizes more olivine. The point at which the Herzberg and O'Hara (2002) LLD intersects the 0.5 GPa Toplis (2005) contour, which in this example is at Mg/Fe_{liq}=1.7 and $K_D^{Ol/L}{}_{(FeO/MgO)}$=0.317 (Fig. 4B), is the taken as the compositional starting point for 1 GPa olivine crystallization. From that point onwards, $K_D^{Ol/L}{}_{(FeO/MgO)}$ is estimated from Mg/Fe_{Liq} using the Toplis (2005) parameterization at a fixed pressure of 1.0 GPa. Whereas the intersection point in Fig. 4b is unique to a specific primary magma, it is mainly influenced by Mg/Fe (and therefore also T_P and P*i*) of the primary magma and P*f*. Consequently, for a magmatic province with relatively consistent values T_P and P*f* such as the BPIP (Hole and Millett 2016) a single crystallization model is probably sufficient to describe the LLD of most basalts and the CLD of their component olivines, and that is the approach which has been taken here.

An additional complication comes from the expansion of the clinopyroxene stability field at the expense of olivine with increasing pressure (Fig. 2; Whitaker et al., 2007; Villger et al., 2007). Magmas that pause in the crust are likely to crystallize on the Ol+Cpx+Liq cotectic rather than along the olivine liquidus. Investigations using Petrolog3 show that $K_D^{Ol/L}{}_{(FeO/MgO)}$ remains nearly constant for the Ol+Cpx+L crystallization interval, but the role of olivine in the crystallizing assemblage diminishes substantially with continuing crystallization (Fig. 2). Consequently, for crystallization at elevated crustal pressures, olivine should be less abundant than for crystallization of the same magma near the surface. This probably naturally limits the number of olivine analyses that can be generated for olivines that crystallized on the Ol+Cpx+L cotectic. For the purposes of this study it has been assumed that for crystallization of Ol+Cpx+L, $K_D^{Ol/L}{}_{(FeO/MgO)}$ is constant at the pressure of interest.

The method used for estimating the Ni content of a primary magma was that of Herzberg (2011);

$$\text{Ni ppm} = 21.6\text{MgO} - 0.32\text{MgO}^2 + 0.051\text{MgO}^3 \quad (5)$$

$D^{Ol/L}_{NiO}$ was determined using the method of Beattie et al. (1991) which was re-examined by Herzberg et al. (2016) and found to remain applicable in the light of new experimental results;

$$D^{Ol/L}_{NiO} = 3.346\, D^{Ol/L}_{MgO} - 3.665 \quad (6)$$

Because $D^{Ol/L}_{MgO}$ is determined from $K_D{}^{Ol/L}_{(FeO/MgO)}$ then magmas which pause at depth in the crust are pressure-compensated for $D^{OL/L}_{NiO}$ by the $K_D{}^{Ol/L}_{(FeO/MgO)}$ calculation method outlined above and in Fig. 4.

Matzen et al. (2013; 2017) showed that the temperature dependence of $D^{Ol/L}_{NiO}$ can ultimately result in olivine crystallizing from near-primary magmas at near-surface pressures, having higher Ni contents than olivine crystallizing from the same magma at the pressure of melt segregation. The relationship between the NiO content of an olivine crystallizing from the same magma at 1 bar and at the pressure of melt segregation is given by;

$$NiO^{Ol}T_{P0}/NiO^{Ol}T_{Pf} = \exp\,(4505 - (1/T_{P0} - 1/T_{Pf})) \quad (7)$$

Where $Ni^{Ol/L}T_{P0}$ and $NiO^{OL/L}T_{Pf}$ are the NiO contents, in weight units, of olivine crystallizing from magma at the surface and close to the pressure of melt segregation respectively, and T_{P0} and T_{Pf} are the temperatures of the olivine saturated magma at 0 GPa and at the pressure of melt segregation respectively. Olivine-saturated T_{Pf} was taken from T_{Ol} of the PRIMELT3 solution for the magma of interest (Herzberg and Asimow, 2015; Hole and Millett, 2016). Since subsequent crystallization was assumed to take place near to the surface $K_D{}^{Ol/L}_{(FeO/MgO)}$=0.30 was used in all calculations. Application of equation (7) to primary magma compositions therefore yields the maximum possible Ni content of an olivine

crystallizing from a primary magma at near-surface pressure. Such olivines are referred to hereafter as 'Matzen olivines'.

3.2 Calculation methods – Ca in olivine

Three different methods are available for calculating the model olivine Ca compositions of primitive magmas. Two of these (Beattie et al., 1991; Herzberg and O'Hara, 2002) are based on variation in $D^{Ol/L}_{CaO}$ as a function of $D^{Ol/L}_{MgO}$. The Beattie et al. (1991) method, which is appropriate to near-surface pressures, and is given by;

$$D^{Ol/L}_{CaO} = 0.0056\, D^{Ol/L}_{MgO} + 0.0135 \quad (8)$$

And for pressures close to those of melt segregation in the range 3-7 GPa, the equation of Herzberg and O'Hara (2002) can been applied;

$$D^{Ol/L}_{CaO} = -0.019\, D^{Ol/L}_{MgO} + 0.007\, D^{Ol/L}_{MgO} + 0.0063/\, D^{Ol/L}_{MgO} \quad (9)$$

Gavrilenko et al. (2016) provided a further method of calculating $D^{Ol/L}_{CaO}$ using only the MgO content of an anhydrous magma based on new melting experiments. This method is applicable over a wide range of pressures (1atm to 14 GPa) and temperatures (1150-2050°C). For magmas containing <11.1 wt% MgO;

$$D^{Ol/L}_{CaO} = -0.0043\ \mathrm{MgO} + 0.072 \quad (10)$$

And for magmas containing >11.1 wt% MgO;

$$D^{Ol/L}_{CaO} = 0.00042\ \mathrm{MgO} + 0.0196 \quad (11)$$

Fig. 5A shows Petrolog3 forward crystallization models of two BPIP model primary magmas (SK982 and MU1.1) at a nominal pressure of 1 atm for the three olivine-liquid CaO partitioning models given in equations (8)-(11). In addition, the CaO contents of olivine in equilibrium with 49 model primary BPIP magmas calculated for equations (8)-(11) are also shown in Fig. 5A. The uncertainty in $D^{Ol/L}_{CaO}$ (±0.004) for the Gavrilenko et al. (2016) model for compositions with >11.0 wt% MgO propagates to ±300 ppm Ca in Fig. 5. The Beattie et

al. (1991) and Gavrilenko et al. (2016) models predict very similar primary equilibrium olivine compositions for BPIP magmas, but exhibit significant differences in slope of the CLD, with the Gavrilenko et al. (2016) model initially predicting lower $D^{Ol/L}_{CaO}$ than the Beattie et al. (1991) model for the same range of Fo contents. However, at around 85-87% Fo, equivalent to a whole rock MgO content of 11 wt% (see equations (10) and (11) above) the Gavrilenko et al. (2016) model exhibits a sharp increase in olivine Ca content with decreasing Fo compared to the Beattie et al. (1991) model. The Herzberg and O'Hara (2002) model predicts lower Ca contents of primary olivine than either of the other two models.

Fig 4b illustrates the effects of crystallization of magmas at varying pressures on Ca and Fo contents of olivine. A single model primary BPIP magma (SK982) has been selected and Petrolog3 forward models at pressures in the range 1atm to 2.2 GPa generated. CLDs for olivine have then been calculated from equations (9)-(11). The Beattie et al. (1991) model has not been investigated because it is applicable only to crystallization at 1 atm. The key features of Fig. 5 are that both the Herzberg and O'Hara (2002) and Gavrilenko et al. (2016) models develop an inflection on the CLD at the point at which clinopyroxene joins the crystallizing assemblage, which is also reflected in the major element data for BPIP lavas (Fig. 3). According to the Gavrilenko et al. (2016) model, crystallization of the assemblage Ol+Cpx+L causes the Ca contents of equilibrium olivine to decrease relative to the primary olivine compositions, whereas the Herzberg and O'Hara (2002) model suggests a buffering of Ca content of equilibrium olivine for the same aasemblage. Additionally, for the Gavrilenko et al. (2016) model, the CLD for Fo and Ca for the assemblage Ol+L has a relatively shallow slope for Fo contents in the range 85.5-91.5, which is equivalent to about 11 wt% MgO in the whole rock (see equation (11)). For the purposes of consistency, the most recent parameterizations for $D^{Ol/L}_{CaO}$ of Gavrilenko et al. (2016) are primarily used below, but the Herzberg and O'Hara model (2002) is also considered if necessary.

Also shown in Fig. 5B are data for natural olivines in near-primary Siqueiros Fracture Zone MORB. These have Ca=2060±63 ppm at Fo=89.9±0.5 (64 samples from Gavrilenko et al., 2016). Olivine in equilibrium with PRIMELT3 model primary magma compositions (Herzberg and Asimow 2015) have predicted Ca=2204±58 ppm and Fo= 89.9±0.3 using the method of Gavrilenko et al. (2016), which is lower than the observed abundances. However, for MORB, predicted and observed data fall within the limits of the regressions used in the Gavrilenko et al. (2016) model.

4. Olivine in MPLF lavas

Data for olivine in MPLF lavas are taken from Sobolev et al. (2007) who analyzed olivine grains from 14 different samples giving a total data set of 842 individual determinations. Spice et al. (2016) provide a further 64 analyses from Skye, Mull and Rum picrites all of which have whole-rock MgO contents in the range 24.8-31.9 wt% MgO. These picrites will be treated as a separate group of rocks from the MPLF because their stratigraphical affinity is unclear they are unlike any samples found within the main MPLF lava pile.

Covariations between Fo content and Ni content for selected analyses are shown in Fig. 6. The data have been selected to be representative of all MPLF olivine, and particularly the range of Fo contents which is from ~75-90, although the bulk of the data have Fo >80. Olivine with compositions in the range Fo 80-90 would be in equilibrium with whole-rock compositions with Mg# 54-73 and MgO 7.7-15.8 wt% at 1 atm based on forward models of the primary magma to SK982. This range in whole-rock compositions encompasses the majority of that for MPLF lavas (Fig. 3). The CLDs in Fig. 6 were calculated both for the Beattie et al. (1991) and the Herzberg and O'Hara (2002) models. For olivine in MPLF lavas, Ni correlatives positively with Fo and the data falls into two distinct groups which relate to the position of data relative to the 1 atm Beattie CLD; data for samples BR2, BR6 and BHL15 (Fig. 6A) plots closer to the 1 atm CLD than the remaining samples, the latter all

having a higher Ni for a given Fo content than, for example, sample BR2. Olivine from picrites from Mull, Skye and Rum (Spice et al. 2016) plot close to the position expected of olivine in equilibrium with primary magmas. Using these data and equation (7) above, gives Matzen olivines with Fo 91.2–91.8 and Ni = 3560-3570 ppm which are within the range of the analyzed values for olivine in the Skye and Mull picrites. Indeed, Matzen olivines calculated to be in equilibrium with all 49 BPIP PRIMELT3 primary magmas (Fig. 6B) show considerable overlap with the olivine data from Spice et al. (2016). The picrites of Spice et al. (2016) which contain high Fo and high Ni olivines must therefore have been formed by rapid emplacement of a near-primary magma at the surface followed by olivine crystallization at close to 1 atm. This allows the maximum Ni content of BPIP olivines to be constrained to ~3600 ppm at Fo ~91.5, values which are within the normal range expected for dry melting of mantle peridotite at T_P ~1500°C (Matzen et al., 2017) and within the range of those calculated for lavas from west Greenland (Herzberg et al., 2016; Matzen et al., 2017).

Since it is likely that MPLF lavas equilibrated at pressures ≥1.6 GPa, the CLD for SK982 at 1.6 GPa has been calculated and is shown in in Fig. 6. It shows a remarkable correspondence with the data from MPLF samples BR2, BR6 and BHL15, including an apparent inflection in the data trend which corresponds to clinopyroxene joining the liquidus. The inflection occurs because $D^{Cpx/L}_{NiO}$ ~0.25 × $D^{OL/L}_{NiO}$, (Herzberg et al., 2016) and therefore crystallization along the Ol+Cpx+L cotectic results in a smaller bulk mineral-melt distribution coefficient for Ni than for olivine crystallization alone. This, in turn, results in liquid compositions that have fractionated Ol+Cpx having higher Ni contents than for the same liquid fractionating only olivine, at the same Mg#. It is also noticeable that the data for near CLD MPLF lavas terminates at the Ol+Cpx+Pl+L cotectic. Mixing between primary and derivative magmas along the LLD and their subsequent crystallization of olivine would produce olivine compositions that fall on the mixing lines shown in Fig. 6. The remaining

data for MPLF olivines fall along these mixing lines. This is a similar situation to that described by Herzberg et al. (2016) for mixing relationships in olivines and primary and derivative magmas from Theistareykir, Iceland. The mixing lines shown in Fig. 5 relate to specific MgO contents of the derivative magma along the LLD. So, for sample BR5, mixing between a primary magma and a derivative magma with ~6 wt% MgO could produce the observed array of olivine compositions, whereas sample BHL34 would require a derivative magma with higher MgO content to produce its component olivine compositions.

Fig. 7 shows covariations between Fo and Ca content of the same olivines as shown in Fig. 6. Because Ca is incompatible with respect to olivine ($D^{Ol/L}_{CaO}$ typically 0.025-0.031) then a negative covariation between Fo and Ca content might be expected, but this is not observed. A feature of Fo-Ca covariations in MPLF olivines is the relatively consistent Ca content of 1800-2400 ppm over a range of Fo = 80-89. The predicted range of olivine compositions calculated for the fractional crystallization of 49 BPIP PRIMELT3 solutions from primary MgO contents to 8 wt% MgO, using the Beattie et al. (1991) 1atm crystallization and Gavrilenko et al. (2016) olivine liquidus models are also shown in Fig. 7. The field for olivine calculated using the Beattie *et al.* (1991) model has a considerably steeper slope than that for the Gavrilenko et al. (2016) model. It is noticeable that olivine in the Skye picrites mostly fall within the range of the Beattie et al. (1991) model and close to primary olivine compositions predicted by the Gavrilenko et al. (2016) model, which is also consistent with their position in Ni–Fo space (Fig. 6). Olivine in Mull picrites appear to have consistently lower Ca for a given Fo content than the Skye olivines.

Very few of the data for olivine grains from MPLF lavas fall within the region reserved for 1 atm olivine crystallization from primary and derivative magmas using the Gavrilenko et al. (2016) model. CLDs at varying pressures, calculated as described earlier, are also shown in Fig. 7, and mirror the data trends shown in Fig. 3 such that once Cpx joins olivine on the

liquidus, the CaO content of olivine decreases slightly at a given pressure. Therefore, as in Fig. 4 for whole-rock data, some of the MPLF olivines exhibit patterns of distribution of Fo and CaO that are consistent with crystallization along the Ol+Cpx+L cotectic. However, the position of isobars in Fig. 7 cannot be predicted with certainty because the CaO abundances of BPIP primary magmas vary considerably, such that at ~1.6 GPa the variation within primary magmas is equivalent to a variation of ~500 ppm Ca in the olivine data set. In addition, slow diffusion of Ca in olivine can result in consistent Ca but variable Fo contents in individual grains, which is not evident for faster-diffusing Ni data (Coogan et al., 2005; Chakraborty, 2010). Consequently, the apparent sub-horizontal arrays delineated by olivines from individual MPLF samples could in part be a result of slow Ca diffusion, and it is the Ca content of the most Fo-rich samples that best reflects crystallization conditions. However, the Ca and Fo content of the MPLF lavas shown in Fig. 7 seems to require crystallization at ≥1.4 GPa

Covariations between NiO and CaO are shown in Fig. 8 for all the Ca partitioning models in equations (8)-(11) based on the primary magma to Skye lava SK982, and for the Herzberg and O'Hara (2002) and Gavrilenko et al. (2016) methods, at varying pressures. Ca-Ni covariations for the Gavrilenko et al. (2016) model exhibit a series of negative 'spikes' which relate to the composition at which clinopyroxene joins olivine in the crystallizing assemblage, which is a predictable consequence of augite fractionation. Because clinopyroxene joins the crystallizing assemblage at progressively higher MgO contents with increasing pressure (Fig. 3), the negative 'spikes' occur at higher Ni contents with increasing pressure. However, an added complication is that for pressures >1.2 GPa, clinopyroxene joins the crystallizing assemblage at >11.1wt% MgO so equation (11) applies to the assemblages Ol+L and Ol+Cpx+L, whereas for pressures <1.2 GPa clinopyroxene joins the crystallizing assemblage at <11.1wt% MgO and so equation (11) only applies to the olivine liquidus.

Once crystallization takes place along the Ol+Cpx+Pl+L cotectic Ni-Ca variations define shallow concave upwards trends, Ca contents decreasing with increasing pressure of fractionation. The Herzberg and O'Hara (2002) model is less complex and predicts lower Ca for a given Ni content than the Gavrilenko et al. (2016) model.

Data for olivine in Skye picrites falls close to the extension of the trajectory for low pressure (~1 atm) crystallization of Ol+L and close to the position of Matzen olivines calculated to be in equilibrium with BPIP primary magmas at 1 atm. Data for olivine in Mull picrites generally hove lower Ca for a given Fo than those from Skye picrites, and lower than the model Matzen olivines. This may suggest that the Mull picrites may have experienced clinopyroxene fractionation in the mantle (Herzberg and Asimow, 2008). The data for MPLF olivines shown in Fig 7c plots significantly below the olivine liquidus of Gavrilenko et al. (2016) and close to, or below, the olivine liquidus for the Herzberg and O'Hara (2002) model. Consequently, data for the samples shown in Figs 6 and 7 are consistent with crystallization of Ol+Cpx+L at elevated pressures up to ~2.2 GPa. Given that the final pressure of melting for many BPIP lavas is ~2.7 GPa (Hole and Millett, 2016) then in some cases, crystallization of olivine must have commenced at or close to the lithosphere-asthenosphere boundary, as suggested by Matzen et al. (2017). In Fig. 8A data are shown for MPLF olivines that falls between the Gavrilenko et al. (2016) and Herzberg and O'Hara (2002) olivine liquidii, and therefore close to the expected range of Ca and Ni content for crystallization of the assemblage Ol+L. BPIP Matzen olivines fall on the extension of the Ol+L trajectory and have higher Fo contents ~92 (Fig. 7) than the observed values for MPLF lavas (maximum ~Fo88). Crystallization of ~15-20% olivine from a Skye picrite composition could produce the observed Ni, Ca and Fo contents of the MPLF olvines shown in Figs 7A and 8A. On the basis of Ni and Ca distributions in olivines discussed above all MPLF lavas could have been generated by crystallization from a peridotite-derived magma at

variable, but elevated pressures of up to ~2.2 GPa. Consequently, there is no evidence to suggest the involvement of pyroxenite in the source of the MPLF lavas.

Herzberg (2011) showed that Fe/Mn>70 at any Fo content is characteristic of olivine that crystallizes from pyroxenite compared to Fe/Mn 60-70 for olivine in peridotite-derived magmas. The mean Fe/Mn for MPLF lavas is 69.2±2.6 (Fig. 9) but two samples (BCH14 and AM7a) fall exclusively above 70 with a maximum Fe/Mn of 75 (Fig. 9A). However, Herzberg et al. (2013) demonstrated that clinopyroxene fractionates Fe from Mn causing elevated Fe/Mn in lavas that undergo clinopyroxene fractionation. Consequently, the elevated Fe/Mn in the MPLF lavas that crystallized at the highest pressures (Fig. 9B) may solely be due to clinopyroxene fractionation and not because they were derived from pyroxenite. Furthermore, the lavas shown in Fig. 9B contain olivine which carry a lower pressure crystallization signature than those in Fig. 9A, and also have Fe/Mn<70. Low and high SiO_2 pyroxenite-derived lavas from Hawaii (HSDP-2) contain olivines with Fe/Mn = 73.8±1.7 and up to a maximum of 81 all of which are higher than the MPLF samples again suggesting that pyroxenite was not an important component of the course of MPLF lavas.

5. Olivine in magmas from Iceland, Baffin Island and west Greenland

The distribution of Ni in olivines in lavas from Thesitareykir (Iceland), Baffin Island and Disko Island (west of Greenland) were discussed in detail by Herzberg et al. (2016). A feature of olivines within lavas from Theistareykir are the existence of two populations, one primitive population crystallizing close to the 1 atm CLD and the other falling on mixing lines with derivative magmas along the CLD (Herzberg et al., 2016). However, the two populations of olivines are mutually exclusive with respect to their host lavas. When the same data are considered in terms of Ni-Ca covariations (Fig. 10A), olivines that exhibit evidence of an origin by magma mixing in terms of Fo-Ni correlations, have lower CaO contents over the same range of Ni contents than the more primitive olivines that fall close to the 1 atm

CLD. Simple magma mixing cannot account for these variations because mixing lines for reasonable MgO contents of derivative magmas (≥7 wt% MgO) do not intersect both groups of olivines. Indeed, mixing between a primary magma formed at depth with magmas formed at progressively shallower levels would necessarily fall along the predicted pathway for the Herzberg and O'Hara (2002) Ni-Ca partitioning model (Fig, 9). Similarly, mixing between primitive or near primary magmas (those which would crystallize Matzen olivines) and derivative magmas close to the surface would follow the predicted pathway for the Beattie et al. (1991) Ni-Ca partitioning model.

Inspection of Fig. 7 shows that for BPIP lavas crystallizing only olivine, Ca contents of olivines should be lower for crystallization occurring at higher pressures compared to those at lower pressures. Maclennan et al. (2003) showed that some lavas at Theistareykir crystallized at >0.8 GPa and showed evidence of crystallization along the Ol+Cpx+L cotectic. So, rather than being a result of mixing it is more likely the low CaO olivines found in some Theistareykir lavas are those which crystallized at ~1.0 GPa. The variation in $D^{Ol/L}{}_{NiO}$ because of fractionation at higher T (Matzen et al. 2017) would not be great enough to cause any discernible variation in Ni content between high and lower pressure olivines. Nevertheless, $K_D{}^{Ol/L}{}_{(FeO/MgO)}$ would be higher (~0.310) for the higher pressure olivines than those which crystallized at 1 atm (~0.298) thus resulting in differences in distribution of the data in terms of Ni-Fo covariations. Also, because crystallization along the Ol+Cpx+L cotectic results in a smaller bulk mineral-melt distribution coefficient for Ni than for olivine crystallization alone, liquid compositions that have fractionated Ol and Cpx have higher Ni contents than for the same liquid fractionating only olivine, resulting in higher Ni contents in olivine for a given Fo content, as is observed at Theistareykir.

Covariations between Ca and Ni in data for olivines from Baffin Island (Fig. 10B) follow the predicted CLDs defined by the Beattie et al. (1991) and Gavrilenko et al. (2016)

models and the data therefore follow trends that are consistent with crystallization at or near the surface. The most Ni-rich and Ca-poor olivines overlap with the composition of Matzen olivines calculated to be in equilibrium with PRIMELT3 primary magmas Consequently, some of the olivines in Baffin Island lavas can be considered to be truly primary and crystallized after rapid emplacement of magma close to the surface. Importantly, there is no evidence for crystallization along the Ol+Cpx+L cotectic, the projection of which falls well below the observed data in Fig. 10B. Olivines in lavas from Disko Island (Fig. 10C) have systematically lower Ca contents at a given Fo content compared to the values predicted by the Gavrilenko et al. (2016) model for crystallization at 1 atm, and lower Ca contents than olivines from Baffin Island with similar Fo contents. Hole and Millett (2016) showed that at Baffin Island P*f*~2.1 GPa whereas at Disko island P*f* ~2.8 GPa which most likely reflects a deeper asthenosphere-lithosphere boundary at Disko Island Baffin Island (Matzen et al., 2017). One possibility is that Disko Island magmas underwent minor clinopyroxene fractionation in the mantle before being emplaced, whereas the Baffin Island magmas only crystallized olivine and underwent rapid emplacement to shallow levels. Alternatively, the low Ca and high Ni contents of some Disko Island olivines could be interpreted as a result of their derivation from a low CaO pyroxenite source. However, the involvement of pyroxenite cannot be substantiated by the Fe/Mn for Disko Island olivines (Fig. 9). Consequently, the observed differences between Baffin and Disko island olivines might relate to the differences in magmatic plumbing at the two locations rather than to source heterogeneities.

6. Clinopyroxene stability during polybaric fractionation

MPLF and SMLS lavas do not contain augite phenocrysts, only olivine. Augite tends to form as groundmass poikilitic anhedra in sparsely olivine-phyric lavas regardless of Mg# (Thompson, 1982; Bailey et al., 1923). Nevertheless, there appears to be ample evidence to

suggest that augite was an important crystallizing phase during the evolution of the BPIP plateau lavas, which sets them apart from other NAIP lavas. On a regional scale, there were large volumes of pyroxene gabbro intruded throughout the lifetime of the BPIP. The Ben Buie gabbro complex on Mull forms part of the intrusive complex beneath the Mull volcano and is considered to be a product of the crystallization of a tholeiitic magma (Thompson 1982).

The estimates of ~1.0 GPa crystallization pressure of some of the more evolved lavas along the Ol+Cpx+Pl+L cotectic, coupled with the high pressure Ol+L or Ol+Cpx+L crystallization trends evident in the olivine data, strongly suggests that polybaric fractional crystallization was important in the BPIP, as was originally postulated by Thompson *et al.* (1980) and developed further by other workers (e.g. Kerr et al., 1999; Fowler et al., 2003; Font et al., 2008; Hole et al., 2015a). Herzberg and Asimow (2008) noted that deep crystallization of high CaO augite can have the same effect as shallow augite fractionation on the CaO contents of high MgO primary magmas, and Keshav et al. (2007) argued that clinopyroxene can accumulate in the mantle and evidence of its existence is found in mantle xenoliths. Consequently, the Ni-Ca relationships shown in Fig. 8 for MPLF lavas could result from initial crystallization of augite at mantle depths, close to the top of the melting column (~2.7 GPa) in the region. The distribution of the most Fo-rich olivines (Fo~92) from Mull in Fig. 8B, and the fact that they have lower Ca content but the same Ni contents as Matzen olivine compositions suggests that mantle augite accumulation is a possibility. Furthermore, olivines in Skye picrites exhibit Ni-Ca covariations that are suggestive of limited or no mantle augite accumulation (Fig. 8B). As discussed above, the sub-horizontal arrays delineated by the MPLF lavas in Fig. 8B might be a result of slower diffusion of Ca relative to Ni in olivine (Coggan et al., 2005; Chakraborty, 2010) and the Ca contents of these olivines reflect the accumulation of augite in the mantle.

An alternative explanation for the lack of early-formed augite phenocrysts in MPLF lavas relates to differences in clinopyroxene and olivine stability in primitive melts. Sugawara (2000) and Chen and Zhang (2008; 2009) provide empirical relationships between pressure, temperature and the MgO and CaO content of olivine and pyroxene saturated liquids. The Sugarawa (2000) parameterizations show that for a given melt MgO content and pressure, augite saturation occurs at ~50°C lower temperature than olivine saturation. The Chen and Zhang (2008; 2009) studies relate to the dissolution of mantle clinopyroxene (diopside $Wo_{49.5}En4_{8.5}Fs_{2.0}$) in basaltic melt. It is appreciated that extrapolating such a study to pyroxenes with compositions of around $Wo_{45}En_{41}Fs_{14}$ such as those found in mafic BPIP magmas (Hole et al. 2015a) may not be strictly valid, but these are the most applicable parameterizations in the literature. Chen and Zhang (2009) showed that saturation of Mg- and Ca-rich clinopyroxene may be determined by the three major components MgO, CaO and SiO_2. Chen and Zhang (2009) developed a relationship between $C_0^{MgO} \times C_0^{CaO}$, pressure and temperature to define clinopyroxene stability in a basaltic melt, where C_0^{MgO} C_0^{CaO} are the concentrations of MgO and CaO in a liquid at the point of saturation. Fig. 11 is a plot of CaO *versus* MgO for the MPLF whole-rock samples from which olivine data were derived plotted alongside clinopyroxene and olivine saturation curves calculated from Chen and Zhang (2008; 2009). Here it is assumed that polybaric fractional crystallization took place in two distinct phases; firstly at 1.5 GPa with Cpx joining the liquidus at ~1390°C (the Cpx-in temperature for SK982 at 1.5 GPa) and secondly at 1.0 GPa with an accompanying fall in temperature to 1365°C (~55°CGPa^{-1}; Sugawara, 2000; Matzen et al., 2017). Olivine saturation is independent of CaO content of the liquid, and over the temperature interval in question, olivine saturation is little effected. However, augite saturation occurs at considerably higher CaO content for a given MgO at 1.0 GPa compared to its saturation at 1.5 GPa. The whole-rock analyses of MPLF lavas fall close to the join the between olivine

and clinopyroxene saturation curves at 1.5 GPa. However, at 1.0 GPa the same liquid composition is saturated with respect to olivine, but not with respect to clinopyroxene. Consequently, is it possible during polybaric fractional crystallization under the range of pressure conditions applicable to the MPLF, to render clinopyroxene unstable. Consequently, the lack of observed phenocrysts of augite in MPLF lavas might result from their dissolution during magma storage and fractionation at ≤1.0 GPa.

7. Predicting pyroxenite in the source of continental flood basalts

Olivines from low SiO_2-pyroxenite-derived magmas from Mauna Loa (HSDP-2) have Ni contents of ~4000 ppm at Fo ~90 whereas high SiO_2 pyroxenite derived magmas from Koolau (Makapuu stage) have even more extreme Ni contents of up to 4660 ppm at Fo ~89 (Herzberg, 2006; 2011; Sobolev et al., 2005). Both of these Ni contents are in excess of the highest Ni Matzen olivines from Disko Island which have ~3600 ppm Ni at Fo ~91.5. Since the Matzen olivines from West Greenland represent the highest possible Ni contents attainable for olivines in the NAIP, the values of up to 3000 ppm Ni at Fo ~90 for MPLF lavas does not require a high Ni pyroxenite source. Additionally, CaO contents of low and high SiO_2 pyroxenite-dervied magmas are <2000 and <1700 ppm respectively which are lower than the most CaO-poor MPLF lavas (Figs 5 & 6).

Olivines from mafic magmas in some Karoo LIP lavas (e.g. N356 of Sobolev et al., 2007) which have whole-rock with ~6wt% CaO at ~15wt% MgO (Ellam and Cox 1989) exhibit extreme depletions in Ca (100-1400 ppm), enrichment in Ni (up to 4500 ppm at Fo 88) and have Fe/Mn 75-82. However, sample N356 comes from the Lebombo monocline and is one of a suite of high TiO_2 lavas with εNd_{190}= −4 to −10 and εHf_{190}=−3 to −11 and is likely to be a sample of Proterozoic lithosphere (Ellam and Cox, 1989; 1992; Ellam et al., 1992; Ellam, 2006) and not necessarily recycled oceanic crust in the sense of Sobolev (2005) and Herzberg (2006). Extreme depletions in CaO (~8 wt% at MgO ~9.5 wt%) in Si-oversaturated

(SiO_2 ~54 wt%) whole rock samples from part of the Karoo LIP in the Falkland Islands were also reported by Hole et al. (2015b) and these too have εNd_{190} as low as −11, although they are olivine-free. It is beyond the scope of the current study to discuss the role of pyroxenite in continental LIPs, but a picture is emerging that the continental lithosphere might also be a source of pyroxenite which contributes to CFB magmatism. Data for olivines in lavas from the Siberian Traps (Sobolev et al. 2007; 2009) have Ni contents of ~3200ppm at $Fo_{83.0}$ which would project to higher Ni contents than those of Matzen olivines (~3200ppm at $Fo_{91.8}$) calculated from PRIMELT3 solutions at the same Fo content, regardless of pressure of crystallization. These same olivine phenocrysts contain <2000 ppm Ca. Consequently, the olivines must have crystallized from partial melt of pyroxenite, and not from mantle peridotite (Sobolev et al. 2009).

Given the intricacies of interpreting the whole-rock and olivine record of fractionation of magmas in the crust, it is not surprising that the positive identification of pyroxenite involvement in magmagenesis at LIPs using major elements is highly problematical. It is quite clear that any attempts to utilize CaO content of lavas to identify pyroxenite sources will be ambiguous in their outcomes. Perhaps a step closer can be made by considering the fractionation of basaltic magmas at varying pressures without utilizing CaO abundances. Fig. 12 shows SiO_2/MgO versus Mg# for basalts from Hawaii (HSDP-2), the MPLF and Theistareykir. LLDs at 1 atm have been calculated from PRIMELT3 primary magmas using Petrolog3, including for HSDP samples, a few of which are derived from mantle peridotite (Herzberg and Gazel 2009). Because Cpx is saturated with respect to silica, when it joins the liquidus it fractionates SiO_2 and MgO relative to one another at a different rate from olivine crystallization resulting in infections on the LLD as seen in Fig. 12. Data for HSDP lavas mostly fall on the 1 atm LLD implying olivine crystallization alone is responsible for their evolution. The majority of HSDP samples have lower CaO for a given MgO than would be

expected for olivine crystallization alone and consequently the source from which they were derived must be similarly CaO deficient indicating a role for pyroxenite which is also consistent with olivine trace element data (e.g. Sobolev et al., 2005; Herzberg, 2006). By contrast, MPLF lavas show significant deviations from the 1 atm LLD as a result of crystallization of Ol+Cpx. Consequently, the CaO deficiency of these lavas need not be attributed to the involvement of pyroxenite, which the olivine trace element data also indicates. For Theistareykir, the majority of lavas follow the 1 atm LLD with some deviation at Mg# <65 towards lower SiO_2/MgO than the 1 atm LLD, which is most likely a consequence of the crystallization of Ol+Cpx. Crystallization of Ol+Cpx at ~0.8 GPa is consistent with the melt inclusion studies of Maclennan et al., (2003) as well as the olivine trace element data discussed above. So, whereas the representation of data in Fig. 12 cannot be used to identify pyroxenite in the source of LIPs, it can be used to identify lavas that have crystallized Cpx+Ol at depth, without the use of CaO data, which therefore removes some ambiguity from the interpretation of MgO and CaO data for continental flood basalts.

8. The NAIP – a peridotite-dominated LIP

It is generally accepted that many of the shield-building lavas of Hawaii are likely to have been derived from melting of a pyroxenite-rich source lithology (e.g. Herzberg 2006; 2011; Sobolev et al., 2005; 2007). This pyroxenite is thought to be derived from the recycling of oceanic crust at depth and was subsequently entrained in a mantle plume. The transformations that oceanic crust may undergo during recycling are complex and involve rock-melt, melt-melt and rock-rock interactions (e.g. Herzberg, 2011; Lambart et al., 2016; Lambart, 2017). Sobolev et al. (2005; 2007) argued that the rising mantle plume beneath Hawaii contains eclogite bodies that start melting at about 190–180km depth. Melting of eclogite produces high SiO_2 initial melts which infiltrate into, and react with, the adjacent peridotite eliminating olivine and producing a solid pyroxenite. Both the reaction pyroxenite

and unreacted peridotite melt at depths between 140 and 100 km, producing hybrid magmas by mixing in conduits and crustal magma chambers. Nevertheless, data from Mauna Kea reveal that low- and high-SiO_2 pyroxenite-sourced magmas coexist as discrete batches along with peridotite-derived magmas (Rhodes et al., 2012; Sobolev et al., 2005; 2007) leading Herzberg (2011) to promote the hypothesis that melts of pure pyroxenite may segregate from their source without mixing and be erupted at the surface as lavas.

In the case of LIPs formed above thick continental lithosphere (e.g. Siberian Traps and parts of the NAIP) the composition of magmas should be almost exclusively controlled by the melting of reaction pyroxenite because thick lithosphere restricts the amount of melt that can be derived from mantle peridotite (Sobolev et al., 2005; 2007; 2009; Hole and Millett, 2016). The model proposed by Sobolev et al. (2005; 2009) for the petrogenesis of lavas of the Siberian Traps relies on the fact that SiO_2 rich olivine-free pyroxenite (that which plots to the right of the Cpx-CaTs-Opx plane) has a lower solidus temperature at a given pressure than peridotite (Sobolev et al., 2005; Lambart et al., 2012; 2016; Lambart 2017) and consequently for a given T_P, pyroxenite will melt at a higher pressure than peridotite. On this basis, Sobolev et al. (2009) concluded that early tholeiites from the Gudchikhinsky Formation of the Siberian Traps were 100% pyroxenite melts with the contribution from pyroxenite decreasing to 40-50% (Tuklonsky and Nadezhdinsky formations) as peridotite was entrained in the melting zone. Sobolev et al. (2009) further argued that differences in the compositions of lavas from the Hawaii and Siberian LIPs was simply a function of lithospheric thickness and not the amount of recycled material present in the mantle, implying that all mantle plumes could have, and should have, a similar petrological structure.

Matzen et al. (2017) provided estimates of 100 and 32 km for the depths to the LAB beneath Disko Island and Iceland rift zones respectively. Hole and Millett (2016) showed that P*f* was ~2.7 GPa for BPIP magmas and was not significantly different from that for

Disko Island, West Greenland (P*f*~2.8 GPa) suggesting a similar depth to the LAB in both areas. A pyroxenite melting signature would therefore be expected to be most evident in lavas of the MPLF and Disko Island (Fig. 13). However, it is apparent that none of the NAIP lavas under consideration here provide any evidence of melting of 100% pyroxenite, or indeed any significant proportion of pyroxenite, once the effect of high pressure fractionation on major element compositions is accounted for. In the case of Iceland, existing studies provide estimates for the overall contribution from pyroxenite which vary from <5% (Brown and Lesher, 2014) through 10% (Sobolev et al., 2007; Lambart, 2017) to 30% (Matthews et al., 2016). Lambart (2017) showed that the observed crust thickness of the Icelandic rift zones is consistent with about 10% of recycled crust in the form of a *low* SiO_2 pyroxenite lithology and that diversity of trace element and isotopic compositions observed in Icelandic rift zone basalts does not require a contribution from melts derived directly from a recycled basalt component, but results from the melting of hybrid olivine-bearing lithologies formed by solid state reactions between recycled crust and peridotite (Lambart, 2017).

Low SiO_2 olivine pyroxenites (those which plot to the left of the Cpx-CaTs-Opx plane) melt under P-T conditions that are not much different from that of peridotite but are characterized by higher melt productivity than peridotite at the same temperature and pressure (e.g. Lambart et al., 2016; Lambart, 2017). A contribution from low SiO_2 pyroxenite is therefore most likely to take the form of a hybrid lithology formed by solid state reactions (Lambart, 2017) and the resultant melt may not have an identifiable 'pyroxenite signature'. Melting experiments at 2.0 and 2.5 GPa on low SiO_2 pyroxenite SL77-582 (Keshav et al., 2004) show that large extents of melting (>70%) of pyroxenite can produce magmas with whole-rock compositions that are similar to peridotite-derived magmas, and in particular, such melts occupy the same position as some peridotite-derived melts in terms of CaO and MgO contents (Fig. 2). Lambart (2017) further showed that most of the variations in Ni

content of olivine in Icelandic lavas reported by Sobolev et al. (2007) and Shorttle and Maclennan (2011) can be explained by varying the sampling pressure of the aggregated melts in the melting column, with the compositions richest in Ni sampled at the highest pressure where the contribution of pyroxenite is the largest. However, modelling carried out during the current study does not require a pyroxenite source to explain the Ni-Ca-Fo relationships of Icelandic basalts, but merely requires fractionation of olivines at varying pressures. Nevertheless, a contribution from a pyroxenite lithology is not necessarily precluded on the basis of Ni contents of olivines in Icelandic basalts.

Fig. 13 shows the predicted CLDs for Matzen olivines with 0.365 and 0.600 wt% NiO which are in equilibrium with experimental melt #370 (Keshav et al., 2004) which itself represents 70% melt of low SiO_2 pyroxenite SL77-582 at 2.0 GPa and 1385°C. Herzberg et al. (2016) showed that olivine with 0.365 wt% NiO was characteristic of high-precision analysis of olivines having an Mg number of 89.5 that represent near solidus melts of mantle peridotite. Pyroxenite melts, and their near solidus olivines, have considerably higher NiO than melts from peridotite (e.g. Sobolev et al., 2007) and a value of 0.600 wt% NiO in near solidus pyroxenite olivine has been chosen here for illustrative purposes. The CLD for 0.365 wt% NiO intersects the data for olivine from Theistareykir which crystallized at low pressures (~0 GPa) whereas the CLD for 0.600 wt% NiO intersects the data field for pyroxenite-derived magmas from Mauna Kea recovered during the Hawaiian Scientific Drilling Programme (HSDP-2; Sobolev et al., 2007; Herzberg, 2006). In addition, the 0.600 wt% NiO CLD falls immediately below the field for olivines in lavas from Koolau (Hawaii) which were derived by melting of a high SiO_2 pyroxenite. Reverse modelling from the Matzen olivines shown in Fig. 13 to whole-rock Ni contents gives primary magma compositions which contain 463ppm and 792ppm Ni for 0.365 and 0.600 wt% NiO in olivine respectively; the former is within the estimates for near-primary high SiO_2 pyroxenite-

derived magmas given in Sobolev et al. (2005) and the latter is within the estimates for primary peridotite-derived magmas. Hybridization of melts derived from peridotite and pyroxenite must therefore fall between the 0.600 and 0.365 wt% NiO CLDs and this is indeed the region where data for all olivines from the NAIP are found. However, the Theistareykir olivines with the higher Ni for a given Fo content are also those which fractionated at ~1.0 GPa (Fig. 10) and while their relatively elevated Ni content does not *require* an input from a pyroxenite-derived melt it does not preclude it. Consequently, there is no necessity to involve a significant proportion of pyroxenite in the petrogenesis of any NAIP lavas on the basis of the trace element content of olivine.

It is interesting to speculate on the fact that more than 320 lavas from the NAIP yield PRIMELT3 solutions for melting of dry peridotite (Hole and Millett 2016), which does not include peridotite-derived magmas that crystallized at elevated pressures, compared to ~18 lavas from the Siberian Traps and ~14 lavas from Maua Loa and Mauna Kea, even though the data bases for each area are of a similar magnitude. This is probably also an indication of the dominance of peridotite-derived melt in the NAIP. Why then, if the NAIP was the site of a mantle plume that has been active from ~61 Ma until the present, do lavas show an overwhelming signature of peridotite melting? Variations in the depth to the LAB cannot provide a viable explanation which leads to the conclusion that pyroxenite was never a significant component in the source of the NAIP magmas, and where present, it had thoroughly hybridized with peridotite. If pyroxenite was not present in any significant volume, then this suggests that the NAIP did not have the same petrological structure as that envisaged for the commonly accepted mantle plume models such as those for Hawaii or the Siberian Traps. In this connection, it may be beneficial to consider alternative models for magmatism at LIPs which do not require large scale recycling of oceanic lithosphere (e.g. Foulger 2012; Anderson and Natland 2014).

9. Conclusions

Some plateau forming lavas of the BPIP have major element compositions that indicate they crystallized at <1 GPa with plagioclase joining the liquidus before clinopyroxene, the majority crystallized clinopyroxene before plagioclase feldspar over the pressure range 1.0-2.0 GPa. However, the majority crystallized olivine and clinopyroxene before plagioclase feldspar and therefore must have crystallized at >~1 GPa. Olivine within the plateau lavas have Ni and Ca contents that suggests that magmas paused at >1.6 GPa and crystallized Ol±Cpx at that depth. A few examples of near-primary magmas that underwent crystallization of olivine near the surface are found on Skye and their component olivines can be successfully modelled using the method of Matzen et al. (2017) giving a maximum Ni content for BPIP olivine as 3600 ppm. MPLF lavas which fractionated Ol+Cpx in the crust exhibit a CaO deficieny for a given MgO compared to lavas from west of Greenland and Iceland which crystallized olivine alone near the surface. Low CaO high MgO in lavas is often considered to be a characteristic sign of the involvement of pyroxenite in the source of basalts. However, olivines within MPLF lavas have Fe/Mn <70 and Ni and Ca contents that are entirely consistent with and origin solely from mantle peridotite. Therefore, apparent CaO deficiency in these lavas results from augite crystallization within the crust. The absence of augite phenocrysts in lavas may be a consequence of change from augite saturation to under-saturation with decreasing pressure, and consequent augite dissolution. The commonly accepted petrological structure of mantle plumes involving entrainment of recycled oceanic crust and significant contributions to magmatism from pyroxenite-rich sources cannot be applied to the flood basalts of the NAIP which is dominated by peridotite-derived melts.

Acknowledgements.

Prof. Claude Herzberg is thanked for a thoughtful, critical and technical review of this manuscript. John Millett is thanked for his comments on earlier drafts of the paper. Members of the NAIP workshops at Durham University provided significant background information and a context for this study.

References cited

Anderson, D.L., Natland, J.H., 2014. Mantle updrafts and mechanisms of oceanic volcanism. Proc. Nat. Acad. Sci. Am. 111, E4298-E4304.

Bailey, E.B., Clough, T.C., Wright, W.B., Richey, J.E., Wilson, G.V., 1924. The Tertiary and post-Tertiary geology of Mull, Lochaline and Oban. Mem Geol Surv UK. His Majesty's Stationery Office, Glasgow. 422pp.

Beattie, P.D., Ford, C.E., Russell, D.G., 1991. Partition coefficients for olivine-melt and orthopyroxene-melt systems. Contrib. Mineral. Petrol. 109, 212-224.

Beattie, P.D., 1994. Systematics and energetics of trace-element partitioning between olivine and silicate melts: Implications for the nature of mineral/melt partitioning. Chem. Geol. 117, 57-71.

Beattie, P.D. 1995. Olivine-melt and orthopyroxene-melt equilibria. Contrib. Mineral. Petrol. 115, 103-111.

Bell, B.R., Claydon, R.V., Rogers, G., 1994. The petrology and geochemistry of cone-sheets from the Cuillin igneous complex, Isle of Skye: Evidence for combined assimilation and fractional crystallization during lithospheric extension. J. Petrol. 35, 1055–1094.

Brown, E.L., Lesher, C.E., 2014. North Atlantic magmatism controlled by temperature, mantle composition and buoyancy. Nature Geosci. 7, 820-824.

Chakraborty, S., 2010. Diffusion coefficients in olivine, wadsleyiteand ringwoodite. In: Zhang, Y. & Cherniak, D. J. (eds) Diffusion in Minerals and Melts. Mineralogical Society of America and Geochemical Society, Reviews in Mineralogy and Geochemistry 72, 603–639.

Chen, Y., Zhang, Y., 2008. Olivine dissolution in basaltic melt. Geochim. Cosmochim. Acta 72, 4756-4777.

Chen, Y., Zhang, Y., 2009 Clinopyroxene dissolution in basaltic melt. Geochim. Cosmochim. Acta. 73, 5720-5747.

Coogan, L.A., Hain, A., Stahl, S., Chakraborty, S. 2005. Experimental determination of the diffusion coefficient for calcium in olivine between 900°C and 1500°C. Geochim. Cosmochim. Acta, 14, 3683-3694.

Coogan, L.A., Saunders, A.D., Wilson, R.N., 2014. Aluminium-in-olivine thermometry of primitive basalts: Evidence of an anomalously hot mantle source for large igneous provinces. Chem. Geol. 368, 1-10.

Danyushevsky, L.V., Plechov, P., 2011. Petrolog3: Integrated software for modeling crystallization processes. Geochem. Geophys. Geosys. 12. doi:10.1029/2011GC003516.

Danyushevsky, L.V., 2001. The effect of small amounts of H_2O on crystallization of mid-ocean ridge and back-arc basin magmas. J. Volcanol. Geotherm. Res. 110, 265-280.

Ellam, R.M., 2006. New constraints on the petrogenesis of the Nuanetsi picrite basalts from Pb and Hf isotope data. Earth. Planet. Sci Lett. 245,153-161.

Ellam, R.M., Cox, K.G., 1989. A Proterozoic lithospheric source for Karoo magmatism: evidence from the Nuanetsi picrites. Earth. Planet. Sci. Lett. 92, 207–218.

Ellam, R.M., Cox, K.G., 1991. An interpretation of Karoo picrite basalts in terms of interaction between asthenospheric magmas and the mantle lithosphere. Earth. Planet. Sci. Lett. 105, 330–342.

Ellam, R.M., Carlson, R.W., Shirey, S.B. 1992. Evidence from Re–Os isotopes for plume-lithosphere mixing in Karoo flood basalt magmatism. Nature 359, 718–721.

Font, L., Davidson, J.P., Pearson, D.G., Nowell, G.M., Jerram, D.A. Ottley, C.J. 2008. Sr and Pb Isotope Micro-analysis of Plagioclase Crystals from Skye Lavas: an Insight into Open-system Processes in a Flood Basalt Province. J. Petrol. 49, 1449-1471.

Foulger, G., 2012. Are 'hot spots' hot? J. Geodynamics 58, 1-28.

Fowler, S.J., Bohrson, W.A., Spera, F.J., 2003. Magmatic Evolution of the Skye Igneous Centre, Western Scotland: Modelling of Assimilation, Recharge and Fractional Crystallization. J. Petrol. 45, 2481-2505.

Gavrilenko, M., Herzberg, C., Vidito, C., Carr, M.J., Tenner, T., Ozerov, A., 2016. A calcium-olivine hygrometer and its aoolication to subduction zone magmatism. J. Petrol. 57, 1811-1832.

Gurenko, A.A., Geldmacher, J., Hoernle, K.S., Sobolev, A.V., 2013. A composite, isotopically-depleted peridotite and enriched pyroxenite source for Madeira magmas: Insights from olivine. Lithos 170, 224-238.

Herzberg, C., Asimow, P.D., 2008. Petrology of some oceanic island basalts: PRIMELT2.XLS software for primary magma calculation. Geochem. Geophys. Geosys. 9. Doi: 10.1029/2008GC002057 .

Herzberg, C., Asimow, P.D., 2015. PRIMELT3 MEGA.XLSM software for primary magma calculation: Peridotite primary magma MgO contents from the liquidus to the solidus. Geochem. Geophys. Geosys. 16, 563-578.

Herzberg, C., Gazel, E. 2009. Petrological evidence for secular cooling in mantle plumes. Nature 458, 619-623.

Herzberg, C., O'Hara, M.J. 2002. Plume-associated ultramafic magmas of Phanerozoic age. J. Petrol. 43, 1857-1883.

Herzberg, C. 2004. Partial Crystallization of Mid-Ocean Ridge Basalts in the Crust and Mantle. J Petrol. 45, 2389-2405 .

Herzberg, C. 2006. Petrology and thermal structure of the Hawaiian plume from Mauna Kea volcano. Nature, 444, 605-609.

Herzberg, C., 2011. Identification of source lithology in the Hawaiian and Canary Islands: implications for origins. J Petrol. 52, 113-146.

Herzberg, C., Asimow, P.D., Ionov, D.S., Vidito, C., Jackson, G., Geist, D. 2013. Nickel and helium evidence for melt above the core–mantle boundary. Nature 493, 393-398.

Herzberg, C., Vidito, C., Salter, N. 2016. Nickel–cobalt contents of olivine record origins of mantle peridotite and related rocks. Am. Min. 101, 1952-1966.

Hole, M.J., Millett, J.M. 2016. Controls of mantle potential temperature and lithospheric thickness on magmatism in the North Atlantic Igneous Province. J. Petrol. 57, 417-436.

Hole, M.J., 2015. The generation of continental flood basalts by decompression melting of internally heated mantle. Geology 43, 311-314.

Hole, M.J., Millett, J.M., Rogers, N.W., Jolley, D.W. 2015a. Rifting and mafic magmatism in the Hebridean basins. J. Geol. Soc. Lond. 172, 218-236

Hole, M.J., Ellam, R.M., Macdonald, D.I.M., Kelley, S.P. 2015b. Gondwana break-up related magmatism in the Falkland Islands. J. Geol. Soc. Lond. 173, 108-126.

Jennings, E.S., Holland, T.B.J. 2015. A simple thermodynamic model for melting of mantle peridotite in the system NCFMASOCr. J. Petrol. 56, 869-892.

Jennings, E.S., Holland, T.J.B., Shorttle, O., Mclennan, J., Gibson, S.A. 2016. The composition of melts from a heterogeneous mantle and the origin of ferropicrite: Application of a thermodynamic model. J. Petrol. 57, 2289-2310.

Kashev, S., Gautam, S., Presnall, D.C. 2007. Garnet-bearing Xenoliths from Salt Lake Crater, Oahu, Hawaii: High-Pressure Fractional Crystallization in the Oceanic Mantle. J. Petrol. 48, 1681-1724.

Kerr, A.C., 1998. Mineral chemistry of the Mull-Morvern Tertiary lava succession, western Scotland. Mineral. Mag. 6, 295-312.

Kerr, A.C., Kempton, P.D., Thompson, R.N. 1995. Crustal assimilation during turbulent magma ascent (ATA); new isotopic evidence from the Mull Tertiary lava succession, N. W. Scotland. Contrib. Mineral. Petrol. 119, 142-154.

Kerr, A.C., Kent, R.W., Thomson, B.A., Seedhouse, J.K., Donaldson, C.H. 1999. Geochemical Evolution of the Tertiary Mull Volcano, Western Scotland. J. Petrol. 40, 873-908.

Keshav, S., Gudfinnsson, G., Sen, G., Fei, S., 2004. High-pressure melting experiments on garnet clinopyroxenite and the alkalic to tholeiitic transition in ocean-island basalts. Earth. Planet. Sci. Lett. 223, 365-379.

Kress, V.C., Carmichael, I.S.E., 1988. Stoichiometry of the iron oxidation reaction in silicate melt. Am. Mineral. 73, 1267-1274.

Lambart, S. 2017. No direct contribution of recycled crust in Icelandic basalts. Geochem. Persp. Let. 4, 7-12.

Lambart, S., Laporte, D., Provost, A., Schiano, P., 2012. Fate of pyroxenite-derived melts in the peridotitic mantle: thermodynamic and experimental constraints. J. Petrol. 53,451-476.

Lambart, S., Laporte, D., Provos, A., Schiano, P. 2013. Markers of the pyroxenite contribution in the major-element compositions of oceanic basalts: Review of the experimental constraints. Lithos 160-161, 14-36.

Lambart. S., Baker, M.B., Stopler, E.M., 2016. The role of pyroxenite in basalt genesis: Melt-PX, a melting parameterization for mantle pyroxenites between 0.9 and 5GPa. J. Geophys. Res. doi: 10.1002/2015JB012762.

Larsen, L.M., Pedersen, A.K., 2000. Processes in high-Mg, high-T magmas: evidence from olivine, chromite and glass in Paleogene picrites from West Greenland. J. Petrol. 41,1071–1098.

Larsen, L.M., Pedersen, A.K., 2009. Petrology of the Paleocene picrites and flood basalts on Disko and Nuussuaq, West Greenland. J. Petrol. 50, 1667-1711.

Lawver, L.A., Muller, R.D., 1994. The Iceland hotspot track. Geology 22, 211-214.

Maclennan, J., McKenzie, D.P., Gronvold, K., Shimuzu, N., Eiler, J.M., Kitchen, N. 2003. Melt mixing and crystallization under Theistareykir, northeast Iceland. Geochem. Geophys. Geosys. 4,8624-8664 doi:10.1029/2003GC000558.

Matthews, S., Shorttle, O., Maclennan, J., 2016. The temperature of the Icelandic mantle from olivine-spinel aluminum exchange thermometry. Geochem. Geophys. Geosys. 17, 4725-4752. doi:10.1002/2016GC006497.

Matzen, A.K., Baker, M.B., Beckett, .J.R., Stolper, E.M., 2013. The temperature and pressure dependence of nickel partitioning between olivine and silicate melt. J. Petrol. 54, 2521–2545.

Matzen, A.K., Baker, M.B., Beckett, J.R., Wood, B.J., 2017. The effect of liquid composition on the partitioning of Ni between olivine and silicate melt. Contrib. Mineral. Petrol. 172. DOI 10.1007/s00410-016-1319-8.

Millett, J.M., Hole, M.J., Jolley, D.W., Schofield, N, Campbell, E., 2016. Frontier exploration and the North Atlantic Igneous Province: New insights from a 2.6 km offshore volcanic sequence in the NE Faroe–Shetland Basin. J. Geol. Soc. Lond. 173, 320-336.

O'Hara, M.J. 1968. The bearing of phase equilibria studies in synthetic and natural systems on the origin and evolution of basic and ultrabasic rocks. Earth. Sci. Rev. 4, 69-133.

Peate, D.W., Peat, I.U., Rowe, M.C., Thompson, J.M., Kerr, A.C., 2012. Petrogenesis of High-MgO lavas of the Lower Mull Plateau Lava Formation, Scotland: insights from melt inclusions. J. Petrol. 53, 1867-1886.

Putirka, K.D., 2008. Thermometers and barometers for volcanicsystems. In: Putirka, K. D. & Tepley, F. J., III (eds) Minerals, Inclusions and Volcanic Processes. Mineralogical Society of America and Geochemical Society, Reviews in Mineralogy and Petrology 69, 61–120.

Putirka, K.D., Ryerson, F.J., Perfit, M., Ridley, W.I., 2011. Mineralogy and Composition of the Oceanic Mantle. J. Petrol. 52, 279-313.

Rhodes, J.M., Huang, S., Frey, F.A., Pringle, M., Xu, G., 2012. Compositional diversity of Mauna Kea shield lavas recoveredby the Hawaii Scientific Drilling Project: Inferences on source lithology, magma supply, and the role of multiple volcanoes. Geochem. Geophys. Geosys. 13. Doi: 10.1029/2011GC003812

Scarrow, J.H., Cox, K.G., 1995. Basalts generated by decompressive adiabatic melting of a mantle plume: a case study from the Isle of Skye, NW Scotland. J. Petrol. 36, 3-22.

Sobolev, A.V., Hofmann, A.W., Kuzmin, D.V., Yaxley, G.M., Arndt, N.T., Chun,g S-L,, Danyushevsky, L.V., Elliott, T., Frey, F.A., Garcia, M.O., Gurenko, A.A., Kamenetsky, V.S., Kerr, A.C., Krivolutskaya, N.A., Matvienkov, V.V., Nikogosian, I.K., Rocholl, A., Sigurdsson, I.A., Sushchevskaya, N.M., Teklay, M., 2007. The amount of recycled crust in sources of mantle-derived melts. Science 316, 412-417.

Sobolev, A.V., Krivolutskaya, N.A., Kuzmin, D., 2009. Petrology of the parental melts and mantle sources of Siberian Trap magmatism. Petrology, 17, 253-286.

Sobolev, A.V., Hofmann, A.W., Sobolev, S.V., Nikogosian, I.K., 2005. An olivine-free mantle source of Hawaiian shield basalts. Nature 434, 590-597.

Spice, H.E., Fitton, J.G., Kirstein, L.A., 2016. Temperature fluctuation of the Iceland mantle plume through time. Geochem. Geophys. Geosys. 17, 234-254.

Starkey, A.A., Stuart, F.M., Ellam, R.M., Fitton J.G., S, Basu & Larsen L. M. 2009. Helium isotopes in early Iceland plume picrites: constraints on the composition of high $^{3}He/^{4}He$ mantle. Earth Planet. Sci. Lett. 277, 91-100.

Sugarawa, T., 2000. Empirical relationships between temperature, pressure, and MgO content in olivine and pyroxene saturated liquid. J. Geophys. Res. B4, 8457-8472.

Thompson, R.N., 1974. Primary basalts and magma genesis I: Skye, North-West Scotland. Contrib. Mineral. Petrol. 45, 317-341.

Thompson, R.N., 1982. Magmatism in the British Tertiary Volcanic Province. Scott. J. Geol. 18, 49-107.

Thompson, R.N., Morrison, M.A., Dickin, A.P., Gibson, I.L., Harmon, R.S., 1986. Two contrasting styles of interaction between basic magmas and continental crust in the British Tertiary Volcanic Province. J. Geophys. Res. 91, 5985–5997.

Thompson, R.N., Gibson, I.L., Marriner, G.F., Mattey, D.P., Morrison, M.A., 1980. Trace element evidence of multistage mantle fusion and polybaric fractional crystallisation in the Palaeocene lavas of Skye, NW Scotland. J. Petrol. 21, 265-293

Toplis, M.J., 2005. The thermodynamics of iron and magnesium partitioning between olivine and liquid: criteria for assessing and predicting equilibrium in natural and experimental systems. Contrib. Mineral. Petrol. 149, 22-39.

Villiger, S., Ulmer, P., Muntener, O., 2007. Equilibrium and fractional crystallization experiments at 0.7 Gpa; the effect of pressure on phase relations and liquid compositions of tholeiitic magmas. J. Petrol. 48, 159-184.

Villiger, S., Ulmer, P., Muntener, O., Thompson, B., 2004. The liquid line of descent of anhydrous, mantle-derived, tholeiitic liquids by fractional and equilibrium crystallization—an experimental study at 1.0 GPa. J. Petrol. 45, 2369-2388

Whitaker, M.L., Nekvasil, H., Lindsley, D.H., Difrancesco. N.J., 2007. The role of pressure in producing compositional diversity in intraplate basaltic magmas. J. Petrol. 48, 365-393.

Williamson, I.T., Bell, B.R., 2012. The Staffa Lava Formation: Graben related volcanism, associated sedimentation and landscape character during the early development of the Palaeogene Mull Lava Field, NW Scotland. Scott. J. Geol, 48, 1–46.

Figure Captions.

Fig. 1. (A) Reconstruction of the North Atlantic region at about 65Ma showing the locations referred to in the text. Pecked lines labelled A6 etc., are seafloor magnetic anomalies. Black dots numbered 55-70 are plume-head positions at the time indicated and are taken from Lawver and Müller (1994). JMFZ, Jan Mayen Fracture Zone. After Hole and Millett (2016). (B) detail of the British Pelaeocene Igneous Province showing the position of the main magmatic centres mentioned in the text and the main structural features of the region. After Hole et al. (2015a).

Fig. 2. Schematic representation of the pressure, temperature and composition (*P, T, X*) relationships for the crystallization of a typical BPIP primary magma. (a) Phase relationships calculated using Petrolog3 for the primary magma to Skye lava SK982 (Thompson, 1982; Hole & Millett, 2016). The white dots are the approximate Fo content (Mg#) of olivine that crystallizes at the Ol+Cpx+L cotectic, and the grey dots the same for the Ol+Cpx+Pl+L cotectic. % figures on the arrows are the approximate % of olivine that can crystallize on the Ol+L liquidus at a given pressure before reaching the Ol+Cpx+L cotectic. The olivine saturation curve was calculated using the method of Sugarawa (2000) with the final pressure of melting (P*f*) from PRIMELT3 solutions (Hole & Millett, 2016) acting as a proxy for the pressure of melt segregation.

Fig. 3 (A) CaO (wt%) *versus* Mg# and b) CaO (wt%) *versus* MgO (wt%) for and Mull Plateau Lava Formation (MPLF) lavas (grey dots), Central Mull Formation (CMF; triangles) and Baffin Island lavas (white dots). The Baffin Island and CMF data shown yield PRIMELT3 solutions for melting of dry peridotite. Liquid lines of descent (LLD) were generated using Petrolog3 (Danyushevsky & Plechov, 2011) using the QFM buffer of Kress & Carmichael (1988) and the plagioclase and clinopyroxene melt liquidus associations of Danyuchevsky (2001). Black diamonds; Cpx-in at the pressure indicated; grey diamonds, Plag-in. The LLD shown is for the PRIMELT3 solution for Syke lava SK982 (Thompson, 1982) which has the following characteristics; Fe^{2+}/Fe_T=0.905 (Fe_2O_3/TiO_2=1.0); T_P=1500°C; MgO=17.4 wt%; P*i*=3.5 GPa; P*f*=2.9 GPa; F-AFM=0.17 (Hole & Millett, 2016). In a) note that for pressures <0.6 GPa the crystallization order is Ol+L → Ol+Pl+L → Ol+Pl+Cpx+L whereas for pressures >0.6 GPa the order is Ol+L → Ol+Cpx+L → Ol+Cpx+Pl+L. In (B) the dividing lines between pyroxenite- and peridotite-derived magmas and the range of possible peridotite-derived primary magmas (fine pecked lines) are taken from Herzberg & Asimow (2008). The black dots in each diagram are the samples for which high-precision olivine trace element data is available (Sobolev *et al.* 2007).

Fig. 4. (A) $K_D^{Ol/L}{}_{(FeO/MgO)}$ *versus* pressure for three BPIP model primary magmas calculated using Petrolog3 for the thermodynamical model of Toplis (2005). MgO contents of the model primary magmas were derived from PRIMELT3 the final pressure of melting (P*f*) being used as a proxy for the pressure of melt segregation PRIMELT3 solutions for S006 (16.0 wt% MgO) and SK982 (17.5 wt% MgO) are given in Hole & Millett (2016) and for MU1.1 (20.0 wt% MgO) in the electronic appendix. (B) variation in $K_D^{Ol/L}{}_{(FeO/MgO)}$ and Mg/Fe_{Liq} (cationic Mg/Fe of the liquid) during crystallization of the model primary magma to SK982 for the Toplis (2005) model at fixed pressures from 0.0 to 2.0 GPa (solid lines). Also shown is the parameterization of Herzberg & O'Hara (2002) SK982 which assumes magma ascent and crystallization along the olivine liquidus from the pressure of melt segregation to the surface. The grey diamonds represent the intersections of the Toplis (2005) contours for a fixed pressure with the Herzberg & O'Hara (2002) ascent path – see text for details. The pecked line is the approximate position of Cpx-in, with the vertical shading on the Ol+Cpx+L side of the cotectic.

Fig. 5 (A) Calculated Fo and Ca content for crystal lines of descent (CLD) for equilibrium olivines crystallizing from two BPIP model primary magmas (SK982 and MU1.1) at 1atm pressure for the models given in equations (8)-(11) in the text. Crystallization models were calculated using Petrolog3 with the following parameters; QFM Buffer of Kress and Carmichael (1988); plagioclase and clinopyroxene equilibria of Danyushevsky (2001). Crosses are at 1% crystallization intervals. The composition of 49 olivines in equilibrium with model BPIP primary magmas (Hole and Millett 2016) are also shown for each calculation method. (B) CLDs for the model primary magma to SK982 at variable pressures for; grey lines, Herzberg and O'Hara (2002); black lines, Gevrilenko et al. (2016) calculation methods (equations (9)-(11) in the text). Pressure in GPa is indicated for each CLD. Grey squares, points at which clinopyroxene joins the crystallizing assemblage for each pressure. SQFZ, Siqueiros Fracture Zone MORB measured olivine compositions (filled triangles) from Gavrilenko et al. (2016) and compositions calculated (open triangles) using the Gavrilenko et al. (2016) model. Vectors relating to various petrological parameters are from Gavrilenko et al. (2016). The line with dot terminations is the approximate uncertainty in Ca content propagated from equation (10) in the text.

Fig. 6. (A) & (B) Ni content (ppm) *versus* Fo content for olivines in MPLF lavas. The CLDs shown were calculated for the primary magma to SK982 and are for; (i) the Beattie *et al.* (1991) model at 1 atm (short dashes line); (ii) the Herzberg & O'Hara (2002) model for crystallization and ascent along the olivine liquidus (long dashes) and (iii) the Herzberg & O'Hara (2002) model until 1.6 GPa and then at a fixed pressure of 1.6 GPa (solid back line). For model (iii) $K_D^{Ol/L}{}_{(FeO/MgO)}$ values were calculated from Mg/Fe_{Liq} as shown in Fig. 2(A), propagating to give $D^{Ol/L}{}_{NiO}$ from equation (3) in the text. The large white diamond represents the Fo content for

Cpx-in, and at this pojnt $D^{Cpx/L}_{NiO}$ was assumed to be 0.25 $D^{Ol/L}_{NiO}$. Grey curves are mixing lines between the primary magma composition and derivative magmas along the CLD (see also Herzberg *et al.,* 2016) with the approximate MgO content of the derivative magma indicated. It was assumed that mixing was complete and that neither liquid contained phenocrysts at the time of mixing. 'Matzen olivines' are model olivine compositions for BPIP primary magmas segregating at P*f*, undergoing rapid emplacement at the surface without crystallizing any olivine, and then crystallizing olivine at 1 atm (equation (7) in the text. The cross-hatched field in (a) is for olivines from Siqueiros Fracture Zone MORB (Sobolev et al. 2007; Gavrilenko et al. 2016) and is shown for comparison. In (b) Skye and Mull olivines are near-primary olivines in picrites (Spice *et al.*, 2016). These include sample MU1.1 for which a Toplis model is shown in Fig. 2.

Fig. 7. (A) and (B) Ca content (ppm) *versus* Fo content for olivines for the same MPLF lavas as in Fig. 6. The cross-hatched area delimits the range of Ca and Fo contents of olivines for 49 forward crystallization models of BPIP primary magmas at 1 atm using the Beattie *et al.* (1991) parameterization for $D^{Ol/L}_{CaO}$ given in equation (4) in the text. The stippled field uses the same primary magma data but for the Gavrilenko et al. (2016) method of calculating $D^{Ol/L}_{CaO}$ given in equations (10) and (11) in the text. Grey squares are the composition at which clinopyroxene joins the crystallizing assemblage. The field labelled SQFZ encompasses measured olivine compositions for Siqueiros Fracture Zone MORB from Gavrilenko et al. (2016)

Fig. 8. (A) calculated CLDs for Ca and Ni content of olivines at variable pressures using the Ni and Ca model of Herzberg and O'Hara (2002) and the Ca model of Gavrilenko et al. (2016). The Ni model has been modified for appropriate final pressure of equilibration as discussed in the text and shown in Fig. 3. The black lines with arrows are for the Herzberg and O'Hara (2002) Ca model at the pressures in indicted in GPa. Fine lines with various ornaments are for the Ni model of Herzberg and O'Hara (2002) with Ca calculated according to the Gavrilenko et al. (2016) model, and the thick grey line if for 1 atm pressure, which is the same as the olivine. Grey squares are the compositions at which clinopyroxene joins the crystallizing assemblage for a given pressure and the white squares the same for plagioclase feldspar. The curved inflections giving negative 'spikes' for pressures >1.2 GPa result from clinopyroxene joining the liquidus before 11 wt% MgO, the MgO content at which the calculation $D^{CaO}_{OL/L}$ changes from equations (10) to (11) in the text. Matzen olivines are for olivine in equilibrium with 49 BPIP model primary magmas. The double-headed arrow illustrates the effect of crystallization of ~15% olivine at 1 atm. (B) and (C) Ni and Ca contents of MPLF olivines. The cross hatched area represents the range of compositions for forward crystallization of BPIP model primary magmas at 1 atm and therefore represents the olivine liquidus. The thick grey line is the CLD for

sample SK982 at 1 atm, and the lines labelled 'Beattie' and 'H&O' are 1atm CLDs for the Beattie et al. (1991) and Herzberg and O'Hara (2002) calculation methods.

Fig. 9. Fe/Mn (ppm) *versus* Fo content for olivine in BPIP, Baffin Island and West Greenland (Disko Island) lavas. The fields for primary olivines derived from melts of mantle peridotite are labelled with their source mineralogy i.e. harzburgite or lherzolite. The two pecked horizontal lines (Fe/Mn 60 and 70) are the upper and lower boundaries respectively for olivines that crystallize from peridotite-derived magmas. After Herzberg (2011).

Fig. 10. covariations between Ni and Ca content of lavas from (A) Theistareykir, Iceland, (B) Baffin Island and (C) Disko Island, west Greenland. Stippled areas are the range of predicted Ni and Ca contents for the crystallization of model primary magmas (Hole and Millett 2016) at 1 atm from each location. The grey line on each diagram is the calculated Ol+L CLD at 1 atm for a model primary magma from each location. Model primary magmas are as follows; Disko Island, #410188 (Larsen and Pedersen 2000); Baffin Is, BI/CS/14 (Starkey et al. 2009); Theistareykir, #9302 (Maclennan et al. 2003). In (c) grey symbols are olivines considered by Herzberg et al. (2016) to be near primary, and open circles are olivines considered by Herzberg et al. (2016) to be the result of crystallization from mixed magmas. The Ni content of Matzen olivines were calculated from PRIMELT3 solutions using equation (7) and the Ca content using equation (10). The cross-hatched area is the field for olivine data from MPLF sample BHL15 for comparison with Fig. 7. Data are from Sobolev *et al.* (2007) and Herzberg *et al.* (2016).

Fig. 11 Olivine (vertical lines) and clinopyroxene (curves) saturation calculated using the method of Chen & Zhang (2008; 2009). To the left of the curves, liquids are undersaturated with rescpect to olivine or clinopyroxene. At 1.5 GPa, the temperature estimate of 1390°C is the temperature estimate immediately prior to the Cpx-in temperature from a Petrolog3 forward crystallization model for the primary magma to lava SK982. The temperature at 1.0 GPa assumes a 55°CGPa^{-1} gradient on the olivine liquidus (Sugawara 2000; Matzen et al. 2017). Black dots are the whole-rock compositions of the MPLF lavas for which olivine data are available. The shaded area is the region of instability of Cpx in the melt caused by decompression.

Fig. 12. SiO_2/MgO versus Mg# for (A) Hawaii Scientific Drilling Project lavas, (B) MPLF lavas and (C) lavas from Theistareykir. For each sample set forward crystallization models have been generated at varying pressures from 0.0 to 1.8 GPa using Petrolog3, and starting with PRIMELT3 primary magma compositions. The shaded area on each diagram is the field for

Ol+Cpx+L. The insets are CaO *versus* MgO for the same lavas, the black line indicating the dividing line between peridotite- (above the line) and pyroxenite-derived magmas taken from Herzberg & Asimow (2008). The CaO-MgO relationships for MPLF lavas are shown in Fig. 2. Note the extended scale in (C).

Fig. 13. Ni (ppm) *versus* %Fo in olivine for basalts from Theistareykir, and pyroxenite-derived lavas recovered during the Hawaii Scientific Drilling Project (HSDP-2) and from Koolau (shield stage). Only olivine with Fo>86 are given in Sobolev et al. (2007) for HSDP-2. The open diamond is the composition of Matzen olivine, assuming an NiO content 0.365 wt%, in equilibrium with experimentally generated melt #370 of Keshav et al. (2004) which represents 70% melt of pyroxenite SL77-582. The whole-rock content of this magma would be ~460 ppm Ni which is within the range for natural olivine in peridotite-derived magmas. Black diamond is the composition of Matzen olivine, assuming and NiO content of 0.600 wt%, in equilibrium with melt #370. In this case the whole-rock composition would be 792 ppm Ni which is within the range of parental melts to Hawaiian pyroxenite-derived magmas (Sobolev et al., 2005). The pecked lines represent the CLD at 1 atm from the Matzen olivine indicated.

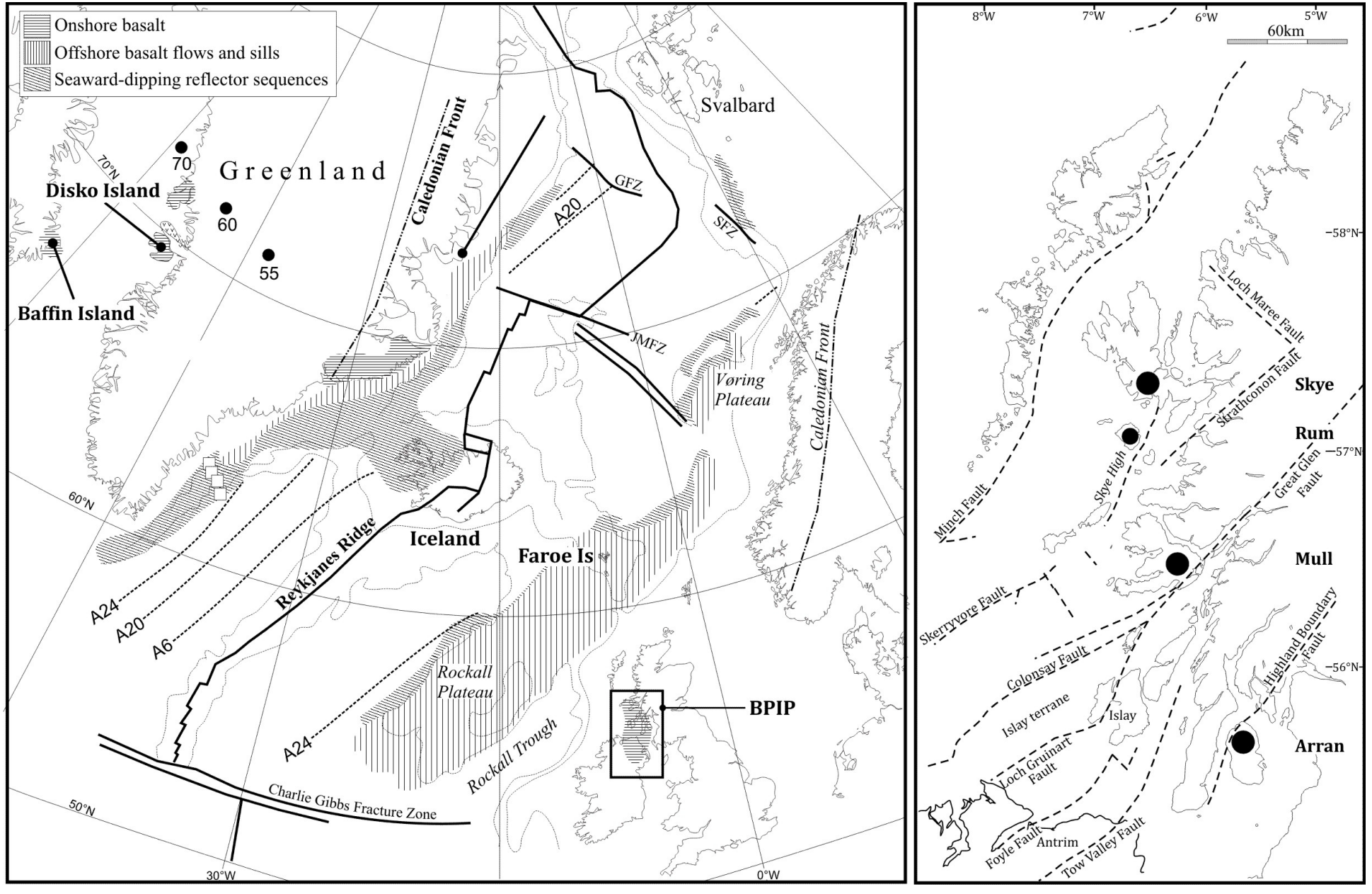
Onshore basalt
Offshore basalt flows and sills
Seaward-dipping reflector sequences
Greenland
Svalbard
Disko Island
Baffin Island
Iceland
Faroe Is
BPIP
Caledonian Front
Caledonian Front
GFZ
SFZ
A20
JMFZ
Vøring Plateau
Rockall Plateau
Rockall Trough
Reykjanes Ridge
A24
A20
A6
A24
Charlie Gibbs Fracture Zone
70
60
55
70°N
60°N
50°N
30°W
0°W
8°W
7°W
6°W
5°W
60km
58°N
57°N
56°N
Loch Maree Fault
Strathconon Fault
Skye
Rum
Great Glen Fault
Skye High
Minch Fault
Mull
Skerryvore Fault
Colonsay Fault
Islay terrane
Islay
Loch Gruinart Fault
Highland Boundary Fault
Arran
Foyle Fault
Antrim
Tow Valley Fault

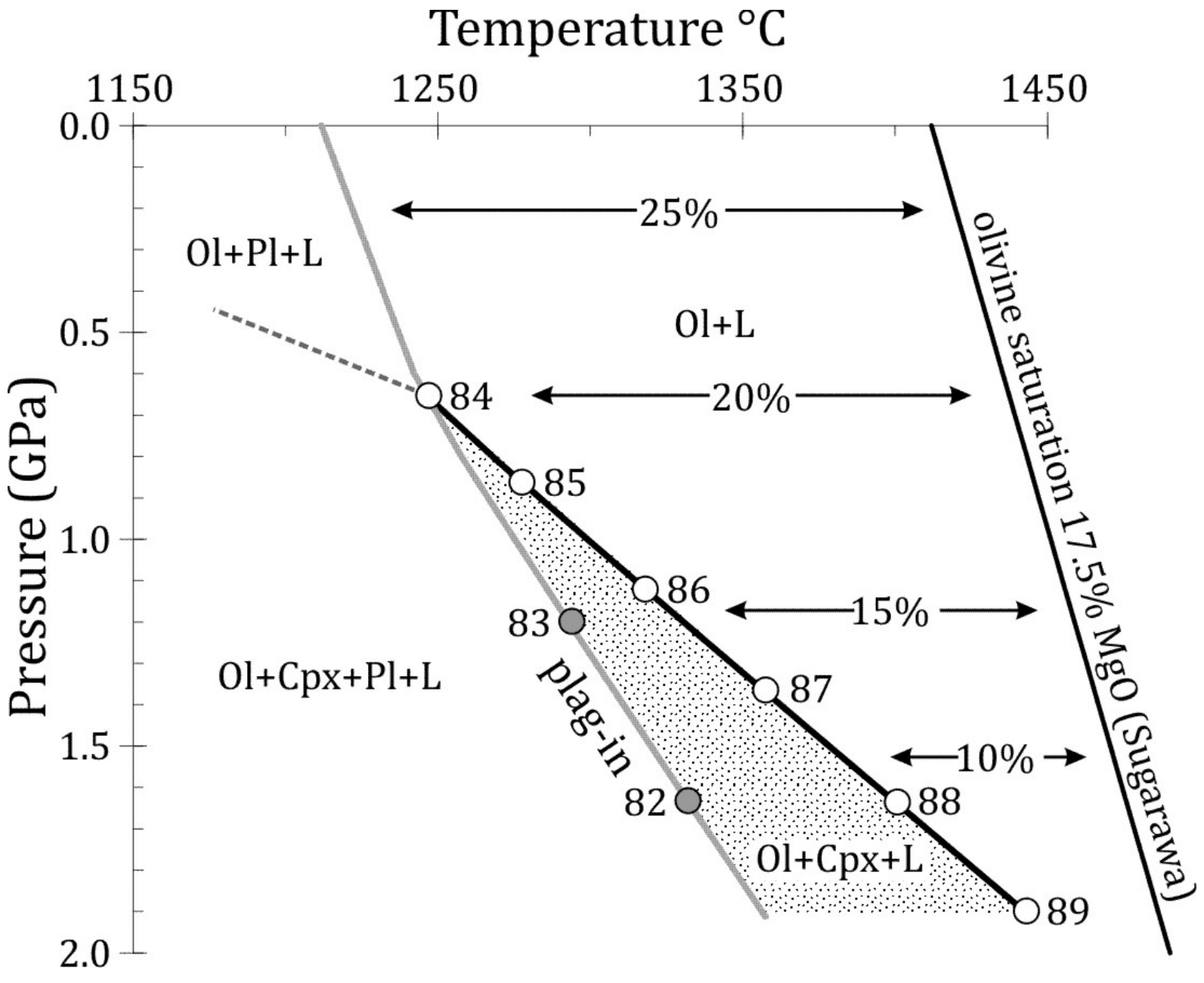
Temperature °C
1150
1250
1350
1450
0.0
0.5
1.0
1.5
2.0
Pressure (GPa)
Ol+Pl+L
Ol+L
Ol+Cpx+Pl+L
Ol+Cpx+L
25%
20%
15%
10%
84
85
86
87
88
89
83
82
plag-in
olivine saturation 17.5% MgO (Sugarawa)

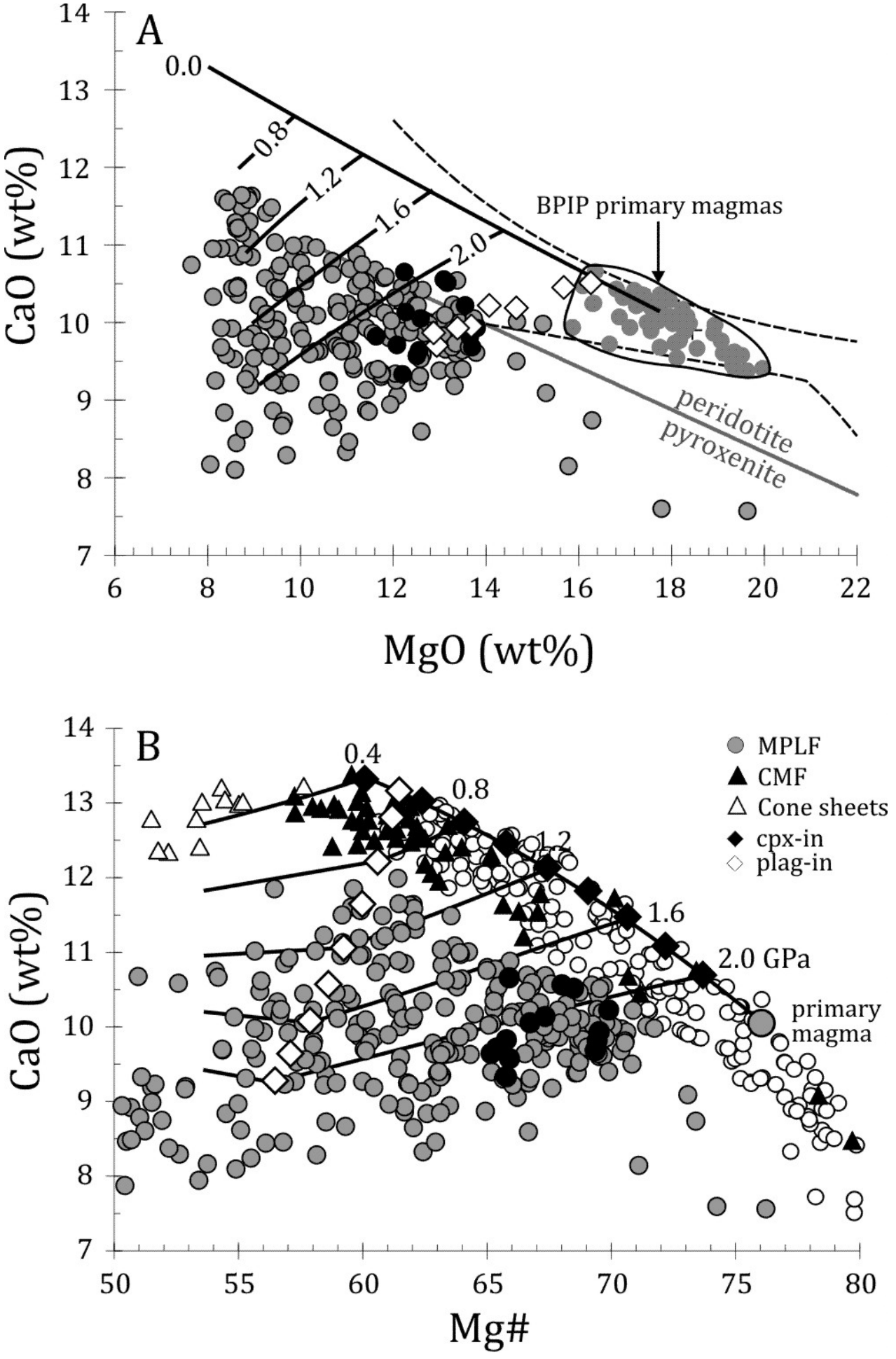
A
0.0
0.8
1.2
1.6
2.0
BPIP primary magmas
peridotite
pyroxenite
CaO (wt%)
MgO (wt%)
B
0.4
0.8
1.2
1.6
2.0 GPa
primary magma
MPLF
CMF
Cone sheets
cpx-in
plag-in
CaO (wt%)
Mg#

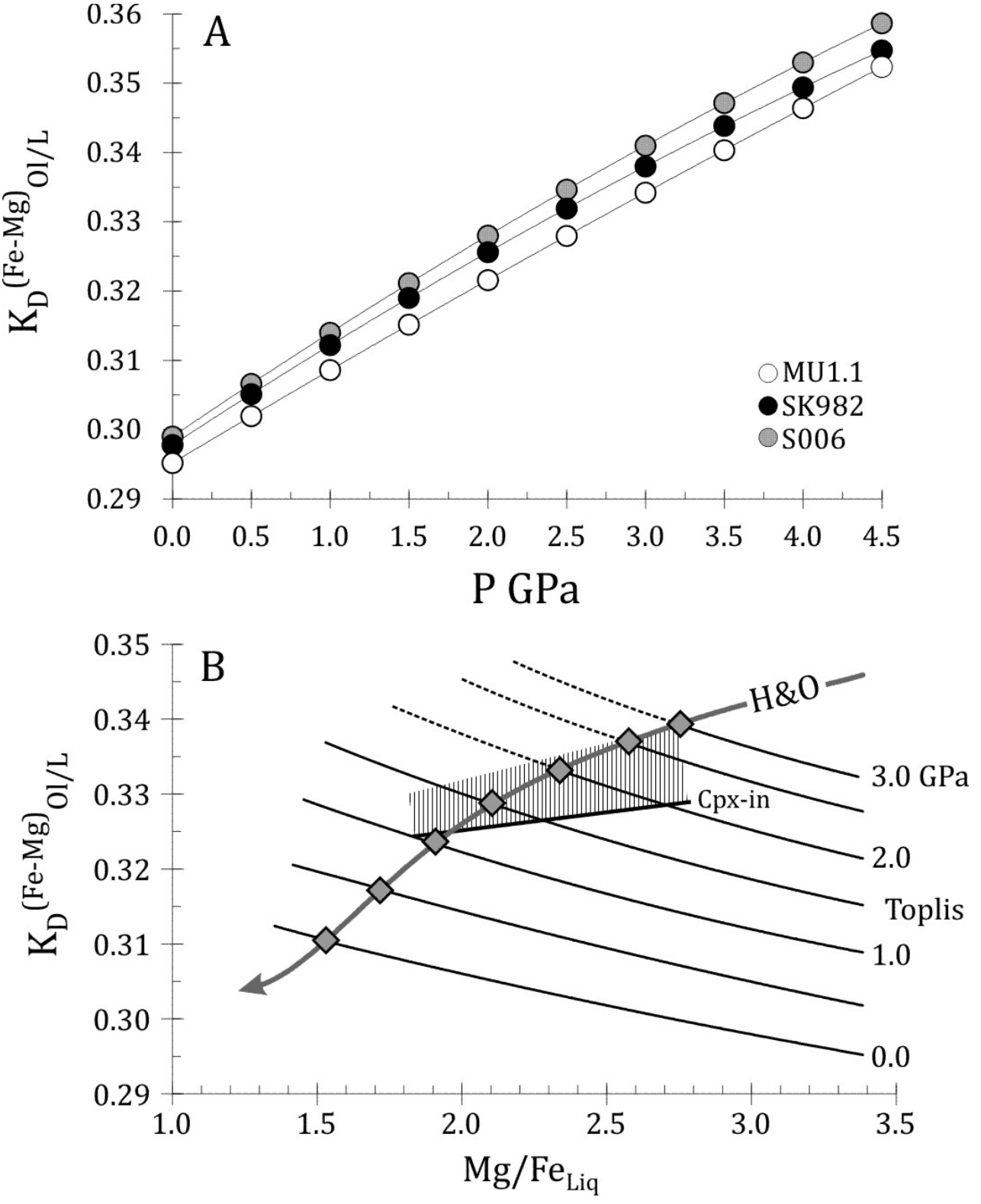
A
0.36
0.35
0.34
0.33
0.32
0.31
0.30
0.29
$K_D^{(Fe\text{-}Mg)}{}_{Ol/L}$
MU1.1
SK982
S006
0.0
0.5
1.0
1.5
2.0
2.5
3.0
3.5
4.0
4.5
P GPa
B
0.35
0.34
0.33
0.32
0.31
0.30
0.29
$K_D^{(Fe\text{-}Mg)}{}_{Ol/L}$
H&O
3.0 GPa
Cpx-in
2.0
Toplis
1.0
0.0
1.0
1.5
2.0
2.5
3.0
3.5
Mg/Fe_{Liq}

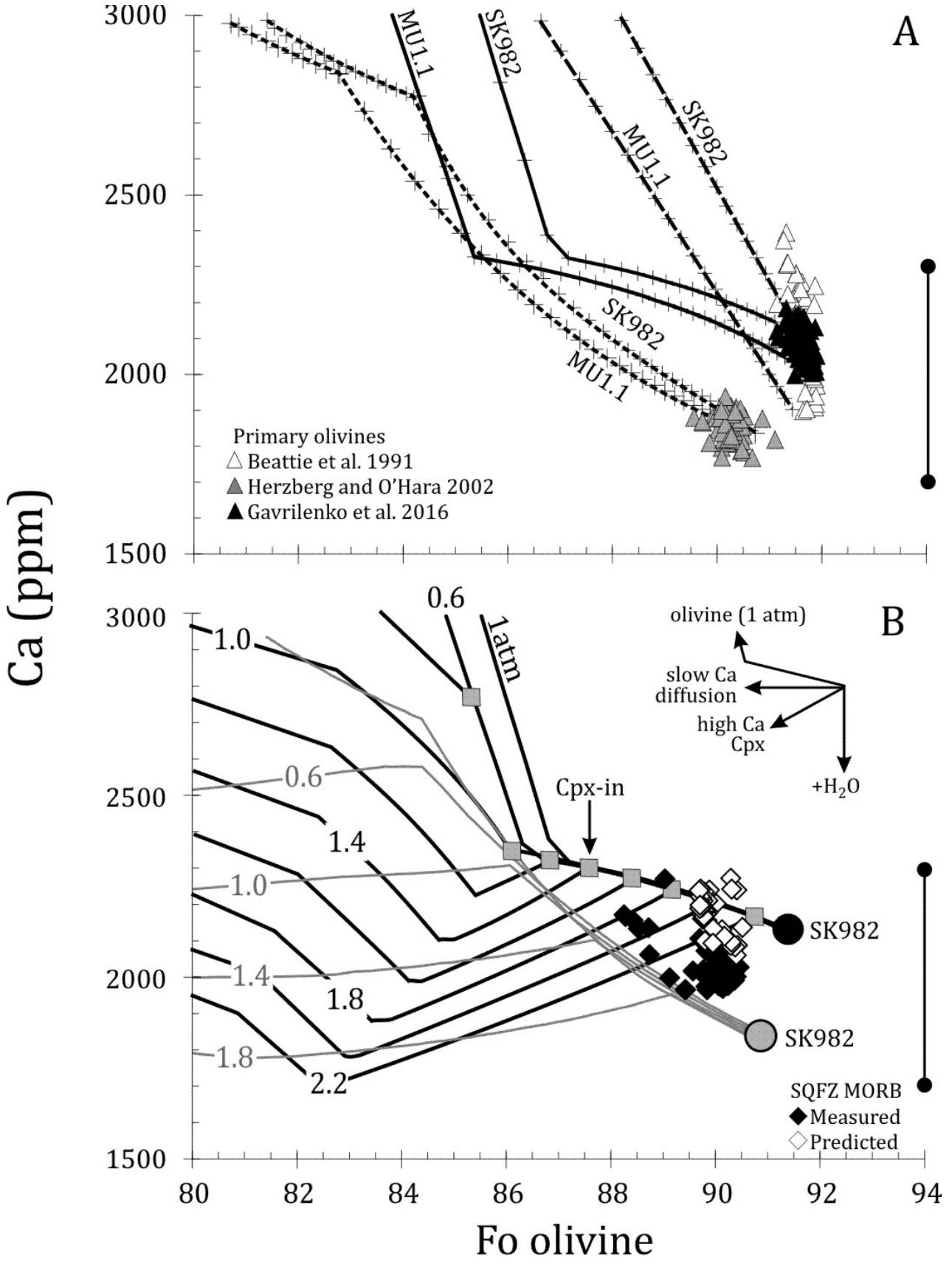
A
MU1.1
SK982
MU1.1
SK982
SK982
MU1.1
Primary olivines
Beattie et al. 1991
Herzberg and O'Hara 2002
Gavrilenko et al. 2016
B
0.6
1atm
1.0
olivine (1 atm)
slow Ca diffusion
high Ca Cpx
+H2O
Cpx-in
0.6
1.4
1.0
1.4
1.8
1.8
2.2
SK982
SK982
SQFZ MORB
Measured
Predicted
Ca (ppm)
Fo olivine
3000
2500
2000
1500
80
82
84
86
88
90
92
94

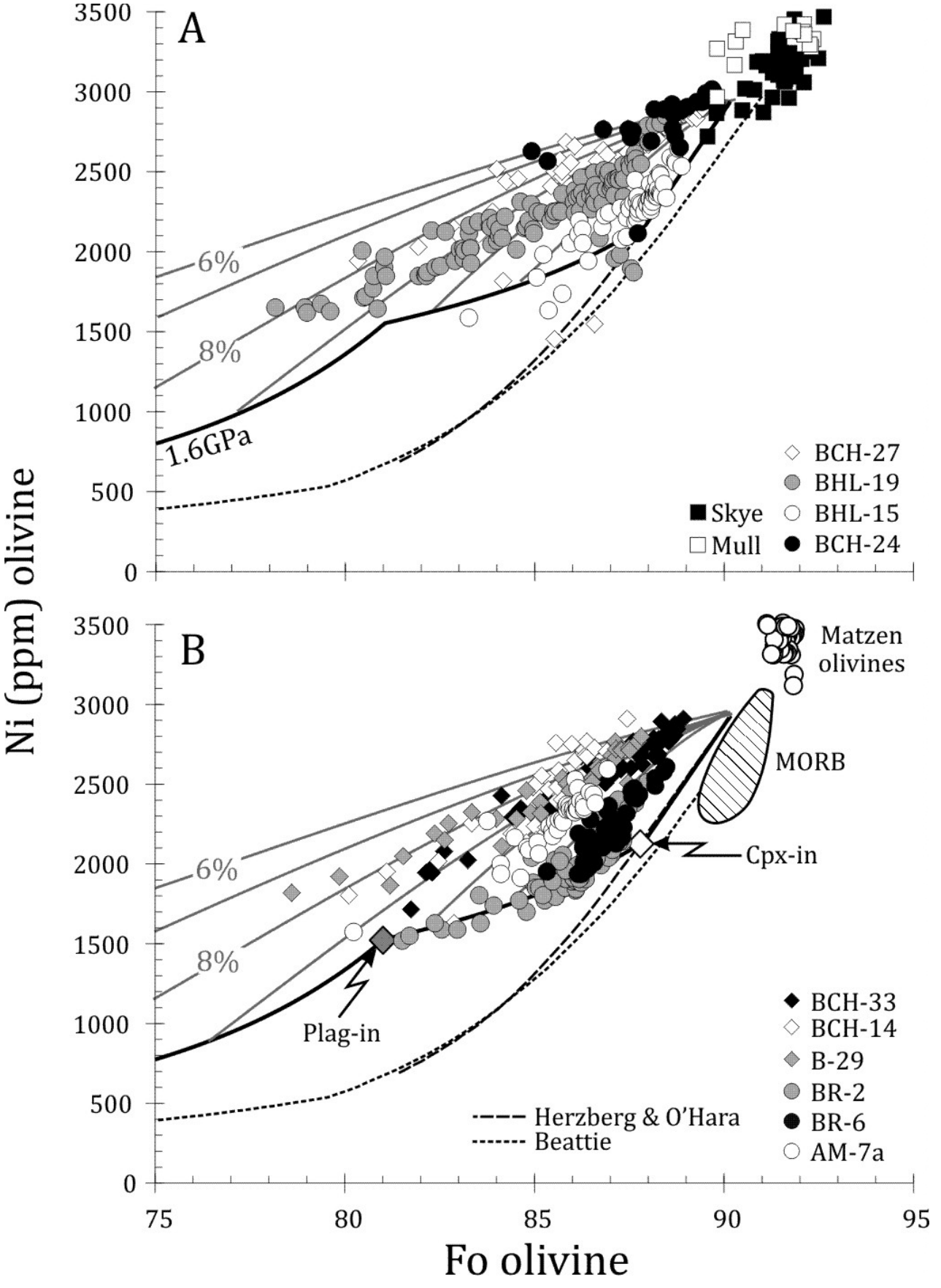
A
B
Ni (ppm) olivine
Fo olivine
3500
3000
2500
2000
1500
1000
500
0
75
80
85
90
95
6%
8%
1.6GPa
BCH-27
BHL-19
BHL-15
BCH-24
Skye
Mull
Matzen olivines
MORB
Cpx-in
Plag-in
BCH-33
BCH-14
B-29
BR-2
BR-6
AM-7a
Herzberg & O'Hara
Beattie

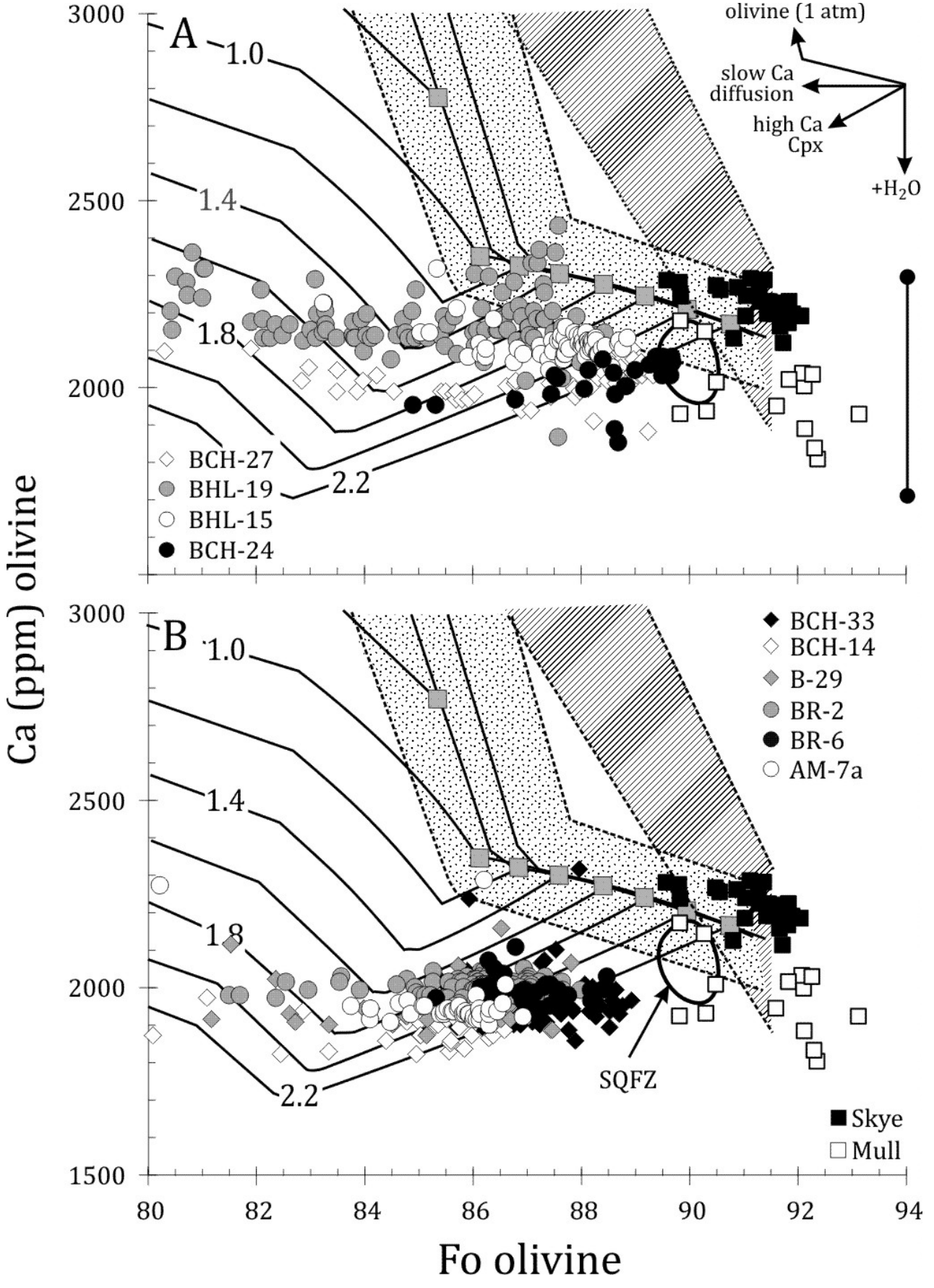
A
B
1.0
1.4
1.8
2.2
olivine (1 atm)
slow Ca diffusion
high Ca Cpx
+H2O
BCH-27
BHL-19
BHL-15
BCH-24
BCH-33
BCH-14
B-29
BR-2
BR-6
AM-7a
SQFZ
Skye
Mull
Ca (ppm) olivine
Fo olivine
3000
2500
2000
1500
80
82
84
86
88
90
92
94

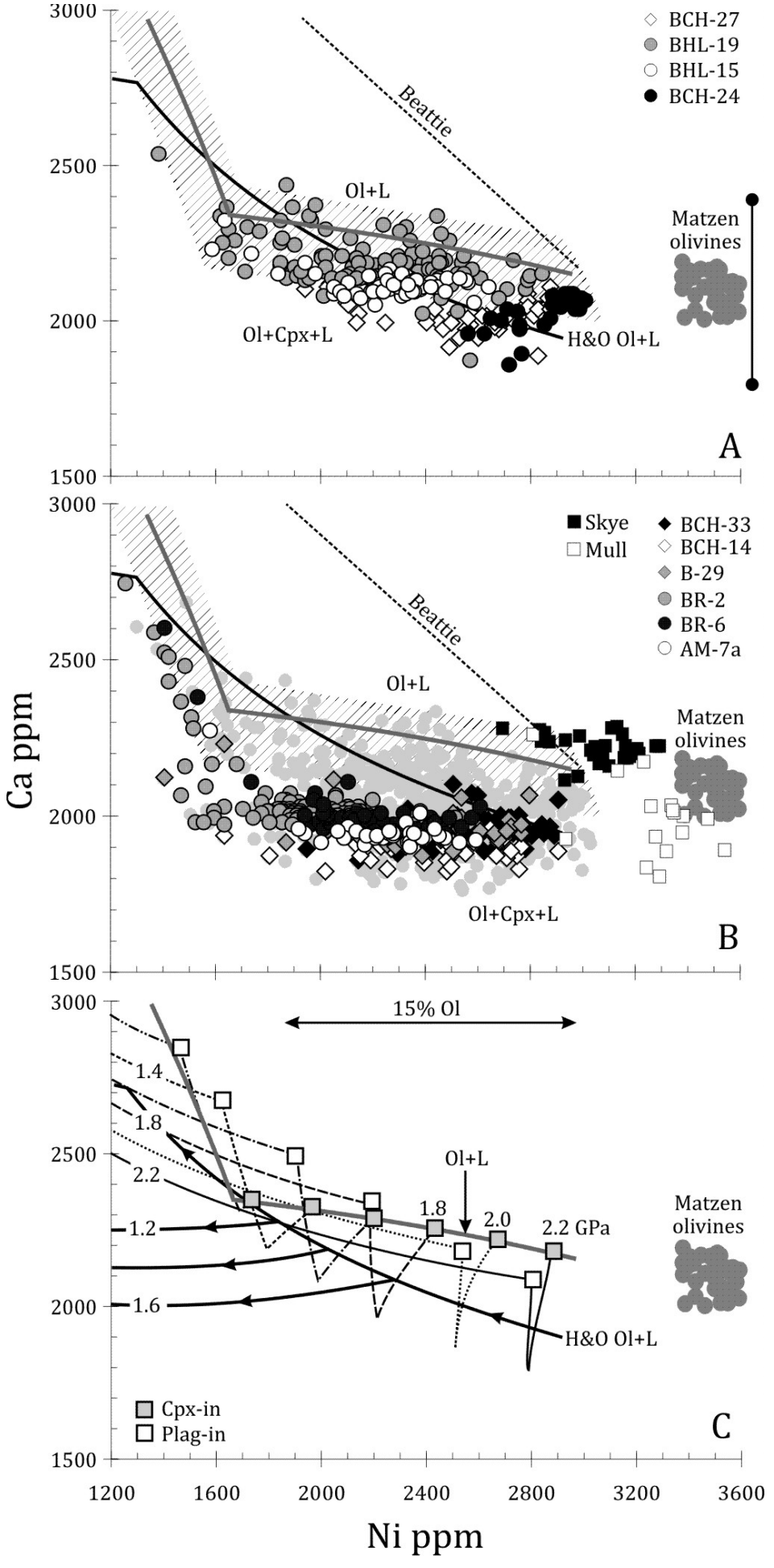
BCH-27
BHL-19
BHL-15
BCH-24
Beattie
Ol+L
Ol+Cpx+L
H&O Ol+L
Matzen olivines
A
Skye
Mull
BCH-33
BCH-14
B-29
BR-2
BR-6
AM-7a
Beattie
Ol+L
Matzen olivines
Ol+Cpx+L
B
15% Ol
1.4
1.8
2.2
1.2
1.6
Ol+L
1.8
2.0
2.2 GPa
Matzen olivines
H&O Ol+L
Cpx-in
Plag-in
C
Ca ppm
Ni ppm
3000
2500
2000
1500
1200
1600
2000
2400
2800
3200
3600

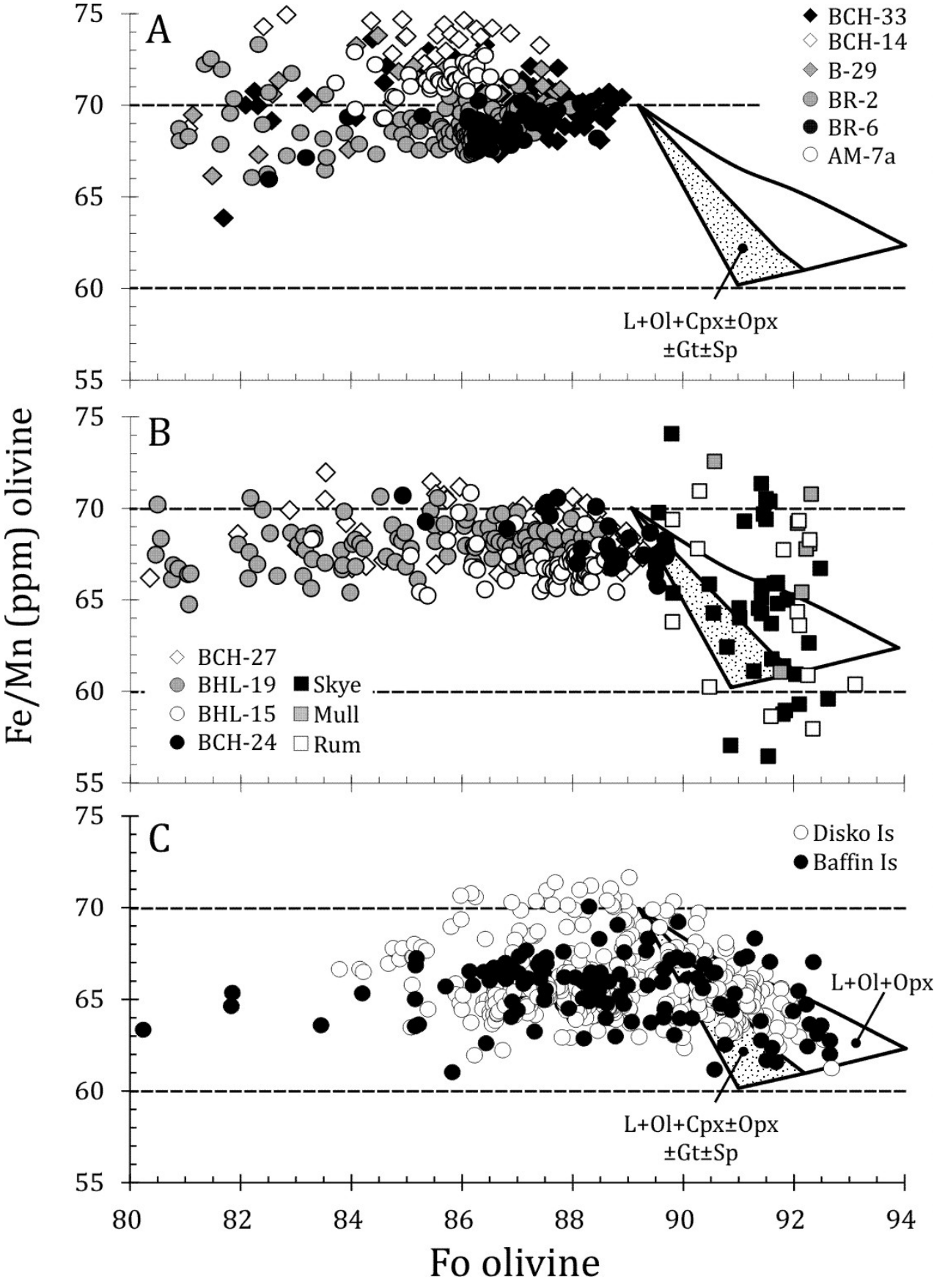
A
B
C
BCH-33
BCH-14
B-29
BR-2
BR-6
AM-7a
L+Ol+Cpx±Opx
±Gt±Sp
BCH-27
BHL-19
BHL-15
BCH-24
Skye
Mull
Rum
Disko Is
Baffin Is
L+Ol+Opx
L+Ol+Cpx±Opx
±Gt±Sp
Fe/Mn (ppm) olivine
Fo olivine
75
70
65
60
55
80
82
84
86
88
90
92
94

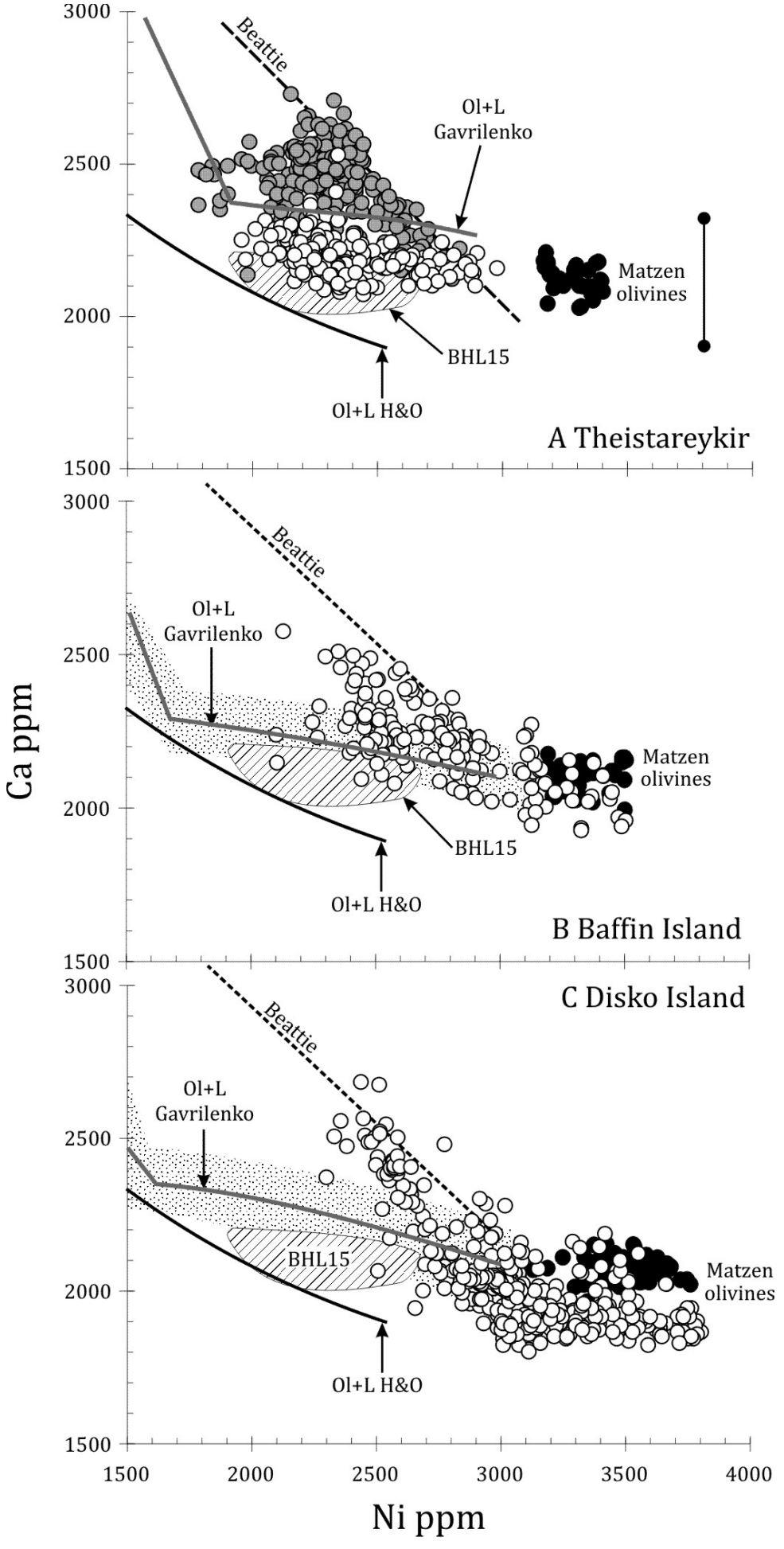
Ca ppm
Ni ppm
Beattie
Ol+L
Gavrilenko
Matzen
olivines
BHL15
Ol+L H&O
A Theistareykir
B Baffin Island
C Disko Island
3000
2500
2000
1500
1500
2000
2500
3000
3500
4000

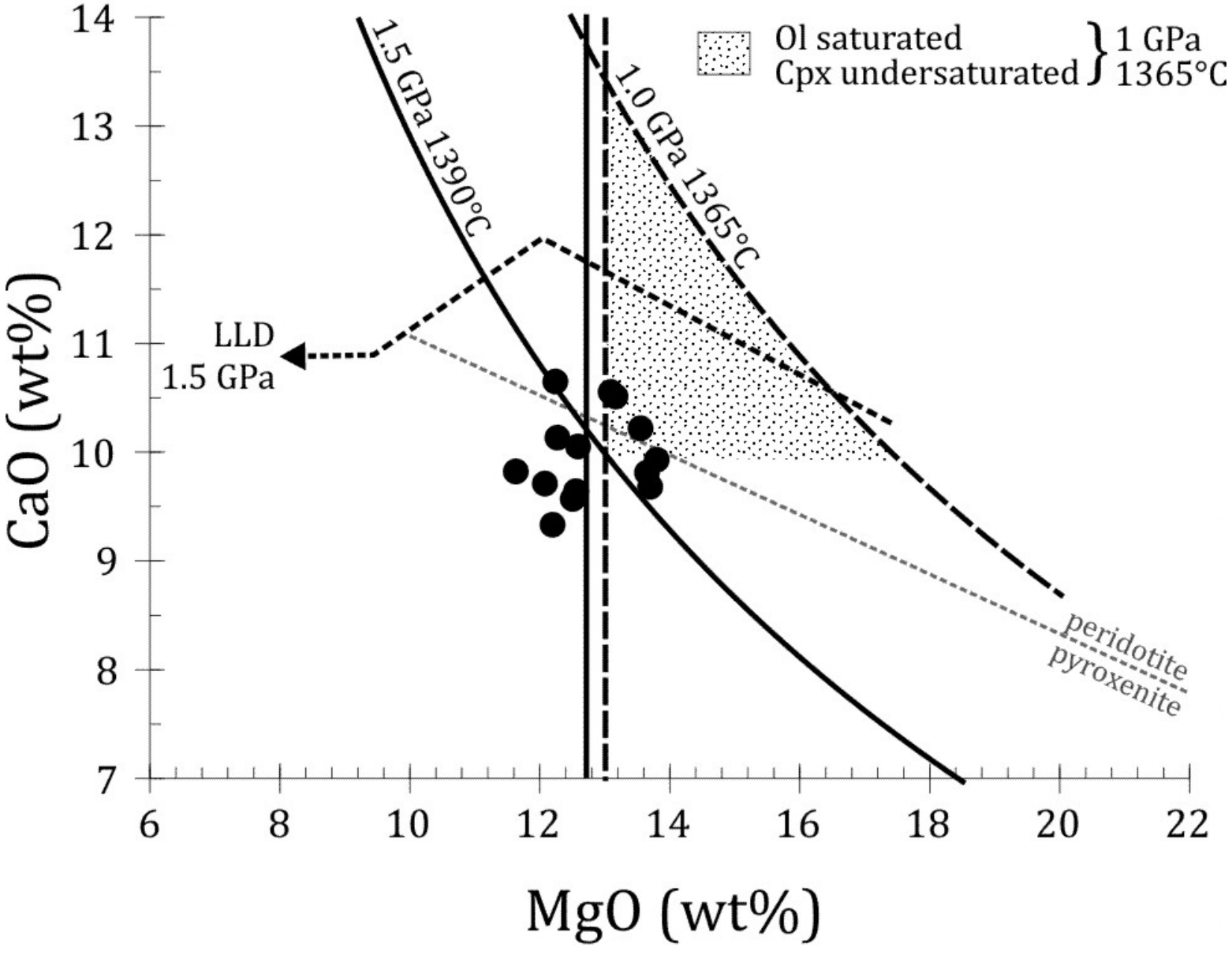
Ol saturated
Cpx undersaturated
1 GPa
1365°C
1.5 GPa 1390°C
1.0 GPa 1365°C
LLD
1.5 GPa
peridotite
pyroxenite
CaO (wt%)
MgO (wt%)
14
13
12
11
10
9
8
7
6
8
10
12
14
16
18
20
22

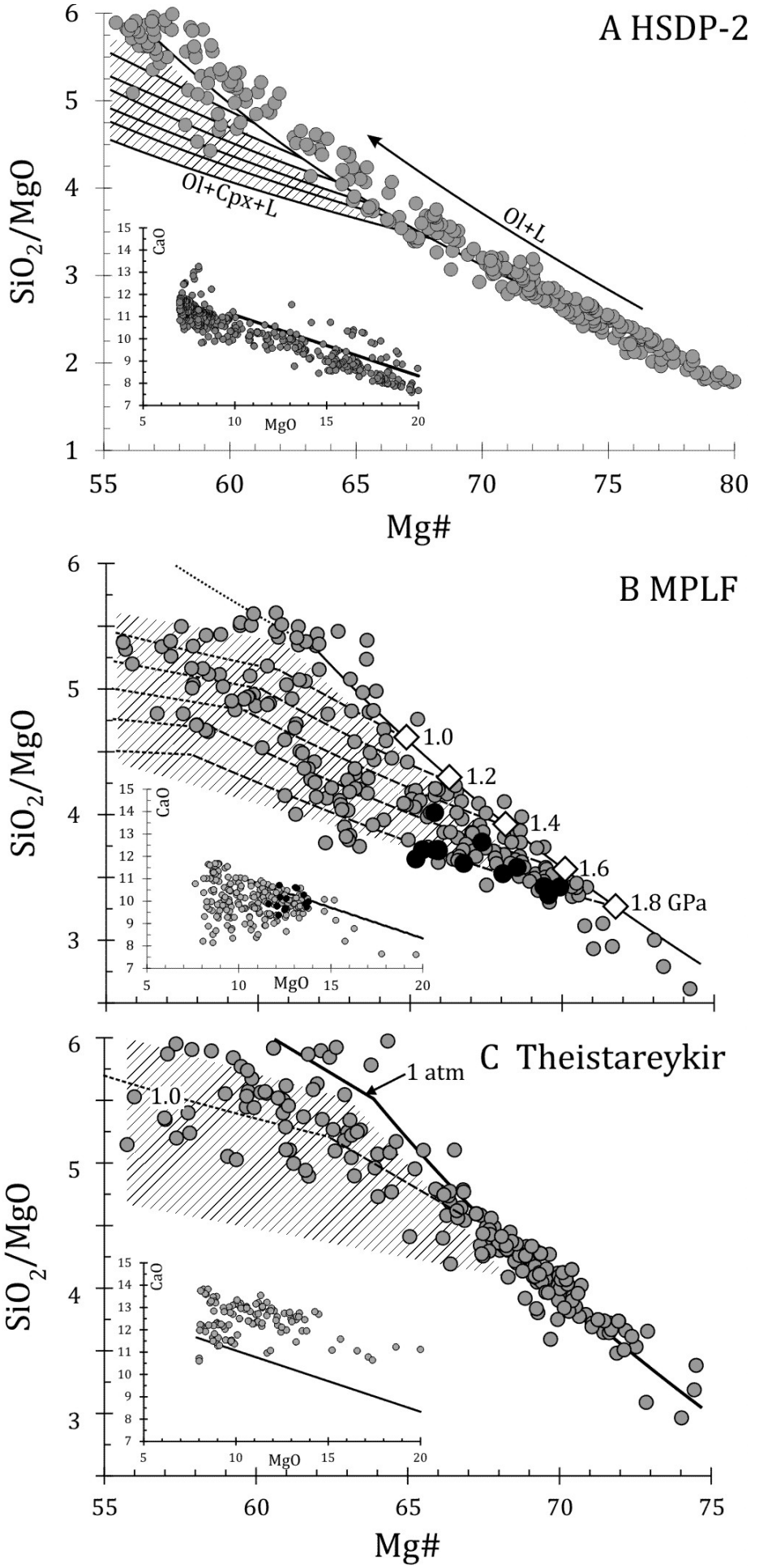
A HSDP-2
Ol+Cpx+L
Ol+L
SiO2/MgO
Mg#
CaO
MgO
B MPLF
1.0
1.2
1.4
1.6
1.8 GPa
C Theistareykir
1 atm
1.0

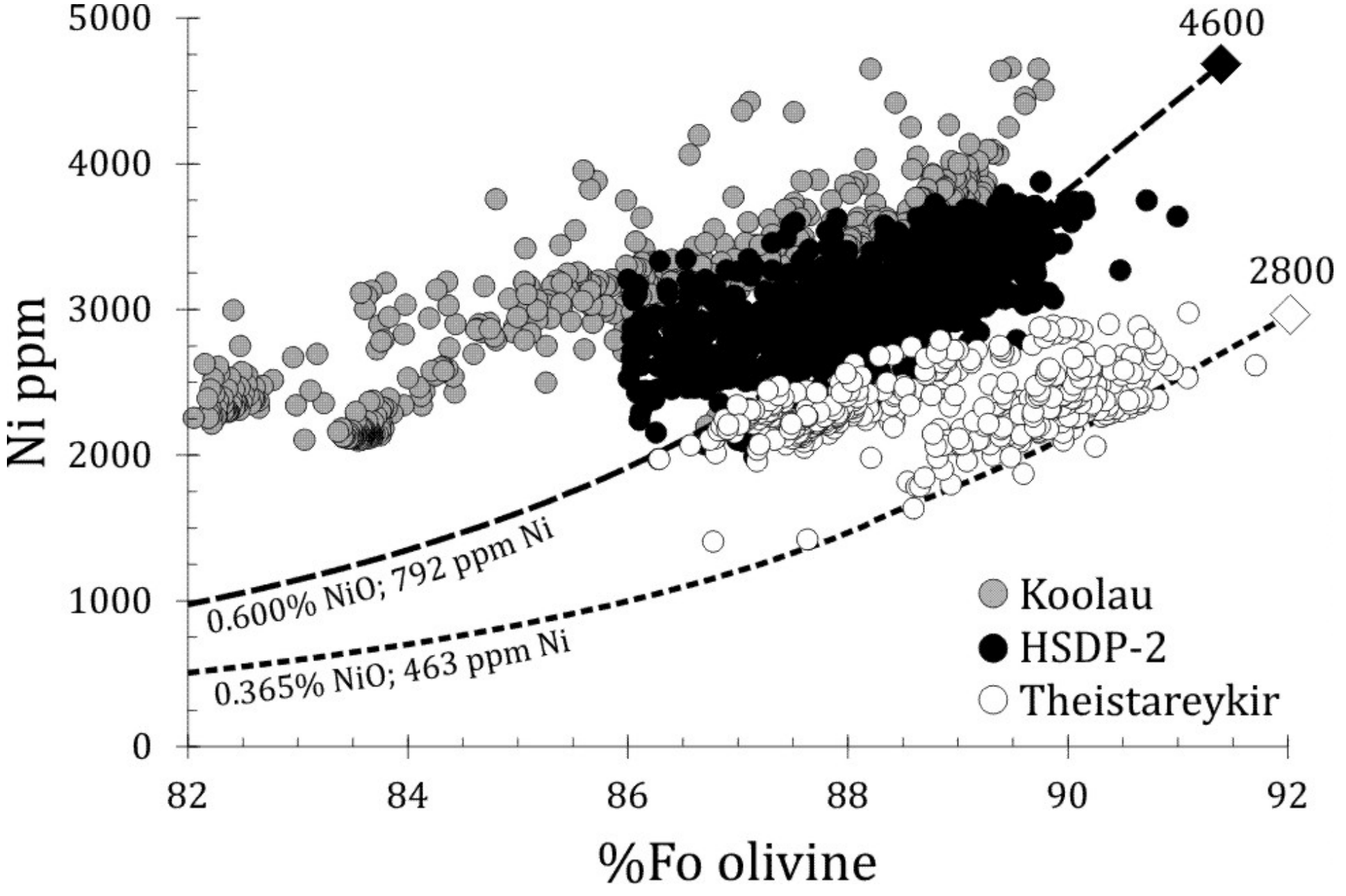
5000
4000
3000
2000
1000
0
Ni ppm
82
84
86
88
90
92
%Fo olivine
4600
2800
0.600% NiO; 792 ppm Ni
0.365% NiO; 463 ppm Ni
Koolau
HSDP-2
Theistareykir